



Performance of road markings and road surfaces

Kai Sørensen, 21 March 2011

Foreword

This textbook on road markings has been prepared by the NMF with the scope to collect the knowledge that has been obtained in a number of projects carried out by the NMF or with the assistance of members of the NMF, to put this knowledge into an international and practical perspective, and make it available for future use, in particular for the education of persons working in the field of road marking.

It is the intention that the textbook itself is translated to Nordic language, when this is relevant, while the annexes A to F with more detailed information remain in the English language only. It may also be useful to translate the annex X on light and units.

It is a further intention to prepare similar textbooks on other types of road equipment on which the NMF has worked; including at least retroreflective road equipment, variable message signs, road lighting, signal heads and yellow flashing lights at road works.

NMF (Nordisk Møde for Forbedret vejudstyr – translates to Nordic Meeting for improved road equipment) was founded in 1973 and is a well established forum in the Nordic countries for co-operation between the national road administrations and researchers in the field of development and improvement of road equipment. It is the scope of the NMF to provide – through FoU activities – the knowledge basis for improvement of the visibility and/or legibility of the road and its various components (road markings, road signs, road lighting, retroreflectors, delineators, signal and warning lights etc.).

The road road users orientation and understanding of the road and current traffic situations is to be supported through improvement of the transfer of information between the road and the road user.

An important activity of the NMF is to take part in the European standards work within the CEN. Through the conduction of research, whose results should have direct consequences for the drafting of standards for road equipment, the Nordic countries together have the possibility of playing a positive and decisive role in this work.

Contents	page
Introduction	3
1. Types of road markings	4
2. Materials for road markings and application methods	6
3. Reflection of road markings and road surfaces in daylight and under road lighting	9
4. Reflection of road markings and road surfaces in the illumination by the drivers own headlamps	12
4.1 Introduction	12
4.2 Reflection in a surface	13
4.3 Reflection by glass beads	15
4.4 Wet conditions	16
5. Reflection of road markings and road surfaces in the illumination by opposing headlamps	20
6. Road marking performance characteristics, classes of performance and measuring methods	21
6.1 Introduction	21
6.2 The luminance coefficient under diffuse illumination Q_d	21
6.3 The luminance factor β	23
6.4 The coefficient of retroreflected luminance R_L	24
6.5 The x, y chromaticity co-ordinates	25
6.6 Skid resistance	25
7. The visibility of road markings	27
7.1 Introduction and summary	27
7.2 Principles of the visibility of road markings in headlamp illumination	28
7.3 Principles of the visibility of road markings in daylight and under road lighting	30
Literature	31
Annex A: Reflection of road markings and road surfaces under road lighting or in daylight	33
Annex B: Retroreflection of road markings and road surfaces	49
Annex C: Specular reflection of road markings and road surfaces	71
Annex D: Measurement of the retroreflection of road markings and road surfaces	85
Annex E: Measurement of the reflection in diffuse illumination of road markings and road surfaces	119
Annex F: The visibility of road markings	133
Annex X: Lighting concepts and units used for road equipment	145

Introduction

Chapter 1 provides a brief account of the different types of road markings. Chapter 2 provides an additional brief account of materials and application methods for road markings, and mentions relevant European standards for these materials.

The chapters 3 to 7 may be considered as summaries of annexes A to F that give more extensive accounts of:

Annex A: Reflection of road markings and road surfaces under road lighting or in daylight

Annex B: Retroreflection of road markings and road surfaces

Annex C: Specular reflection of road markings and road surfaces

Annex D: Measurement of the retroreflection of road markings and road surfaces

Annex E: Measurement of the reflection in diffuse illumination of road markings and road surfaces

Annex F – The visibility of road markings

Chapters 3, 4 and 5 cover the scopes of annexes A, B and C respectively.

Chapter 6 covers the scopes of the two annexes D and E and provides also a short description of all the performance characteristics for road markings and performance classes of those as provided in EN 1436 “Road marking materials – Road marking performance for road users”

Chapter 7 covers the scope of annex F.

It is the intention that the chapters 3 to 7 should be easier to read than the annexes and that the interested reader can find more detailed information in the annexes themselves.

The focus is on road markings and in particular on longitudinal road markings of the different types mentioned in chapter 1. However, road surfaces are included as well because road markings and road surfaces share the same types of properties and because the same characteristics and measuring methods apply. Further, the visibility of road markings is depending on the properties of the road surfaces on which they are applied.

An additional annex X explains light and units and it intended for reference regarding characteristics and units for illumination and reflection.

1. Types of road markings

Road markings include the types that are mentioned and illustrated by examples in table 1. Longitudinal markings are those of most extensive use. They are subdivided into the types that are shown in table 2.

Table 1: Types of road markings with examples.


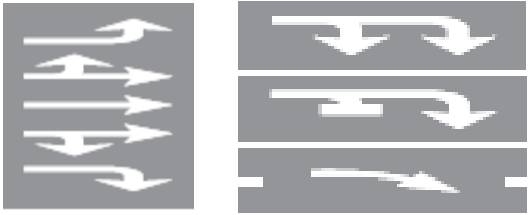









Longitudinal marking	
Arrows	
Transverse marking	
Marking for stopping and parking	
Text and symbols	

Table 1: Types of longitudinal markings.

Lane line	
Warning line	
Barrier line	
Barrier field	
Unbroken edge line	
Broken edge line	

Longitudinal markings are used for centre lines, dividing lines and edge lines.

Centre lines separate traffic with opposite driving directions; they are lane lines, warning lines, barrier lines or barrier fields, and can be single or double lines.

Dividing lines separate traffic with the same driving direction, they are lane lines, warning lines or barrier lines.

Edge lines restrict the part of the carriage way that is intended for motorised traffic; they are unbroken (continuous) or broken.

The geometry of longitudinal markings varies from country to country. The geometries used by the Nordic countries are shown in table 3 for motorways and in table 4 for single carriageway roads. A number of special cases depend on the type and the width of the road; refer to the detailed regulations of the individual countries.

Table 3: Geometry of the longitudinal markings on motorways.

Edge lines			
Country	Width	Length	Gaps
Denmark	30 cm	Unbroken	
Finland	20 cm	Unbroken	
Norway		Unbroken	
Sweden	30 cm	Unbroken	
Dividing lines			
Country	Width	Length	Gaps
Denmark	15 cm	5 m	10 m
Finland	10 cm	3 m	9 m
Norway			
Sweden	15 cm	3 m	9 m

Table 4: Geometry of the longitudinal markings on single carriageway roads.

Centre lines *)			
Country	Width	Length	Gaps
Denmark	10 cm	5 m	10 m
Finland	10 cm	3 m	9 m
Iceland	10 cm	2 m	6 m
Norway			
Sweden	15 cm	3 m	9 m
Edge lines			
Country	Width	Length	Gaps
Denmark	30 cm	Unbroken	
Finland	10 cm	Unbroken	
Iceland	10 cm	Unbroken	
Norway			
Sweden	10 cm	1 m	2 m
*) This applies for the case when the centre line is a single lane line.			

All permanent markings are white in Denmark, Iceland and Sweden, while longitudinal yellow markings are used to separate lanes of opposite driving directions in Finland and Norway. Refer to the individual regulations in Finland and Norway, which differ in some respects.

2. Materials for road markings and application methods

Materials may be subdivided into materials that are to be applied in the liquid form and in materials that are preformed.

Materials to be applied in the liquid form are paints, thermoplastics and cold plastics.

Paints can be based on solvents or they can be water borne. Paints are applied as thin coatings and adhere to the road surface during drying. The drying time depends on the actual paint and on weather conditions.

Thermoplastics contain a binder and are melted prior to application. The cooling into solids happens in a short moment after the application. Thermoplastics are mostly applied as thick coatings with a thickness of up to 3 mm, either with a uniform thickness or as profiles: Thermoplastics can also be applied as "spray plastic" in thin coatings.

Cold plastics include two or more components that are mixed during application. Adesion occurs relatively quickly during hardening. Cold plastics are mostly applied as thick coatings, either with a uniform thickness or as profiles, but can also be applied as thin coatings.

Paints were used relatively frequently in the Nordic countries, but there has been a gradual shift to thermoplastics, so that paints are now primarily used on roads with low traffic volumes. Cold plastics have been used for special products, but are no longer used in significant amounts.

Longitudinal markings are performed by machine application of materials in the liquid form. Other markings are often applied by hand. See figures 1 and 2.



Figure 1: Machine application of an edge line.



Figure 2: Application of thermoplastic by hand followed by spreading of glass beads.

During the application of materials in the liquid forms, glass beads and/or antiskid aggregates are normally applied to the surface as drop-on materials. The glass beads serve to enhance the reflection in vehicle headlamp illumination, while the antiskid aggregates serve to improve the skid resistance.

As the glass beads in the surface gradually disappear because of erosion by traffic, materials to be applied as thick coatings (thermoplastics and cold plastics) mostly contain pre-mixed glass beads. These emerge gradually in the surface as it is eroded by traffic. See figure 3.

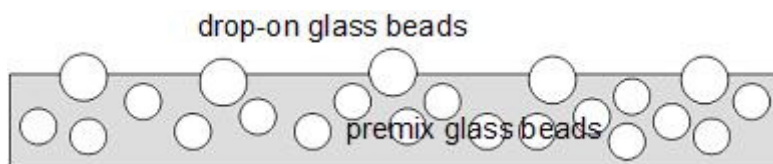


Figure 3: Illustration of drop-on and premix glass beads.

Preformed materials are tapes, or they are preformed text or symbols that are fixed to the road surface by means of glue or heating by a flame. These materials are supplied with glass beads and/or antiskid aggregates during manufacture.

Before the application of tapes it is normally necessary to apply a primer coating to the road surface in order to assure a good adhesion. Tapes exist in both thin versions intended for temporary marking and in relatively thick versions intended for permanent marking.

Text and symbols that are fixed by heating are produced from thermoplastics. The drop-on materials are only loosely attached during the manufacture, but become fixed during the heating.



Figure 4: Application of a symbol by heating.

Road markings applied as thin coatings are normally considered to be less durable than road markings applied as thick coatings. Tender specifications operate, therefore, with the concepts of short and long durability.

Additionally, tender specifications operate with a distinction between road markings with and without performance in wet conditions, where the performance aims at the reflection in vehicle headlamp illumination. This reflection can be strong or adequate, when a road marking is dry, but can fall to virtually zero when the road marking becomes wet. However, some road markings have particular means, such as profiles, structure or large surface beads, to maintain some of the reflection in wet conditions.

Materials for application in the liquid form are covered by EN 1871 "Road marking materials – Physical properties", while preformed materials are covered by EN 1790 "Road marking materials – Preformed road markings".

The following additional standards are relevant:

EN 13212 "Road marking materials – Requirements for factory production control"

EN 12802 "Road marking materials – Laboratory methods and identification"

EN 1824 "Road marking materials – Road trials"

EN 13197 "Road marking materials – Wear simulators".

NOTE 1: These standards are rather old, all dated about the year 2000. At this point in time (February 2011), proposals for revision are at voting. The proposals imply CE marking of the materials in a procedure that includes durability testing in road trials (EN 1824) and/or wear simulators (EN 13197). There is some opposition to these proposals and it is too early to say if or when or if they will come into force.

Drop-on materials are covered by EN 1423 "Road marking materials – Drop on materials – Glass beads, antiskid aggregates and mixtures of the two". An amendment, EN 1423/A1 from 2003, imply CE marking of these materials.

NOTE 2: At this point in time (February 2011), a proposal for revision is at voting.

Premix glass beads are covered by EN 1424 "Road marking materials – Premix glass beads", which does not request CE marking.

An additional relevant standard is EN 1436 "Road marking materials – Road marking performance for road users" in a last edition of 2008. This standard is introduced in chapter 6.

NOTE 3: At this point in time (February 2011), the current edition of EN 1436 is 2008.

3. Reflection of road markings and road surfaces in daylight and under road lighting

The reflection of a field of a surface can be described by the luminance coefficient q , which is the ratio between the luminance of the field caused by illumination and reflection and the illuminance on the plane of the field. Refer to annex A.

Luminance is the stimulus for the eye and is measured in candela pr. square meter, $\text{cd}\cdot\text{m}^{-2}$. Illuminance measures how strong the illumination is and is measured in lux, lx . Thereby, the unit for q is $\text{cd}\cdot\text{m}^{-2}\cdot\text{lx}^{-1}$, but the 1000 times smaller unit of $\text{mcd}\cdot\text{m}^{-2}\cdot\text{lx}^{-1}$ (the m in mcd stands for milli) is used in order to obtain convenient numbers. Refer to annex X regarding lighting units.

In annex A, it is pointed out that the value of q varies with the geometry of illumination as described by an angle of incidence and a side angle. These angles are illustrated in figure 5.

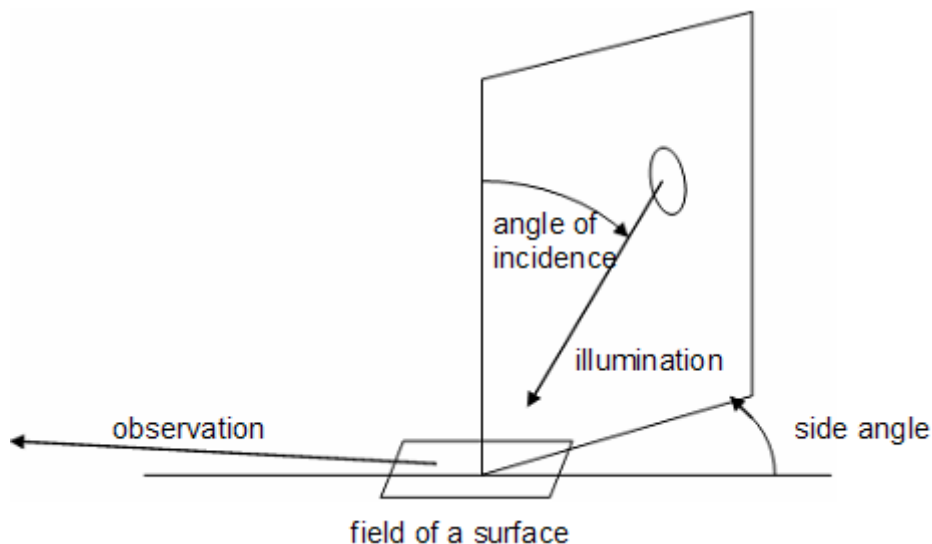


Figure 5: Angle of incidence and side angle.

Additionally, q depends on the lightness of the surface, which can be measured by the luminance coefficient in diffuse illumination Q_d . Diffuse illumination is obtained when the surroundings have a constant luminance, see figure 6. Accordingly, the Q_d value is an average of q values for all directions of illumination.

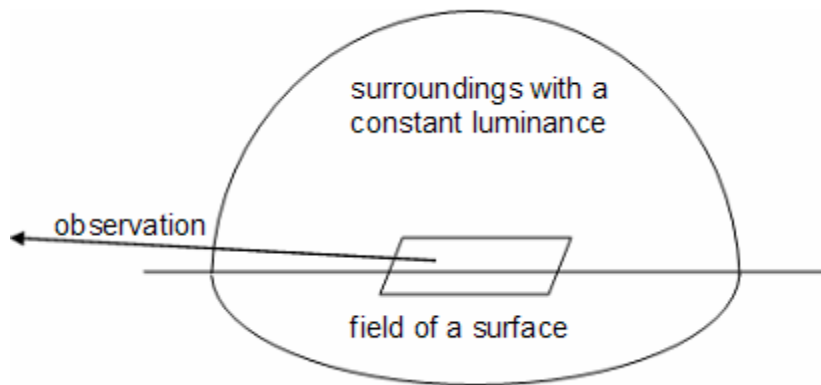


Figure 6: Q_d is the luminance coefficient in surroundings of a constant luminance.

Finally, the value of q values depends on "the degree of specularity" of the surface. This kind of dependence can be illustrated by means of four standard reflection tables N1, N2, N3 and N4 with increasing degrees of specularity. These tables are intended for use with road surfaces under road lighting, but are also applicable for road markings, and for daylight illumination of both road markings and road surfaces.

Figure 7 shows the variation of q with the side angle, when the of incidence is fixed at approximately 80° corresponding for instance to a low sun. It should be stated that the variation is less strong at lower angles of incidence, but of the same character as shown in figure 7.

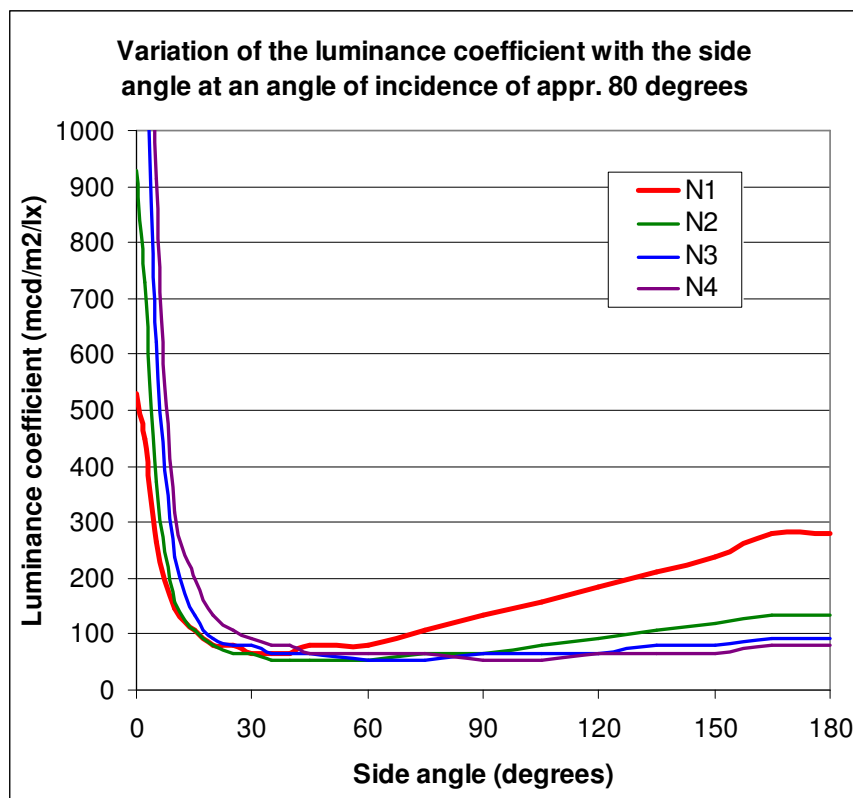


Figure 7: Variation of the luminance coefficient q with the side angle.

The side angle ranges from 0° , which is viewing against the sun, to 180° , which is viewing with the sun.

It is seen that the q value is very high, when viewing against the sun. This is caused by specular reflection in the surface, which gets stronger with less surface texture in the sequence N1, N2, N3 and N4.

The q value is also high, when viewing with the sun. The reason is that the parts of the texture that face the observer are also those that are illuminated. This feature gets stronger with more surface texture in the opposite sequence. For this reason, all the curves of figure 7 cross each other.

The question is if a road marking stands out with a positive contrast to the road surface, when its Q_d value is higher than for the road surface. In the annex A, it is concluded that this is the case when the road marking and the road surface has the same, or at least approximately the same degree of specularly, i.e. when they can be represented by the same N table.

If not, there is a reasonable certainty for a positive contrast in clouded daylight conditions (which has an approximately constant luminance), but not in direct sun.

Additionally, there is a reasonable certainty of a positive contrast under road lighting, when the road lighting has the character that it does not produce strong specular reflections in directions towards the drivers. Road lighting has this character in at least Denmark with the purpose of maintaining some uniformity of the road surface luminance in wet conditions. This applies probably for road lighting in all the Nordic countries.

The common method to provide this character of the lighting is to set the road lighting luminaires to direct the beams at a relatively large angle transverse to the road. Figure 8 shows a road lighting installation on a small traffic road.



Figure 8: A typical road lighting installation on a small traffic road.

In practice, Q_d is used as a characteristic for the reflection of road markings in daylight and under road lighting in EN 1436, refer to chapter 6.

Q_d could also be used as a characteristic for the reflection of road surfaces under road lighting, but this does not happen in practice.

It is noted that the above-mentioned features of reflection, when viewing against or with the light, are much stronger for illumination by vehicle headlamps, because the illumination is at grazing angles (the angle of incidence approaches 90°). This is discussed in the next chapter.

4. Reflection of road markings and road surfaces in the illumination by the drivers own headlamps

4.1 Introduction

The reflection in this type of illumination is measured by the coefficient of retroreflected luminance R_L . The R_L is defined for a field of a surface as the ratio between the luminance L of the field and the illuminance E at the field as measured on the plane perpendicular to the direction of illumination.

In principle, an R_L value can be measured by means of a luminance meter and a luxmeter as shown in figure 9. The figure illustrates the definition of the R_L , but it does not illustrate practical measurements. Such are done with specialized equipment.

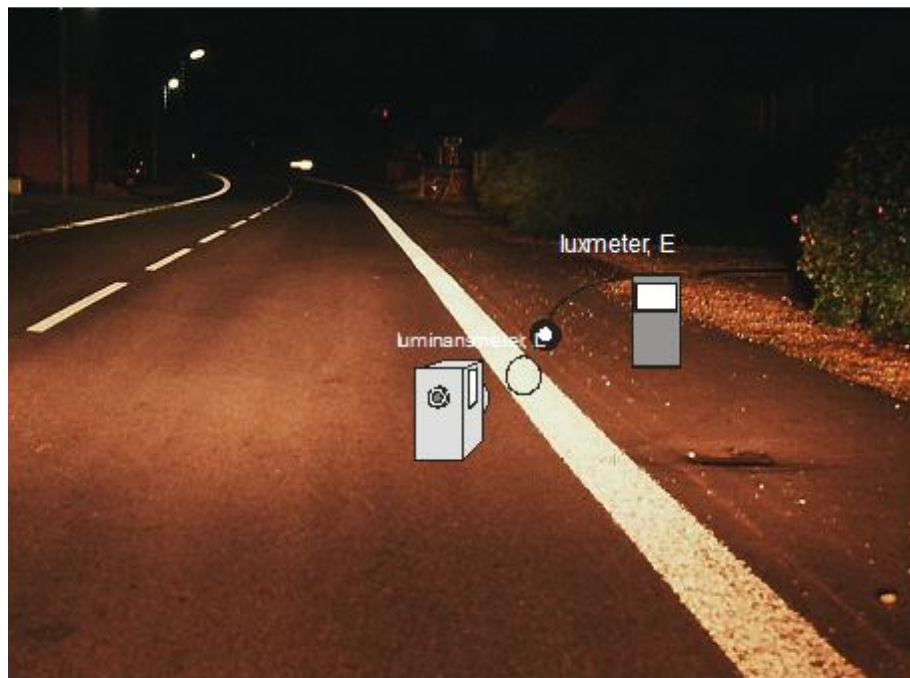


Figure 9: Measurement of the luminance L and the illuminance E entering $R_L = L/E$.

The definition of the R_L is very similar to the definition of the luminance coefficient q , and the unit is the same, $\text{mcd}\cdot\text{m}^{-2}\cdot\text{lx}^{-1}$. The only difference is that the illuminance is measured on the plane of the field for the luminance coefficient q , but perpendicular to the direction of illumination for the coefficient of retroreflected luminance R_L .

The illuminance on the plane of the field is a factor $\cos(v)$ smaller than the illuminance on the plane perpendicular to the direction of illumination. The angle v is the angle of incidence, refer to chapter 3 or annex X regarding the cosine law of illumination.

As the angle ν is close to 90° in relevant cases, $\cos(\nu)$ has a small value and therefore an R_L value could be expected to be numerically small. That is not the case, which shows that the reflection in this type of illumination is fairly strong.

This is discussed in annex B, where mathematical models are provided both for the reflection in the surface itself and for the contribution by glass beads.

These models were established and tested by measurements on panels of road markings and road surfaces cut out from roads in projects carried out by the NMF more than 25 years ago. The conclusion is that the models are sufficiently accurate for practical use. Refer to annex B for details.

The models are briefly accounted for in the following, because they are still not well known and still useful.

In accordance with the models, R_L values can be derived for the interesting range of geometrical situations, if one R_L value has been measured for a single geometrical situation – preferably a central one. This has had deep implications for the practical use of R_L values and for measuring equipment for the R_L .

The R_L is used as a characteristic for the reflection of road markings in vehicle headlamp illumination in EN 1436, refer to chapter 6.

4.2 Reflection in a surface

The mathematical model for reflection in the surface (excluding glass beads) is given by this expression:

$$R_L = 1000 \times \rho \times G \times T / \pi \quad (\text{mcd} \cdot \text{m}^{-2} \cdot \text{lx}^{-1})$$

where ρ is the reflectance of the illuminated parts of the surface

G is a geometrical factor

and T is a texture factor.

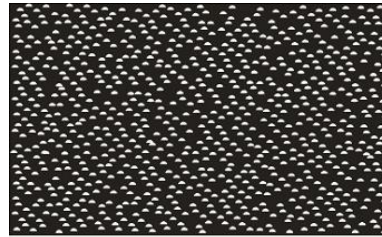
The factor of 1000 is due to the use of milli units ($\text{mcd} \cdot \text{m}^{-2} \cdot \text{lx}^{-1}$) instead of full units ($\text{cd} \cdot \text{m}^{-2} \cdot \text{lx}^{-1}$). The division by π is inherent in the definition of the R_L value. The reflectance ρ has a maximum value of 1.

The geometrical factor G is equal to $\sin(\epsilon)/\sin(\alpha)$, where ϵ is the angle of illumination and α is the angle of observation. These two angles are measured from the respective directions to the plane of the surface.

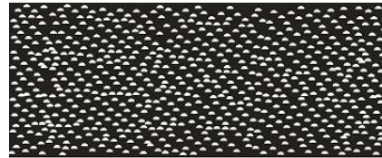
The significance of the factor G is illustrated in figure 10, which shows a field where facets or other parts of the texture are illuminated and stand out as small luminous areas. The illumination direction is fixed, while the field is observed from increasing heights so that the factor G changes as indicated. The small luminous areas remain the same, but the area of the dark background increases with increasing observation height. Because of this, the R_L value decreases in the proportions indicated by the values of G .

The dark background illustrated in figure 10 is at least partly made up of shadows cast by illuminated facets or other parts of the texture. Therefore, the geometrical factor may be considered to take account of shadows in the field as seen by the observer. This is easier to illustrate for a profiled road marking, refer to figure 11.

Observation height of 1,8 m; $G = 0,36$



Observation height of 1,2 m; $G = 0,54$



Observation height of 0,9 m; $G = 0,72$

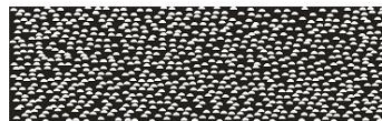


Figure 10: A field that is illuminated from a height of 0,65 m and observed from three different heights.

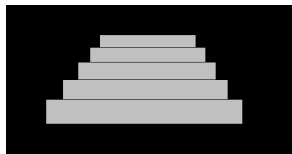


Figure 11: A profiled marking seen from the height of the headlamps (left) and from higher up (right).

Each illuminated facet or other illuminated part of the texture is illuminated with a certain angle of incidence v and, therefore, the illuminance is in proportion to $\cos(v)$ in accordance with the cosine law of illumination. The texture factor T may be considered to be the average for all these cosines.

The value of T has to be quite large in order to explain the typical R_L values of road surfaces and road markings without glass beads. This shows that the illumination, as it sweeps over the surface at a grazing angle, picks out those facets or other parts that have large inclinations and face the direction of illumination. Therefore, the texture factor can be thought as accounting for the proportion of the incoming light that falls on facets facing the direction of illumination with large inclinations.

As also accounted for in annex B, the value of T does not vary strongly with the angle of illumination ϵ within the relevant range. This means that the major variation is with the geometrical factor G , which depends on the vehicle geometry. There may be some variation with distance, but such variation is not systematic and not strong.

The model illustrates that a surface can contribute with a significant R_L value. Road surfaces mostly have R_L values in the range from 10 to 30 $\text{mcd}\cdot\text{m}^{-2}\cdot\text{lx}^{-1}$. Road marking surfaces (excluding the glass beads) normally have at least twice as much.

4.3 Reflection by glass beads

Figure 12 shows how glass beads act to enhance the reflection.

A ray of light enters the upper free part of the bead and is concentrated on a relatively small illuminated field on the road marking material at the back of the bead. Because of the concentration of light on the field, it gets a much higher luminance by reflection than it would have in direct illumination by the ray of light.

Observation occurs in a direction that is close to the direction of the ray of light and is concentrated on an observed field that almost coincides with the illuminated field. This gives the front of the bead a luminance that is almost as high as the luminance of the illuminated field.

The total action is as if the reflectance of the road marking material is amplified by a factor with a relatively high value. In annex B it is stated that the factor is approximately 9 for a glass bead made of ordinary glass with a refractive index of 1,55, when embedded 60 % of the diameter into the road marking material. It is also stated that the retroreflected beam is so wide, approximately $\pm 10^\circ$, that the factor does not vary much within relevant vehicle geometries and distances on the road.

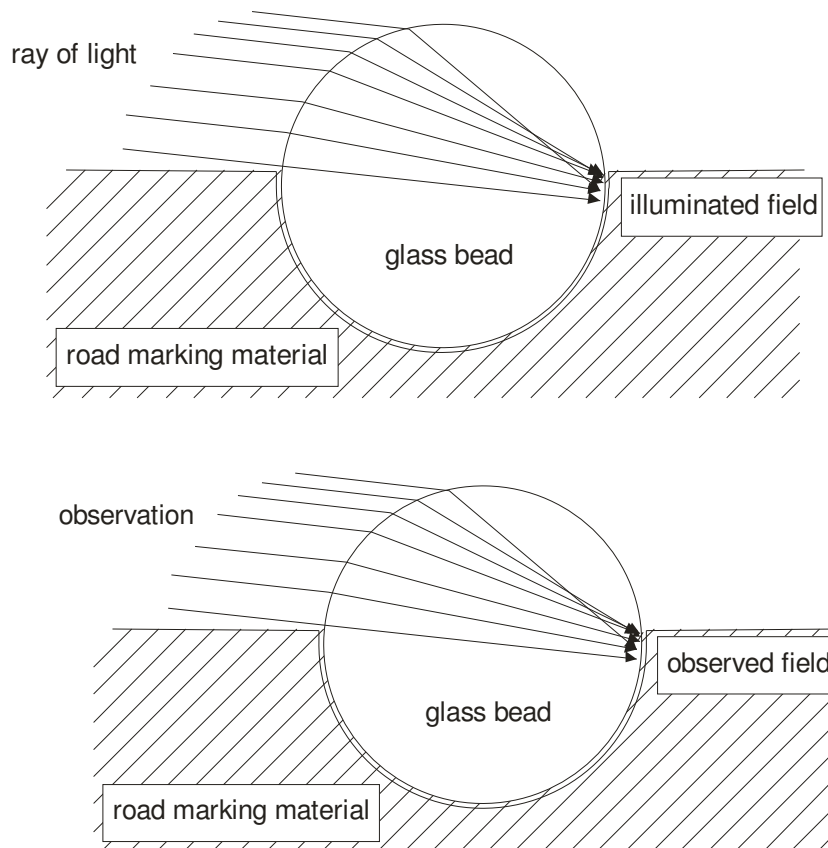


Figure 12: Illumination (top) and observation (bottom) through a glass bead.

The various conditions are discussed in annex B. However, it stands out that the factor of amplification is not very large and that the retroreflected beam is wide. The essential reason for that is that a glass bead does not act as a very good lens in these conditions.

Glass beaded retroreflective sheeting materials used for retroreflective road signs provide more favourable conditions for the glass beads and, therefore, much higher amplification factors and more narrow beams. This can make retroreflective signs stand out with a relatively high luminance that is even fairly constant over a range of distances, as if the signs are self luminous.

Glass beads in road markings do not act like that, they only provide a constant amplification of the reflection by the road marking material.

Because of that, the model presented in annex B for the glass beads is very similar to the model for surface reflection. The only change is that the texture factor T is replaced by the product of the amplification factor A and a bead distribution factor B:

$$R_L = 1000 \times \rho \times G \times A \times B / \pi \quad (\text{mcd} \cdot \text{m}^{-2} \cdot \text{lx}^{-1})$$

where ρ is the reflectance of the road marking material
 G is the geometrical factor equal to $\sin(\epsilon)/\sin(\alpha)$
 A is the amplification factor
and B is the bead distribution factor.

The bead distribution factor accounts for the fraction of the incoming light that falls on glass beads. It may vary some with the illumination angle ϵ , but at least for worn road markings it is relatively constant.

Newly applied road markings with ordinary drop-on beads have R_L values up to approximately $400 \text{ mcd} \cdot \text{m}^{-2} \cdot \text{lx}^{-1}$. This is in good agreement with the model, although in theory values could be somewhat higher. Some tapes, in particular tapes with glass beads of a higher refractive index, can have R_L values up to approximately $800 \text{ mcd} \cdot \text{m}^{-2} \cdot \text{lx}^{-1}$.

When the R_L value is high, it has to be assumed that there are numerous glass beads in the surface and that these catch most of the incoming light. If so, there is less light available for surface reflection which, therefore, is weak.

However, older road markings generally have less glass beads in the surface and often have R_L values of about $100 \text{ mcd} \cdot \text{m}^{-2} \cdot \text{lx}^{-1}$. It is reasonable to assume that the surface reflection and the remaining glass beads contribute roughly equally.

4.4 Wet conditions

The R_L value of most road markings drops to a few units or virtually 0, when the road markings become wet.

The reason for this is that a film of water covers the surface texture and also glass beads in the surface. Figure 13 shows an incoming direction on a road marking surface, which is covered by a water film. Reflection in the water film is strong because of the grazing angle of the direction and, therefore, transmission is weak. The water film acts on both the directions, of illumination and observation, and therefore reduces the R_L value strongly. Additionally, the water film disturbs the focus of the glass beads.

Only road markings with profiles, structure, large glass beads or other special means maintain some R_L values in wet conditions.

Figure 14 shows an incoming direction that hits the front side of a profile. The side may also be covered by the water film, but the direction is directly on and will be transmitted. This provides at least some surface reflection in wet conditions. R_L values as low as 25, 35 and $50 \text{ mcd} \cdot \text{m}^{-2} \cdot \text{lx}^{-1}$ are worthwhile.

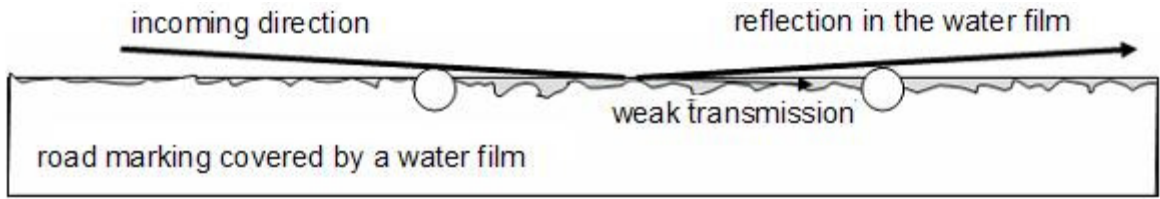


Figure 13: An incoming direction of a road marking surface covered by a water film.

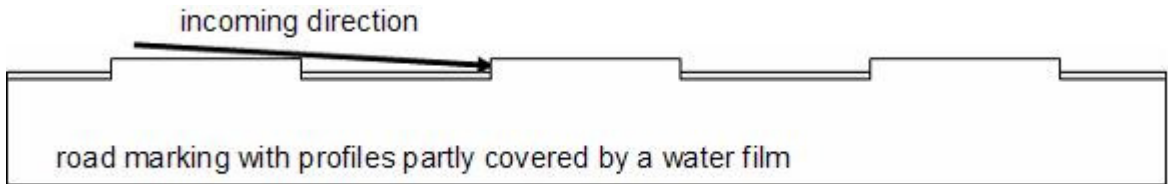


Figure 14: An incoming direction on the front side of a profile.

As an illustration, figure 15 shows road markings at a road trial site in the dry condition and during a light rain. In the last-mentioned situation, only the profiled road markings are clearly visible. Figures 16 and 17 show some of the profiled road markings at the site.



Figure 15: Road markings at a road trial site in the dry condition (top) and during a light rain (bottom).

Figure 16:
An early type of profiled road marking.

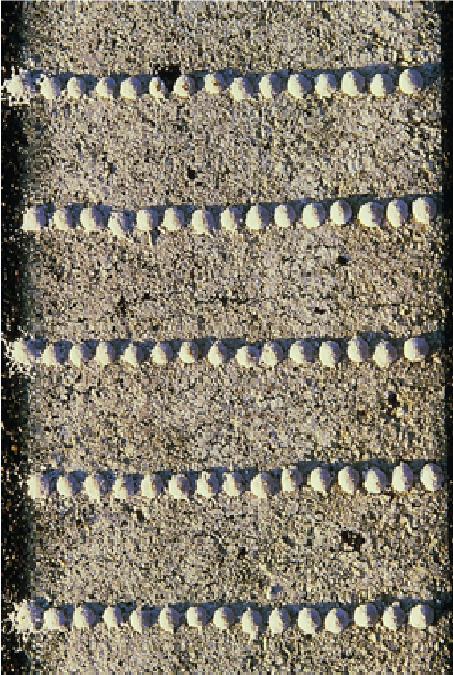


Figure 17: A popular type of profiled road marking.

5. Reflection of road markings and road surfaces in the illumination by opposing headlamps

Drivers are familiar with specular reflections caused by the headlamps of opposing vehicles, and by other low mounted light sources in the road environment. The specular reflections are particularly strong in wet conditions and take the appearance of longish patterns of light stretching in the direction from the light source towards the observer. See the example in figure 18.



Figure 18: A road crossing at night in a wet condition.

This kind of reflection has been studied first in a project organised by the NMF and later in a Nordic project organised in a different organisation.

Specular reflection can be characterised by the R_L value introduced in the previous chapter, in spite that the name of this characteristic “coefficient of retroreflected luminance” is not very suitable.

It is possible to construct a simple formula for the R_L value produced by specular reflection. This formula has been tested by measurements on road surface panels with the conclusion that the factors entering the formula behave in a surprisingly simple manner. It seems that R_L values can be derived for the interesting range of geometrical situations, when one R_L value has been measured for a single geometrical situation – preferably a central one.

Based on this, a portable instrument designed to measure the R_L of retroreflection was converted to measure the R_L of specular reflection. This instrument was used to measure a range of different road surfaces in the Nordic countries.

It was concluded that, at least for wet conditions, specular reflections of opposing headlamps can easily make it difficult to see road markings. Other light sources in the environment may well be able to do the same. Additionally, specular reflections can add so much to the visual complexity that drivers may find it difficult to interpret complex road scenes such as at road crossings and road works.

The R_L for specular reflection has not been included in any standard or national regulation. Refer to annex C for details.

6. Road marking performance characteristics, classes of performance and measuring methods

6.1 Introduction

EN 1436 “Road marking materials – Road marking performance for road users” defines the following performance characteristics for road markings:

- the luminance coefficient under diffuse illumination Q_d
- the luminance factor β
- the coefficient of retroreflected luminance R_L
- the x, y chromaticity co-ordinates
- the skid resistance.

EN 1436 also establishes classes of performance for these characteristics and provides measuring methods.

Additionally, EN 1436 provides some advice on which classes apply for white and yellow road markings, and which to apply for road markings on asphalt and cement concrete road surfaces. In practice, national tender specifications indicate the classes to apply in specific cases.

These performance characteristics are considered in the following.

6.2 The luminance coefficient under diffuse illumination Q_d

The luminance coefficient under diffuse illumination Q_d is used in EN 1436 to represent reflection in daylight or under road lighting. The Q_d has already been introduced in chapter 3, where its application for these purposes has been discussed as well.

The Q_d value is to be measured for a 30 m geometry, which is defined by an observation angle α of $2,29^\circ$, a combined spectral response corresponding to the $V(\lambda)$ distribution (the standard spectral sensitivity of the eye) and the CIE illuminant D65 (corresponds to daylight). Additionally, there is a number of requirements regarding measured field, angular aperture of measurements, quality of approximation to diffuse illumination etc.

The performance classes are those of table 5.

Table 5: Performance classes for the Q_d .

Class	Requirement
Q0	No requirement
Q1	$Q_d \geq 80 \text{ mcd}\cdot\text{m}^{-2}\cdot\text{lx}^{-1}$
Q2	$Q_d \geq 100 \text{ mcd}\cdot\text{m}^{-2}\cdot\text{lx}^{-1}$
Q3	$Q_d \geq 130 \text{ mcd}\cdot\text{m}^{-2}\cdot\text{lx}^{-1}$
Q4	$Q_d \geq 160 \text{ mcd}\cdot\text{m}^{-2}\cdot\text{lx}^{-1}$
Q5	$Q_d \geq 200 \text{ mcd}\cdot\text{m}^{-2}\cdot\text{lx}^{-1}$

The theoretical maximum Q_d value is $1000/\pi = 318 \text{ mcd}\cdot\text{m}^{-2}\cdot\text{lx}^{-1}$. In comparison to the classes of table 5, most road surfaces have Q_d values in the range of 50 to $100 \text{ mcd}\cdot\text{m}^{-2}\cdot\text{lx}^{-1}$.

NOTE: The performance classes apply only for the dry condition. Q_d values are generally higher for wet conditions than for the dry condition due to an increase in specular reflection. This applies for road surfaces as well as for road markings.

The measurement of Q_d is discussed in detail in annex E, and considered briefly in the following.

The first handheld reflectometer for the measurement of Qd was the Qd30 shown in figure 19. It appeared in the mid 1990's and several are still in use.



Figure 19:
A Qd30 in use at a road trial site.

The Qd30 was later displaced from the market by “combination instruments” that are primarily retroreflectometers for the measurement of the R_L , but with secondary illumination systems for the combined measurement of the two characteristics.

It is stated in annex E that the Qd30 meets all the relevant requirements including good repeatability and reproducibility and traceable calibration. In practice, the Qd30 has become the reference instrument.

It is also stated in annex E that this is not the case for the Qd function of the combination instruments, which do not meet the fundamental requirement of providing diffuse illumination due to truncation of the illumination systems. Calibration is probably possible only by comparison to the remaining Qd30's in use.

Finally, it is stated in annex E that it is impossible to develop vehicle based measurement of the Qd.

6.3 The luminance factor β

The luminance factor β is used in EN 1436 to represent reflection in daylight or under road lighting as an alternative to Qd.

The luminance factor β is measured using standard illuminant D65 (corresponds to daylight) defined in ISO 10526. The geometry is the $45^\circ/0^\circ$, which implies illumination at $(45 \pm 5)^\circ$ and measurement at $(0 \pm 10)^\circ$. The angles are measured relative to the normal to the road marking surface.

The performance classes are those of table 6.

Table 6: Performance classes for the luminance factor β .

Class	requirement
B0	No requirement
B1	$\beta \geq 0,20$
B2	$\beta \geq 0,30$
B3	$\beta \geq 0,40$
B4	$\beta \geq 0,50$
B5	$\beta \geq 0,60$

NOTE: The performance classes apply only for the dry condition.

There is no real theoretical maximum value of β , but in practice the value of 1 is considered to be the maximum.

The luminance factor β is measured with small handheld instruments that also measure the chromaticity coordinates x and y . There are several suppliers of such instruments; their accuracy is generally considered to be sufficient.

6.4 The coefficient of retroreflected luminance R_L

The coefficient of retroreflected luminance R_L is used in EN 1436 to represent the retroreflection under vehicle headlamp illumination. The R_L has already been introduced in chapter 4, where its application for these purposes has been discussed as well.

The R_L value is to be measured for a 30 m geometry, which is defined by an illumination angle ϵ of $1,24^\circ$, an observation angle α of $2,29^\circ$, a combined spectral response corresponding to the $V(\lambda)$ distribution (the standard spectral sensitivity of the eye) and the CIE illuminant A (corresponds to headlamp illumination) and a number of requirements regarding the fields of illumination and measurement, angular apertures, etc.

The performance classes for the dry condition are those of table 7.

Table 7: Performance classes for the R_L of dry road markings.

Class	requirement
R0	No requirement
R1	$R_L \geq 80 \text{ mcd} \cdot \text{m}^{-2} \cdot \text{lx}^{-1}$
R2	$R_L \geq 100 \text{ mcd} \cdot \text{m}^{-2} \cdot \text{lx}^{-1}$
R3	$R_L \geq 150 \text{ mcd} \cdot \text{m}^{-2} \cdot \text{lx}^{-1}$
R4	$R_L \geq 200 \text{ mcd} \cdot \text{m}^{-2} \cdot \text{lx}^{-1}$
R5	$R_L \geq 300 \text{ mcd} \cdot \text{m}^{-2} \cdot \text{lx}^{-1}$

There are additional performance classes for road markings during wetness and during rain.

Wetness is obtained 1 min after flooding the surface with water poured from a bucket in a specified manner. The performance classes for road markings during wetness are those of table 8.

The condition during rain is obtained with a specified spray from jets. This condition is not used much in practice and is not considered further.

Table 8: Performance classes for the R_L of road markings during wetness.

Class	requirement
RW0	No requirement
RW1	$R_L \geq 25 \text{ mcd} \cdot \text{m}^{-2} \cdot \text{lx}^{-1}$
RW2	$R_L \geq 35 \text{ mcd} \cdot \text{m}^{-2} \cdot \text{lx}^{-1}$
RW3	$R_L \geq 50 \text{ mcd} \cdot \text{m}^{-2} \cdot \text{lx}^{-1}$
RW4	$R_L \geq 75 \text{ mcd} \cdot \text{m}^{-2} \cdot \text{lx}^{-1}$
RW5	$R_L \geq 150 \text{ mcd} \cdot \text{m}^{-2} \cdot \text{lx}^{-1}$

The measurement of the R_L is discussed in detail in annex D.

The LTL 800 appeared in the early 1980's. It was not the first handheld retroreflectometer for the measurement of R_L , but it was the first that supplied repeatable and reproducible measurements with easy and traceable calibration. This was achieved by the use of suitable optical principles as accounted for in annex D. A picture is shown in figure 20.



Figure 20: An LTL 800 in use at a road trial site.

A later version based on the same optical principles, called the LTL 2000, achieved the status of being the reference instrument. The LTL 2000 has itself been replaced by new versions called LTL-X and LTL-XL. One of these, the LTL-XL is a combination instrument that measures the Q_d in addition to the R_L , refer to the previous section. Some competing instruments by other producers are on the market as well. Refer to annex D for more details.

In total, the handheld retroreflectometers have spurred developments and practical applications in the road marking area. However, attention must be turned to vehicle based retroreflectometers.

Some older types of vehicle based retroreflectometers are also discussed in annex D, where it is pointed out that they have not demonstrated sufficient accuracy.

Additionally, a new development, the LTL-M is discussed. This instrument works by means of a digital camera, and has so much feed-back and so much detail of the images, that the qualities of the handheld retroreflectometers are re-established in mobile measurements.

Accordingly, the accuracy of the LTL-M is much improved compared to the older types of vehicle based retroreflectometers. The real accuracy is difficult to establish, but may be as good as for handheld retroreflectometers.

In the long run, mobile retroreflectometers with properties like the LTL-M may become accepted as reference instruments. If so, this could spur a further development in the road marking field.

6.5 The x, y chromaticity co-ordinates

The x, y chromaticity co-ordinates are measured in the same conditions as the luminance factor β and actually by instruments that incorporate simultaneous measurement of β , x and y.

The permissible colour boxes are shown in figure 21. Yellow 2 is the more limiting colour box and is intended for new road markings, while yellow 1 is the more permissible colour box and is intended for road markings during functional life.

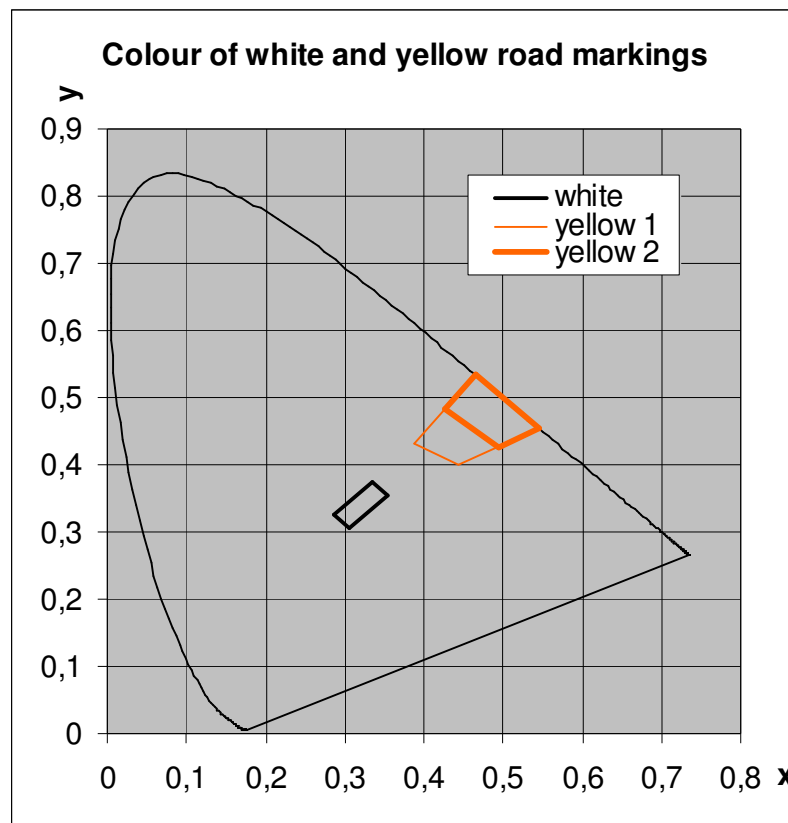


Figure 21:
Colour boxes for
white and yellow
road markings.

6.6 Skid resistance

Skid resistance is measured by means of the pendulum skid resistance tester in SRT units. SRT refers back to the skid resistance tester that is specified by the geometry of the pendulum, specifications for the rubber of

the slider, the watering method and other details. Accordingly, this characteristic is really defined by the measurement method itself.

The performance classes for skid resistance are those of table 9.

Table 9: Performance classes for the skid resistance.

Class	requirement
S0	No requirement
S1	SRT ≥ 45
S2	SRT ≥ 50
S3	SRT ≥ 55
S4	SRT ≥ 60
S5	SRT ≥ 65

The skid resistance tester is awkward in use, refer to the photo in figure 22 and, therefore, there has been attempts to replace it with more convenient instruments. These attempts have not been successful in practice yet.



Figure 22:
Use of the skid resistance tester
at a road trial site.

7. The visibility of road markings

7.1 Introduction and summary

The principles of visibility of road markings in headlamp illumination are explained in 7.2. On the basis of the assumption that conditions are in Ricco's domain at the low lighting levels in headlamp illumination, it is derived that the stimulus for seeing a longitudinal road marking at a particular distance is given by:

$$S = W \times (R_L(\text{road marking}) - R_L(\text{road surface})) \times I / D^4$$

where S is the stimulus

W is the effective road marking width *)

$R_L(\text{road marking})$ is the R_L value of the road marking

$R_L(\text{road surface})$ is the R_L value of the surrounding road surface

I is the total luminous intensity of the headlamps

and D is the distance.

*) The effective width of a broken line is the width of a continuous line with the same surface area.

Whenever the stimulus exceeds a threshold value at a distance, the road marking can be seen at that particular distance.

As accounted for in annex F, this has been one of the scopes of COST Action 331 "Requirements for road markings".

Actual tests of visibility distances confirm the above-mentioned influence of the factors and the distance. A general visibility model found in the literature provides the same conclusion.

This visibility model is useful, as it extends the applications to include factors like the age of the driver and glare from for instance headlamps of oncoming vehicles. Therefore, a freeware program Visibility was developed as a supplement to the COST action based on the visibility model. The program offers the choice among three vehicle geometries and realistic headlamp light distributions as obtained from the literature.

This program offers easy calculation of visibility distances to road markings in a large range of conditions. Input R_L values are those for the 30 m geometry, but these are internally converted to the different vehicles and road situations in accordance with the principles of chapter 4.

An additional scope of the COST Action 331 is the need for visibility distance to longitudinal road markings. Based on tests at the VTI driving simulator, it was concluded that a preview time of 1,8 seconds is the absolute minimum for safe driving, while a preview time of 3 seconds allows driving in some comfort.

Preview time is the time it takes to drive the distance at which the road marking is visible. If too short, it is a difficult and exhausting task for the driver to keep the vehicle within the driving lane. If comfortably long, the driver can find a convenient course through curves and has time for other tasks like looking in the rear view mirror. The Visibility program also provides the preview time at an input driving speed.

Calculations show that even fairly poor road markings (low R_L value and/or small effective width) mostly offer a sufficient preview time, when conditions are good. The road markings have, on the other hand, to be fairly good (higher R_L value and/or larger effective width), when conditions are adverse such as for older drivers, dirty headlamps and glare from opposing vehicles on narrow roads. Refer to the COST Action 331 report. It is also possible to test the conditions by means of the Visibility program.

The most adverse case is the one of wetness, where the R_L values of most road markings fall to very low values. Only road markings with profile or other means to maintain retroreflection in wet conditions will provide some R_L value during wetness. Refer to chapters 4 and 6.

The principles of visibility of road markings in daylight and under road lighting are explained in 7.3. On the basis of the assumption that conditions are in Weber's domain at the high lighting levels in daylight, it is derived that the stimulus for seeing a longitudinal road marking at a particular distance is primarily the contrast of the road marking to the surrounding road surface.

If the contrast is below a small critical value, the road marking is hardly visible at all. However, the visibility distance increases quickly with the contrast, and will in most circumstances be hundreds of metres.

There is an additional influence of the effective road marking width, refer to 7.3.

At the luminance levels obtained by road lighting of traffic roads, several factors influence the visibility of road markings; the actual luminance level, the contrast and the effective road marking width. Illumination by the headlamps improves the visibility somewhat by raising both the luminance level and the contrast. The visibility distances will normally be at least adequate.

It is mentioned that poor visibility can occur in some lighting situations, in particular when the road surface is more shiny than the road markings,

The Visibility program also includes "diffuse illumination" and surface properties described by the Q_d value in diffuse illumination. This extends the applications of the program to daylight and road lighting.

There is no real verification of this application in the tests described in the COST Action 331. However, the extension is a natural implementation of the visibility model for all luminance levels and can be expected to be sufficiently accurate for practical applications.

7.2 Principles of the visibility of road markings in headlamp illumination

Figure 23 shows a background and an object on the uniform background.

The background causes a certain illuminance on the eyes of an observer, while the object causes an additional illumination on the eyes of the observer (additional to what the background alone would have caused).

At the low levels of luminance in headlamp illumination, Ricco's domain of visibility applies. This means that the above-mentioned additional illumination is the stimulus for the visibility of the object. Whenever the stimulus exceeds a certain threshold, the object is visible, else it is not. The threshold itself depends on the visual ability of the observer.

A longitudinal road marking that extends from a distance D and onwards would look like shown in figure 24, when seen by the driver of a vehicle and illuminated by the headlamps of the vehicle.

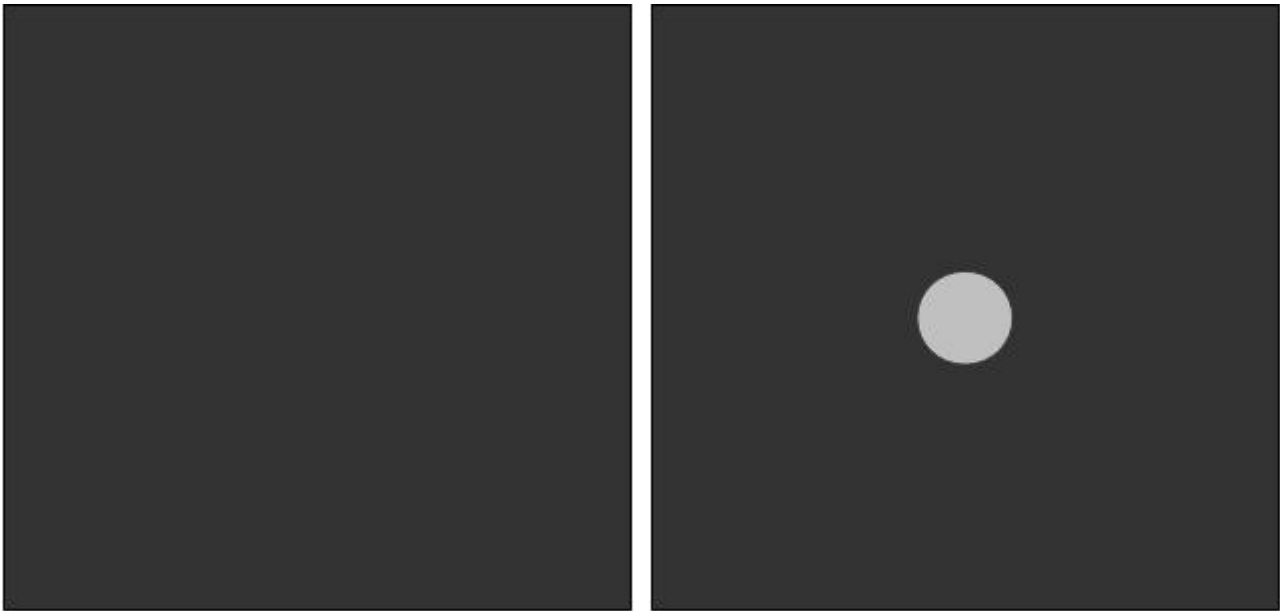


Figure 23: A background (left) and the background with an object (right).

Figure 24: A longitudinal road marking when seen by the driver of a vehicle and illuminated by the headlamps of the vehicle.



It is obviously possible to compute the stimulus provoked by such a longitudinal road marking. It turns out to be in proportion with the product of three factors:

- the effective road marking width
- the R_L value of the road marking minus the R_L value of the road surface
- the total luminous intensity of the headlamps.

For a continuous line, the effective width equals the actual road marking width. However, for a broken line, the effective width is reduced compared to the actual width as shown in figure 25.



Figure 25: The effective width of a broken line (top) is the width of a continuous line with the same surface area (bottom).

The stimulus is also in inverse proportion to the distance D to the road marking to the power of 4. i.e.: to D^4 . This is a strong dependence of distance as illustrated in figure 26.



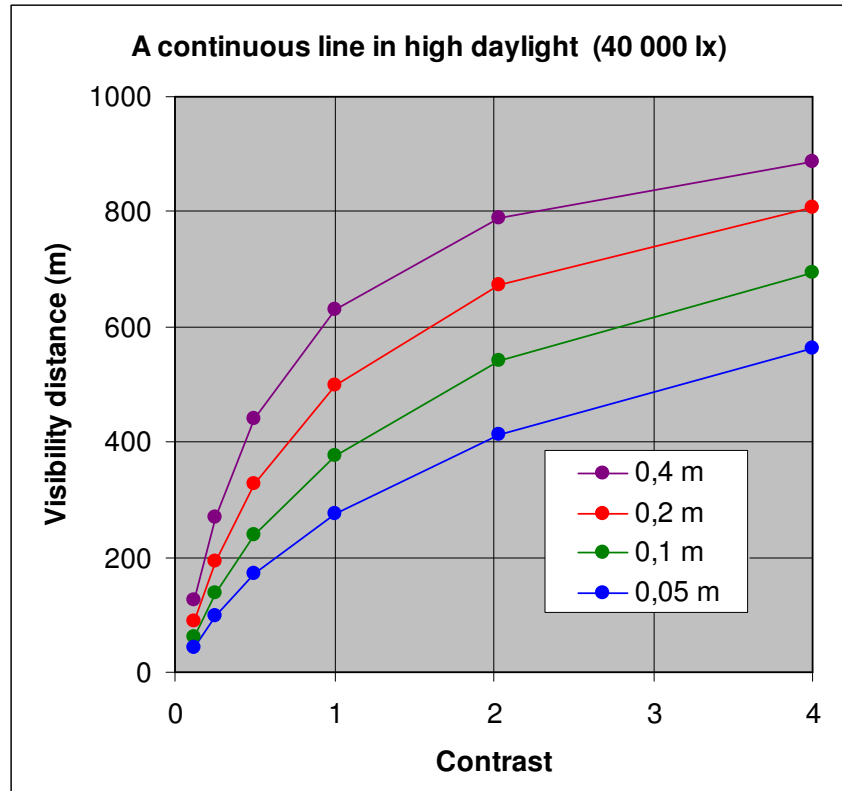
Figure 26: Both luminance and apparent size decrease with distance to a line and, therefore, visibility decreases strongly with distance.

7.3 Principles of the visibility of road markings in daylight and under road lighting

In the high luminance levels in daylight, visibility is in the Weber's domain, where the contrast of a road marking to the surrounding road surface is important. There is some additional influence of the effective road marking width and a small influence of the actual luminance level.

The contrast is measured as $C = (L(\text{road marking}) - L(\text{road surface}) / L(\text{road surface}))$. If the contrast is high, say 1 or more, visibility distances are long, hundreds of metres. If the contrast is low, the visibility distances decrease rapidly with the contrast and approach 0 at a low critical contrast of approximately 0,1. See the diagram in figure 27.

Figure 27:
Variation of the visibility distance with contrast and effective road marking width.



Contrasts estimated by means of Qd values by $C = (Qd(\text{road marking}) - Qd(\text{road surface}) / Qd(\text{road surface}))$ are mostly about 1 or higher. Such estimation leads to the prediction of long visibility distances.

The critical cases are, therefore, when the contrast cannot be evaluated on the basis of the Qd values, for instance when driving against the sun and the road surface is more shiny than the road marking.

In the lower luminance levels of road lighting, typically with an average road surface luminance of 0,5 to 1,5 cd/m^2 , visibility is in neither of the two domains of Ricco and Weber, but somewhere in between. All parameters, including the actual luminance level, influence the visibility of road markings. Illumination by the headlamps of the vehicle improves conditions by raising both the luminance level and the contrast of the road markings.

The visibility distances are normally acceptable, except at locations with a strong specular illumination when the road surface is more shiny than the road marking.

Refer to chapter 3 regarding when contrast can be evaluated on the basis of Qd values.

Literature

Night Traffic Report No. 4 "Reflection properties of road surfaces in headlight illumination", 1982

Night Traffic Report No. 6 "Reflection properties of road markings in headlight illumination", 1983

Influence of pavement marking angular systems on visibility predictions using computer models, Zwahlen, H T; Schnell, T ; Johnson, N ; Hodson, N ; Donahue, T, Transportation Research Record No. 1754, Traffic Control Devices, Visibility, and Rail-Highway Grade Crossings 2001

CIE 54.2 Retroreflection: Definition and measurement, 2001

Annex A: Reflection of road markings and road surfaces under road lighting or in daylight

A.1 Introduction and summary

The reflection of a surface is generally described by the luminance coefficient, which is defined as the luminance of a field of the surface, as produced by illumination and reflection, divided by the illuminance on the plane of the surface at the field.

As luminance is measured in $\text{cd}\cdot\text{m}^{-2}$ and illuminance in lx , the unit of the luminance coefficient is $\text{cd}\cdot\text{m}^{-2}\cdot\text{lx}^{-1}$. However, in order to obtain convenient numerical values the one thousand times smaller unit of $\text{mcd}\cdot\text{m}^{-2}\cdot\text{lx}^{-1}$ is used in this annex.

The value of a luminance coefficient depends in general on the geometry of illumination and observation (measurement).

Standard road reflection tables are introduced in A.2. These provide values of the luminance coefficient that are tabulated for two angles that define the geometry of illumination. The geometry of observation is defined by standard values of two additional angles. It is explained that these standard values normally cover situations that are interesting for traffic situations and, therefore, need not be varied.

A set of standard road reflection tables, the N-tables, are used to explain those variations with the illumination direction that normally occurs for road surfaces. It is mentioned that the same variation occurs for road markings. It is shown that the variations are caused by a mixture of specular surface reflection and ordinary reflection. Surface reflection is strong in situations corresponding to driving against the sun. Ordinary reflection, on the other hand, is strong in situations corresponding to driving with the sun in the back.

The above-mentioned types of reflection are strong enough to be evident in the standard tables, but they are even stronger for illumination by headlamps. Enhanced ordinary reflection is further considered in annex B, where it is called retroreflection, while specular reflection is considered in annex C.

A road reflection table provides a mapping of the reflection properties of a surface. However, as described in A.3, two parameters are used to characterise the reflection. The two parameters are the average luminance coefficient Q_0 , which measures the level of reflection, and the specular factor S_1 , which measures the degree of specular reflection.

It is explained that it was attempted during the 1970's and early 1980's to develop practical in situ equipment for the measurement of the two parameters. However, these attempts were not successful for the reason that the parameters are difficult to measure within the small space of a portable instrument. This applies in particular for the Q_0 . In this sense the choice of the parameters was unfortunate.

In fact, there is a lack of means to test the road surfaces, but in spite of that all the concepts of standard road reflection tables are still being applied in the design of road lighting installations.

As accounted for in A.4, an alternative to Q_0 , the luminance coefficient under diffuse illumination Q_d , was introduced during the 1990's. The Q_d is intended to characterise the reflection of road markings in daylight or under road lighting. Portable instruments are available and are being used in numbers for road markings, and could be used for road surfaces as well. However, no portable instrument is available for the measurement of the specular factor.

Some aspects of Q_d are considered in A.5, in particular that this parameter does include specular reflection, but not to the degree shown by Q_0 . The luminance factor of the surface is mentioned as the alternative in EN 1436 "Road marking materials – Road marking performance for road users".

Qd is a useful measure of reflection of a surface, when the luminance of the surface can be represented to a reasonable approximation by the product of the Qd value and the illuminance.

Even when this is not the case, Qd can still be useful, when the contrast of a road marking to a road surfaces can be represented by the Qd values of the two surfaces. Contrast is relevant for the visibility of road markings.

These matters are considered in A.6 for road lighting by means of an example of a road lighting installation. Distinction is made between a type of road lighting used in the Nordic countries with little illumination in specular directions, and a type of road lighting used in other parts of Europe with more illumination in specular directions. It is concluded that Qd is a good measure of reflection and a reasonably good measure of the contrast between a road marking and the surrounding road surface for the Nordic type of road lighting; but not for the European type.

The matters are considered in A.7 for daylight. It is concluded that Qd is a good measure of contrast in some daylight conditions, but not all. The classic example of driving with or against the sun illustrates this.

The overall conclusion is that standard road reflection tables are still being used in road lighting in spite of many years having passed without any real possibility of measuring the road surface reflection properties. In situ measurement of the characteristic parameters is not available. Even laboratory measurements that were used to form the basis during the 1970's and the early 1980's are hardly available.

One of these characteristic parameters, Q0 could be replaced by Qd for which portable instruments have been made available for use for road markings. Qd is used for road markings, not because it is perfect, but because it is better than the above-mentioned alternative. The measurement of Qd is considered in annex E.

However, it seems that there is little interest in measuring the Qd values of road surfaces in connection with road lighting and probably little interest in testing road surface reflection properties at all. Else laboratory measurements would still have been available.

The explanation is probably that it is unpractical to adapt road lighting installations to individual and changing road reflection properties. All countries have developed some standard assumptions regarding road reflection properties and use those in general for the design of lighting installations. In Denmark, N2 is used with a Qd of $78 \text{ mcd}\cdot\text{m}^{-2}\cdot\text{lx}^{-1}$ (adapted from a Q0 of $90 \text{ mcd}\cdot\text{m}^{-2}\cdot\text{lx}^{-1}$) for the dry condition and W4 for the wet condition. The Qd value is backed up by tender specifications for aggregates used for road surfaces on roads with road lighting.

In this way, the design of road lighting installations is based on assumptions that are practical, but not necessarily accurate at least not backed by updated measurements.

A.2 Standard road reflection tables

Road lighting on traffic roads is generally designed on the basis of the luminance of the road surface in detailed calculations involving the reflection properties of the road surface.

To this purpose some standard road reflection tables are used. One set of such tables was derived on the basis of a collection of hundreds of reflection tables measured at the Danish Illuminating Engineering laboratory, now part of DELTA Light & Optics, during the 1970's and early 1980's.

These tables are labelled N1, N2, N3 and N4 in a sequence that represents a gradual change of the properties.

There are other sets of standard tables in use. R1, R2, R3 and R4 are similar to N1, N2, N3 and N4. C1 and C2 form a reduced set. W1, W2, W3 and W4 correspond to wet or humid road surfaces. Refer to CIE 144 “Road surface and road marking reflection characteristics” for details. However, only the N tables are used in the following in order to illustrate the variation of the reflection with the geometrical conditions.

A reflection table contains in principle the values of the luminance coefficient q for particular directions of illumination. The luminance coefficient q is the ratio between the luminance of a field of a surface and the illuminance at the field measured on the plane of the surface. The unit of the luminance coefficient is $\text{cd}\cdot\text{m}^{-2}\cdot\text{lx}^{-1}$, but in order to obtain convenient values the 1000 times smaller unit of $\text{mcd}\cdot\text{m}^{-2}\cdot\text{lx}^{-1}$ is used in the following.

An illumination direction is given by two angles as illustrated in figure A.1. The figure assumes illumination by the sun, but the illumination can in principle be any other light source.

A side angle defines the vertical plane that contains the direction of illumination, while a zenith angle defines the direction within that plane. All directions in the upper hemisphere are defined by side angle values from 0° to 180° and zenith angle values from 0° to 90° .

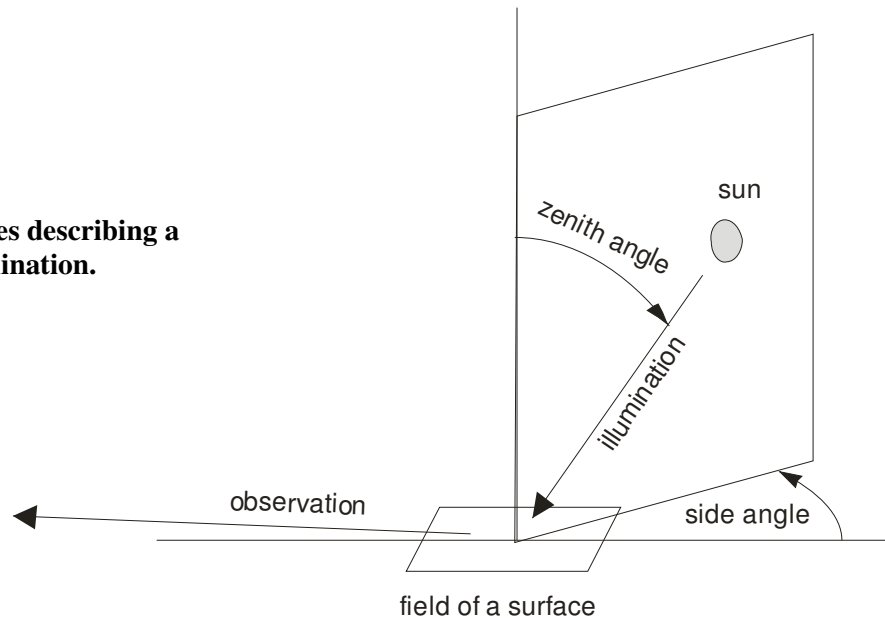


Figure A.1: Angles describing a direction of illumination.

NOTE: In reflection tables, these angles are labelled respectively the angle of incidence γ and the azimuthal angle β . The tables provide values of a reduced luminance coefficient $r = q \times \cos^3 \gamma$ so that values of q can be derived by $q = r / \cos^3 \gamma$.

Figure A.2 shows diagrams for the luminance coefficient values. There is one diagram for each of the tables N1, N2, N3 and N4 and each contains curves for zenith angles of 0° , 45° and 79° . Each of the curves shows the luminance coefficient as a function of the side angle.

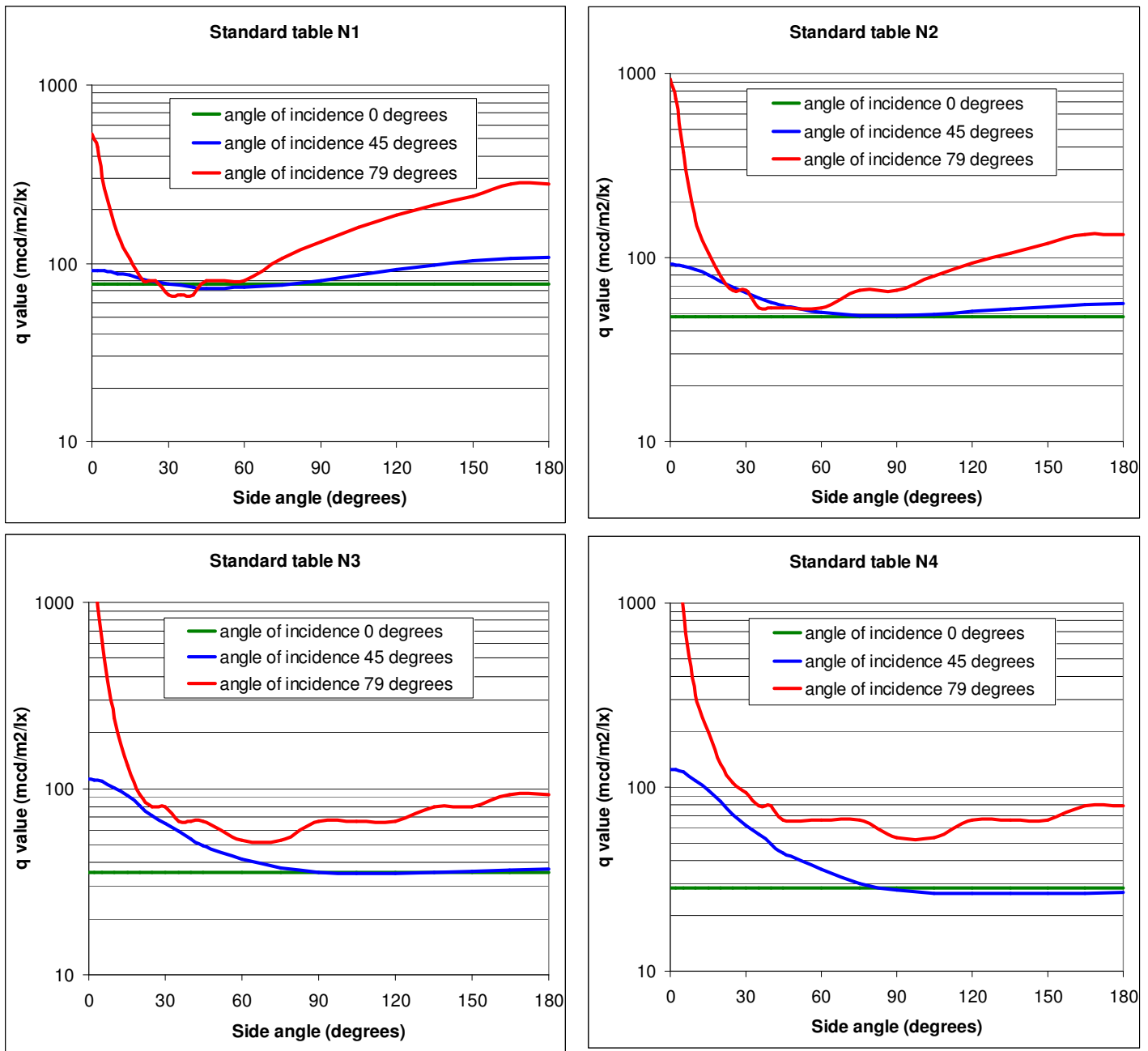


Figure A.2: Curves of the luminance coefficient q for the tables N1, N2, N3 and N4.

For a zenith angle of 0° , the curves are constant. The explanation for this is the simple one that the sun remains at zenith regardless of the side angle and therefore the illumination direction does not change with the side angle.

For zenith angles of 45° and in particular of 79° , the luminance coefficient shows significant variation with the side angle. It is a particular feature that the luminance coefficient is high when the side angle is small. A small side angle means that the sun is in front of the viewing direction and corresponds to driving against the sun. The explanation for this feature is surface reflection in the top parts of the road surface. This feature is called specular reflection in CIE 144 and other publications on the reflection properties of road surfaces.

The specular reflection becomes stronger for the N-series of tables in the sequence N1, N2, N3 and N4. In accordance with that, the tables are distinguished by an increasing “degrees of specularity”.

The specular reflection gets stronger the closer the direction of illumination gets to the plane of the surface. The extreme case is the specular reflection caused by headlamps on opposing vehicles. This type of specular reflection is considered in annex C.

Apart from the above-mentioned specular type of reflection, the reflection affecting the luminance coefficient is ordinary reflection that takes place within the material of the surface. The ordinary reflection does make the luminance coefficient vary with the geometry, but to a smaller degree and more slowly than for specular reflection, and in a way that is dictated by the geometry itself.

Thus, the luminance coefficient has a relatively high value when driving with the sun in the back, because the sun tends to illuminate those parts of the surface that are visible to the observer.

Driving with the sun in the back corresponds to a side angle in the neighbourhood of 180°; refer to figures A.1 and A.2. This feature is caused by ordinary reflection, but may be considered to represent a weak retroreflection where the reflection is strongest in directions back towards the light source. Retroreflection gets stronger the closer the direction of illumination gets to the plane of the surface. The extreme case is the retroreflection caused by the headlamps of the vehicle driven by the observer. This type of retroreflection is considered in annex B.

The retroreflection is strongest for table N1 and decreases with N2, N3 and N4. This is the opposite to the change of specular reflection. The explanation for this is that both features are affected by surface texture in the way that more texture enhances retroreflection, but reduces specular reflection and vice versa. The tables actually reflect decreasing surface texture in the sequence N1, N2, N3 and N4.

It may be noted that the standard tables for wet or humid road surfaces W1, W2, W3 and W4 express a further gradual increase in the degree of specularity in the sequence N1, N2, N3, N4, W1, W2, W3 and W4. Diagrams for the W tables are not provided; they would express the same kind of variation with the angles as in figure A.2, but with less retroreflection and more specular reflection.

The N-series of tables are based on road surfaces, not on road markings. However, several samples of road markings were measured during the 1970's and 1980's and these show higher q values, but else the same type of variation with the angles as road surfaces. In this sense, the N-tables can be considered to be typical for road markings as well as road surfaces.

Table N1, as one of the extremes, might represent structured road markings, while table N4 as the other extreme might represent a painted road marking on a relatively smooth surface. Tables N2 and N3 represent probably most other road markings.

It is noted that the angle of the observation direction, as illustrated in figure A.3 has been fixed at 1° for the standard reflection tables and the underlying collection of measured reflection tables.

The reason for not varying this angle is that the table values do not vary much, at least not in a systematic manner, with the actual value of the angle. This was verified by measurements in the 1970's. The explanation is that the illumination direction lies above the observation direction in all of the table positions and that the texture of the road surface is random of nature. If raising the direction of observation, additional parts of the surface texture will become visible, but these parts reflect the light to the same degree as the previous parts due to the randomness.

NOTE: In the extreme case of headlamp illumination, where the illumination direction is lower than the observation direction, the observation direction has a direct influence on the measured reflection value for both retroreflection and specular reflection. Refer to annexes B and C.

It is also noted that a side angle of view, as measured from a vertical plane containing the observation direction to the direction of the road surface or road marking, has been fixed at 0° for the reflection tables. The justification for not varying this angle is that the road surface is assumed to possess rotational symmetry because of randomness of the surface, or at least not to vary much for the angles of rotation that occur in traffic situations.

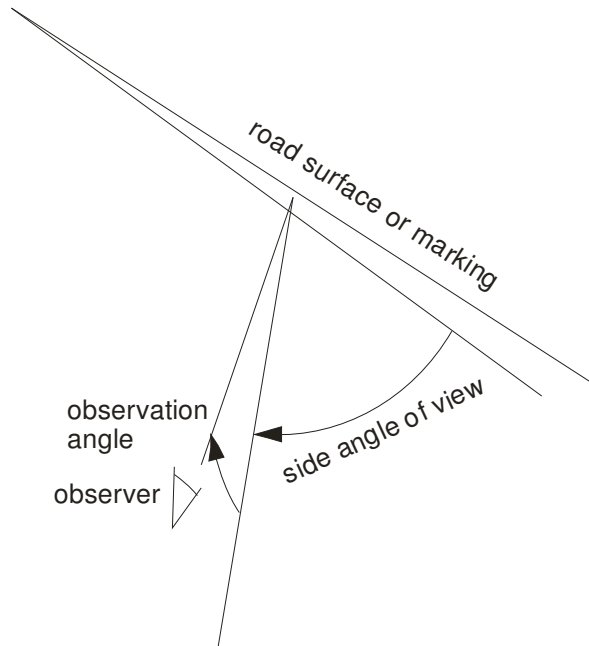


Figure A.3: Angle of observation and side angle of view.

A.3 Characterisation of road surfaces

Each of the standard reflection tables has a characteristic level of reflection and a characteristic degree of specularity. The level of reflection has traditionally been described by the average luminance coefficient Q_0 and the characteristic degree of specularity by the specular factor S_1 .

Q_0 is a weighted average of the luminance coefficients of the reflection table, while S_1 is the number 0,0894 times the ratio between the values of the luminance coefficients q_2 and q_1 in two particular positions of the table. Refer to figures A.4 and A.5.

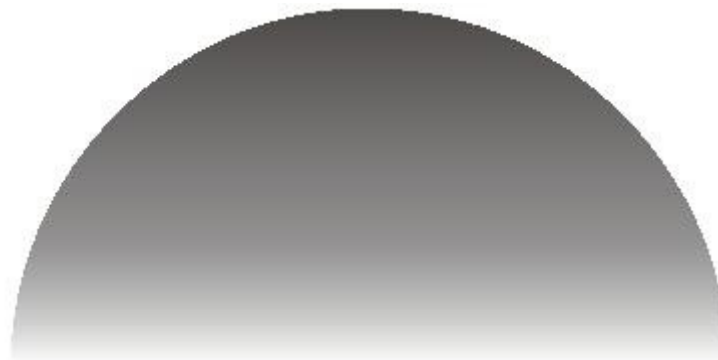


Figure A.4: Weights for the integration of Q_0 .

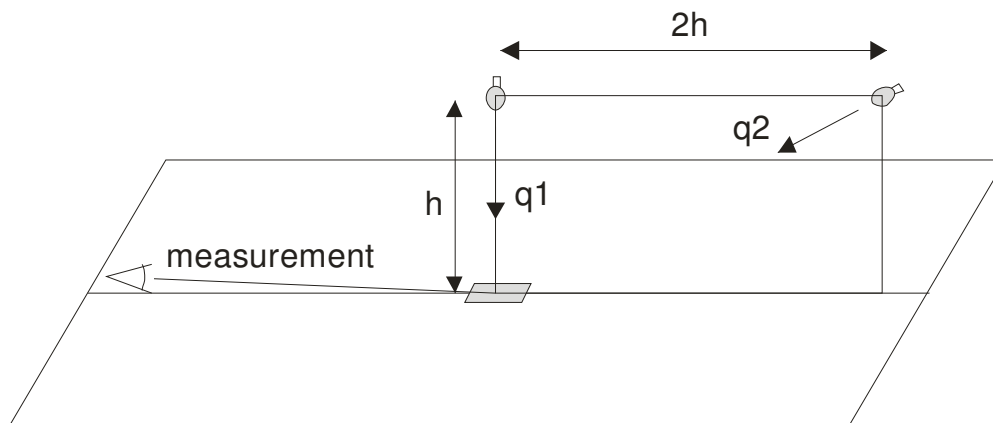


Figure A.5: Two luminance coefficients used to form the specular factor S1.

The idea is that the two characteristics are measured for a road surface by means of a portable instrument. Once measured, the S1 value is used to select one of the standard reflection tables and the Q0 value is used to determine a scaling factor for the luminance coefficient values of that table. The selected table, after rescaling, represents the road surface.

The criteria for the selection of an N-table are given in table A.1. There are similar criteria for other sets of standard tables. The scaling factor is the measured Q0 value in proportion to the Q0 value inherent in the selected N-table. The Q0 values inherent in the N-tables are provided in table A.2.

Table A.1: Criteria for the selection of an N-table.

measured S1	choice of N-table
$S1 \leq 0,28$	N1
$0,28 < S1 \leq 0,60$	N2
$0,60 < S1 \leq 1,30$	N3
$1,30 < S1 \leq 2,00$	N4

Table A.2: Inherent Q0 value for the N-tables.

N-table	inherent Q0 value
N1	$100 \text{ mcd} \cdot \text{m}^{-2} \cdot \text{lx}^{-1}$
N2	$70 \text{ mcd} \cdot \text{m}^{-2} \cdot \text{lx}^{-1}$
N3	$70 \text{ mcd} \cdot \text{m}^{-2} \cdot \text{lx}^{-1}$
N4	$80 \text{ mcd} \cdot \text{m}^{-2} \cdot \text{lx}^{-1}$

A number of portable instruments intended for the measurement of S1 and Q0 were developed during the 1970's and early 1980's. However, comparisons to laboratory measurements showed that they were inaccurate to the degree that the measurements had little practical value. Only one of these portable instruments, called the LTL 200 developed by the Illuminating Engineering Laboratory (now part of DELTA Light & Optics) had a reasonable accuracy. This instrument was, on the other hand, complex. A few copies were made, but only one of these is currently still in use.

The weights for the integration of Q_0 , as illustrated in figure A.4, correspond to a luminous environment, where the luminance is small at zenith and increases gradually towards the horizon. The weights vary according to $1/\cos\gamma$, where γ is the angle of light incidence (equal to the zenith angle). This cosine ($\cos\gamma$) approaches 0 when γ approaches 90° and, therefore, the weights actually approach the infinite as the illumination direction approaches the horizon.

It is very difficult, bordering on the impossible, to provide such a luminous environment within the small space of a portable instrument. It is also difficult to provide the illumination systems needed for the measurement of the values of q_1 and q_2 needed for the determination of the S_1 value.

These are the reasons that a simple portable instrument was not developed. Therefore, the above-mentioned idea actually failed.

The standard reflection tables are still being used for the design of road lighting installations in a conventional manner in the different countries. However, the assumptions regarding average reflection (the average luminance coefficient) and the specularity (the specular factor) are not being tested in practise.

A.4 Introduction of the luminance coefficient under diffuse illumination

The weights used for the integration of Q_0 cause difficulty for portable measurement and also seems a bit strange. The rationale behind the weights is that the Q_0 is intended to represent the average reflection of the road surface under road lighting in this sense:

$$L_{\text{average}} \approx Q_0 \times E_{\text{average}}$$

where L_{average} is the average road surface luminance

and E_{average} is the average illuminance on the road surface.

Q_0 does work this way for some road lighting installations, in particular for installations using lanterns with a very long reach, but not for all lighting installations. In addition, daylight illumination should be considered as well.

Figure A.6 illustrates the CIE standard overcast sky and shows that the luminance is highest at the zenith and decreases towards the horizon. This is the opposite variation compared to the weights for the integration of Q_0 . As could be expected, the Q_0 value provides an overestimation of the road surface reflection in this kind of illumination, actually by 12 %, 18 %, 36 % and 61 % for N_1 , N_2 , N_3 and N_4 respectively.

In sunlight, the relevant road surface reflection is provided by the luminance coefficient that corresponds to position of the sun in the sky. Accordingly, the road surface reflection varies strongly with the position of the sun. However, the weights for the integration of Q_0 are not representative for the frequency of location of the sun, and the Q_0 value can be expected to provide an overestimation of the average road surface reflection in illumination by the sun.



Figure A.6: Luminance according to the CIE overcast sky.

These matters are discussed in some detail in CIE 144, where it is recommended to replace Q_0 with Q_d , which is the average luminance coefficient under diffuse illumination.

The weights for the integration of Q_d are uniform as illustrated in figure A.7 and correspond to a luminous environment with a constant luminance. Such an illumination can be provided by a photometric sphere with indirect illumination for both laboratory measurements and in situ measurements with portable instruments. It is an advantage that there is no preferred location in an environment with constant luminance, so that the measured field does not have to be located accurately. It is also possible to provide a fairly good approximation to diffuse illumination by other means.

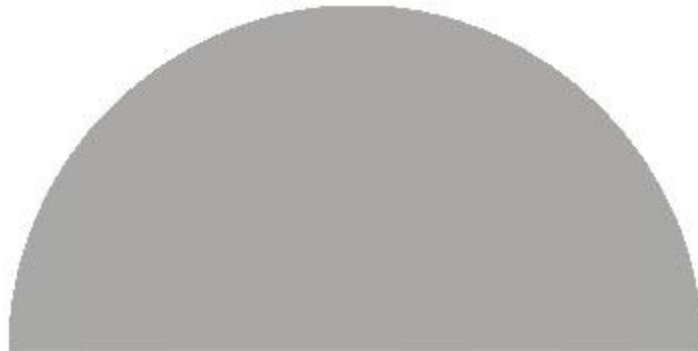


Figure A.7: Weights for the integration of Q_d .

In total, Q_d measurements are practicable, as opposed to Q_0 measurements. Q_d has been introduced in EN 1436 “Road marking materials - Road marking performance for road user” as a characteristic for the reflection of road markings in daylight or under road lighting. Portable instruments for in situ measurement are available and actually used in numbers.

EN 1436 fixes the observation angle at $2,29^\circ$ with a 30 m geometry as opposed to the 1° used for the road reflection tables. In A.2 it is stated that the Q_d value does not depend much on the observation angle. However, the relatively large observation angle of $2,29^\circ$ in the 30 m geometry might allow a view to the bottom surface between profiles of some profiled road markings, so that such road markings may show some variation.

In any case, Q_d should be at least as applicable for road surfaces as for road markings.

Some of these portable instruments combine the measurement of Q_d with the measurement of the coefficient of retroreflected luminance R_L . But these instruments and in fact no portable instrument at all includes measurement of the specular factor S_1 . The reason is probably that this is difficult as stated in A.3.

Therefore, in situ measurement is available for one of the two characteristics of the reflection in daylight or under road lighting – for the level of reflection - but not for the degree of specularity.

A.5 Some aspects of Q_d

EN 1436 defines Q_d as the ratio between the luminance of a field of a surface under diffuse illumination in proportion to the illuminance on the plane on the surface. Q_d is measured with a spectral distribution of the illumination in accordance with standard illuminant D65 representing daylight and with an observation angle of $2,29^\circ$ representing a 30 m geometry.

NOTE 1: Qd is also defined in ASTM E 2302 “Standard Test Method for Measurement of the Luminance Coefficient Under Diffuse Illumination of Pavement Marking Materials Using a Portable Reflectometer”.

The illuminance provided by surroundings of a constant luminance L is $\pi \times L$. The maximum luminance that a field of a surface can obtain, when the surroundings have a constant luminance L, is actually that particular luminance L. Accordingly the maximum value of Qd is $L/(\pi \times L) = 1/\pi = 0,318 \text{ cd}\cdot\text{m}^{-2}\cdot\text{lx}^{-1} = 318 \text{ mcd}\cdot\text{m}^{-2}\cdot\text{lx}^{-1}$.

A surface can approach the maximum value if it reflects the measuring beam with a high reflectance factor. A surface with a matt white finish may approach the maximum, but a shiny surface may also, even if it is black. For instance a black acrylic plate with a smooth upper surface has a Qd value of more than 90 % of the maximum.

This shows that Qd includes specular reflection in the surface, as well as ordinary reflection in the material itself.

In order to estimate the proportions of ordinary and specular reflection, the correlation between Qd and another measure of reflection can be studied. This other measure is the luminance factor β , which is defined in EN 1436 as an alternative characteristic to Qd.

The luminance factor β is measured in the $45^\circ/0^\circ$ geometry with illumination in accordance with standard illuminant D65, and is expressed in percent reflection compared to a perfect diffusing surface.

NOTE 2: EN 1436 also introduces the chromaticity co-ordinates x, and y that are used to express the colour of the material. The chromaticity co-ordinates are measured in the same situation as for β and generally simultaneously to β in a combined instrument. In this sense β , x and y belong together. However, only β is considered in the following.

The value of the luminance factor β does not include much specular reflection, because the geometry dictates that the angle of incidence should be $22,5^\circ$, where surface reflection is weak.

It is sometimes said that there is little correlation between Qd and β , but that would be strange and is not quite true either. Figure A.8 shows the actual correlation as obtained from data collected in the “durability project” carried out by the CEN/TC 226 WG2 on horizontal road markings (which is responsible for EN 1436 and several other standards in the field). The data covers only seven materials, but several countries with a variation in climate. The report is yet to be published by CEN.

Figure A.8 indicates a linear relationship with Qd increasing on the average by $26 \text{ cd}\cdot\text{m}^{-2}\cdot\text{lx}^{-1}$ each time β increases by 10%. The standard deviation of the Qd value with respect to the correlation line is $32 \text{ cd}\cdot\text{m}^{-2}\cdot\text{lx}^{-1}$, the correlation coefficient is 0,90.

NOTE 2: This is useful information to producers of road marking materials and applicators. If the Qd value is to be raised by for instance $30 \text{ mcd}\cdot\text{m}^{-2}\cdot\text{lx}^{-1}$ (one class as defined in EN 1436), then the value of β should be raised by approximately 12 % by adding more colour to the material (normally titaniumdioxide for white materials).

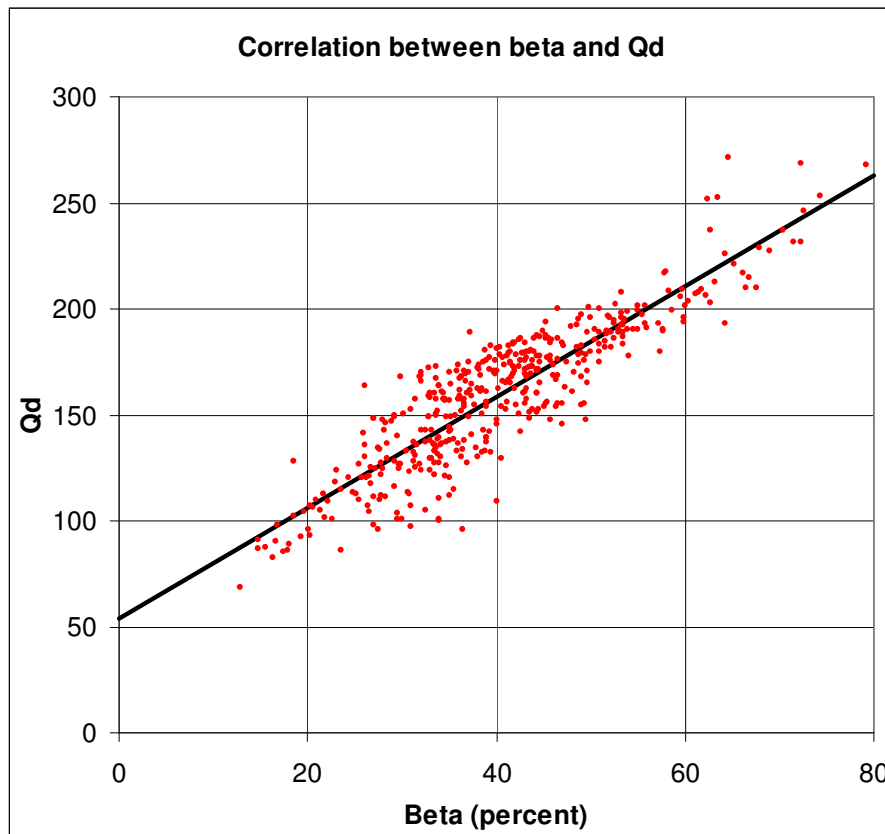


Figure A.8: Correlation between the luminance factor β and the Qd.

The correlation line of figure A.8 predicts a Qd value of $52 \text{ cd}\cdot\text{m}^{-2}\cdot\text{lx}^{-1}$ for $\beta = 0 \%$, i.e. for a material that is pitch black. This value is the average contribution by surface reflection and is clearly not insignificant. It amounts to 16 % of the above-mentioned maximum value and to approximately one third of the Qd value as an average for the data shown in figure A.8.

It is noted that the data of figure A.8 all are obtained for plane road markings. Road markings with structure would not subscribe to the correlation indicated in the figure as the specular reflection would be less.

Table A.3 shows the inherent Qd and Q0 values and their ratios for the N-tables. The ratios decrease with increasing degree of specularity in the sequence N1, N2, N3 and N4 which illustrates that Qd includes specular reflection to a smaller degree than Q0.

Table A.3: Inherent Qd and Q0 values and their ratios for the N-tables.

N-table	inherent Qd value	inherent Q0 value	Ratio Qd/Q0
N1	$92 \text{ mcd}\cdot\text{m}^{-2}\cdot\text{lx}^{-1}$	$100 \text{ mcd}\cdot\text{m}^{-2}\cdot\text{lx}^{-1}$	0,92
N2	$61 \text{ mcd}\cdot\text{m}^{-2}\cdot\text{lx}^{-1}$	$70 \text{ mcd}\cdot\text{m}^{-2}\cdot\text{lx}^{-1}$	0,87
N3	$54 \text{ mcd}\cdot\text{m}^{-2}\cdot\text{lx}^{-1}$	$70 \text{ mcd}\cdot\text{m}^{-2}\cdot\text{lx}^{-1}$	0,77
N4	$54 \text{ mcd}\cdot\text{m}^{-2}\cdot\text{lx}^{-1}$	$80 \text{ mcd}\cdot\text{m}^{-2}\cdot\text{lx}^{-1}$	0,68

The amount of surface reflection depends on the surface texture of the individual road markings, and may be more or less than the above-mentioned value. Profiled road markings have typically less, because the profiles prevent much of the surface reflection. Accordingly, profiled road markings tend to have smaller Qd values than road markings without profile.

Road surfaces also possess a specular reflection that provides a bottom level of the Qd value. This is why road surfaces do not have very small Qd values, even when the material is very dark. Therefore, the contrasts of road markings to the surrounding road surfaces, as expressed by the ratios of Qd values, are not necessarily very high.

A.6 Qd as a measure of luminance and contrast under road lighting

The design parameters for road lighting on traffic roads include the average road surface luminance and the uniformity of that luminance. These are computed in two steps, where the first step is to compute the luminance values in a grid of points that covers a representative area on the road. The second step is to compute the average luminance as the average of the luminance values of the points, and the uniformity as the ratio of the smallest of the luminance values and the average.

The average luminance has to meet a minimum specification, typically 0,5; 0,75; 1,0 or 1,5 cd/m². The uniformity has typically to be minimum 0,4. Refer to national road lighting standards or EN 13201-2, “Road lighting - Part 2: Performance requirements”, which summarizes national requirements in Europe.

NOTE: Other design criteria involve illumination of the near surroundings of the road, limitation of glare and environmental matters.

The design normally involves repeated computations, in which various parameters are varied until the design criteria are met and the installation is deemed to be acceptable in other respects.

One of the parameters that can be varied is the light distribution of the luminaire, which mostly has three or more positions of the light source, or other settings of the optics. The light distribution generally includes two beams of light, one pointing up the road and the other pointing down the road so that the luminaires can be set with a relatively large spacing. The feature that can be varied is “toe-in”, which indicates to what extent the beams are directed at an angle away from the longitudinal direction of the road and towards to opposite side of the road. The optional settings of toe-in are typically small, medium or large.

Figure A.9 shows a road lighting installation on a small traffic road. The calculations involve the reflection tables N1, N2, N3, N4, W1, W2, W3 and W4. The tables N1, N2, N3 and N4 for dry road surfaces are used in a scale corresponding to a constant Qd value. The tables W1, W2, W3 and W4 for wet road surfaces are not used directly in this in scale, but in scales that are natural for wet road surfaces that have the constant Qd in the dry condition.

The calculations also involve three settings of the luminaires to small, medium and large toe-in. The results for the average luminance and the luminance uniformity are shown in figures A.10 and A.11 respectively.

With the small toe-in, the beams of the luminaires have a small angle to the direction of the road and actually point towards the drivers. This produces strong specular reflections and a high average luminance, but also a lower luminance uniformity. With the large toe-in, on the other hand, the beams of the luminaires are more transverse to the road and produce less specular reflection and thereby a lower average luminance, but also a higher luminance uniformity. This applies in particular for the W-tables for wet conditions.

The road lighting standards of the Nordic countries have an additional requirement, which applies for the luminance uniformity in wet conditions. The luminance setting that would be preferred is the large toe-in. With this type of road lighting, the illumination is approximately diffuse as an average over the road surface, and the average luminance is given approximately by Qd times the average illuminance. Accordingly, Qd is a good measure of luminance for the Nordic type of road lighting.

Most countries have no national requirement for the uniformity of luminance in wet conditions. Therefore, the uniformity in wet conditions is not a restriction and the small or medium toe-in would be preferred as they provide the higher average luminance. With this type of lighting, the average luminance is higher than Q_d times the average illuminance, and can be approximately Q_0 times the average illuminance. Accordingly, Q_d is not a good measure of luminance for the European type of road lighting.

The question is now if the Q_d values of the road markings and the road surface can represent the contrast with which the road markings are seen.

Road markings have mostly Q_d values in the range of 100 to 200 $\text{cd}\cdot\text{m}^{-2}\cdot\text{lx}^{-1}$, often in the lower end of the range when the road markings are of some age and wear. Road surfaces, on the other hand, have mostly Q_d values in the range of 55 to 90 $\text{cd}\cdot\text{m}^{-2}\cdot\text{lx}^{-1}$ depending on the type of road surface and the colour of the aggregates. This shows that the contrast of the road marking to the surrounding road surface is not necessarily high and may be critical at the low level of road lighting.

The answer to the question is affirmative if the road markings are of the same reflection table as the road surface. If this is not the case, the actual contrast will vary with the location and may be low at some locations. The variations can be expected to be fairly small with the Nordic type of road lighting, because of the low degree of illumination in specular directions, and higher for the European type of road lighting.

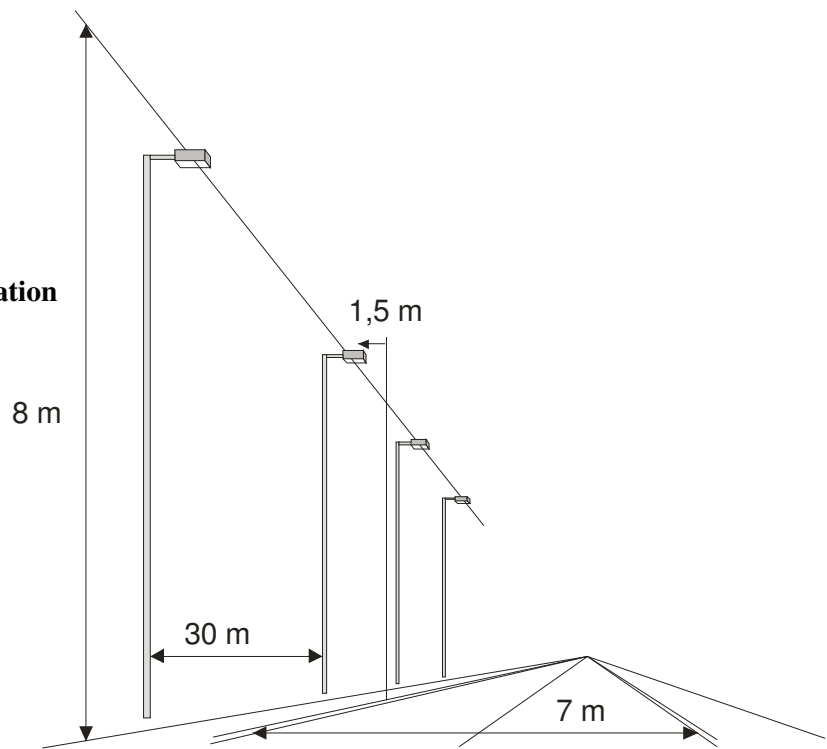


Figure A.9: A road lighting installation on a small traffic road.

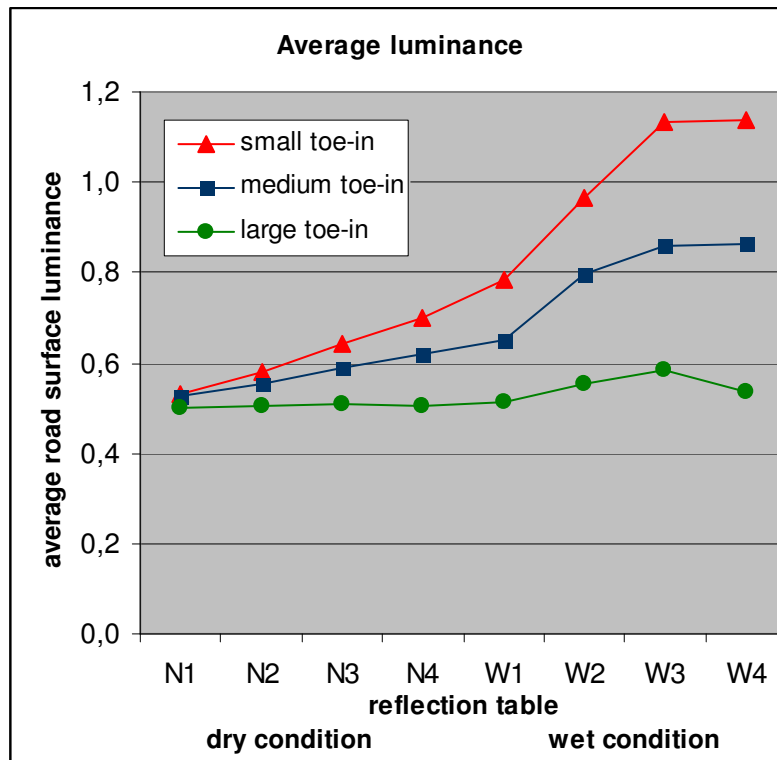


Figure A.10: Average road surface luminance for the lighting installation.

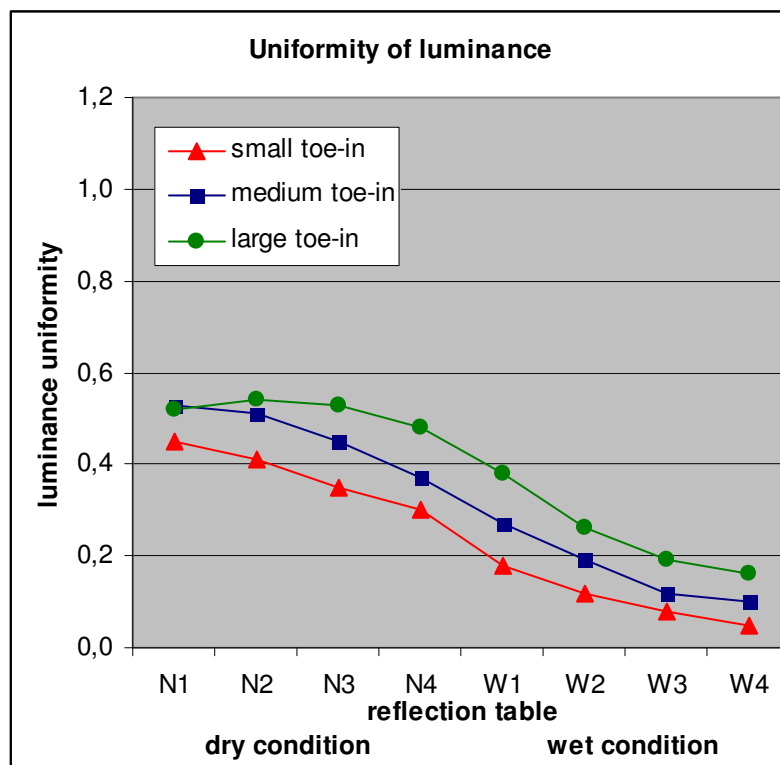


Figure A.11: Uniformity of luminance for the lighting installation.

A.7 Qd as a measure of contrast in daylight

In the high levels of illumination of daylight, road markings can be seen if the contrast to the road surface is higher than a small, critical value.

In conditions of an overcast sky with a reasonable free view to the sky, the luminance of a surface is given as the product of the Qd value and the illuminance to a good approximation (the luminance is actually 3 % to 8 % less than the product for reflection tables N1 to N4). Therefore, the contrast is approximately 2:1 if the Qd value of the road marking is twice the Qd value of the road surface.

This shows that the Qd values represent the contrast to a good approximation in overcast sky conditions.

Additionally, the Qd values represent the contrast when the road markings and the road surface have the same degree of specularly, for instance when they can be represented by the same reflection table.

In order cases, the Qd values may not represent the contrast. A well-known case is shown in figure A.12. Road markings on a test road are seen both with the sun, and against the sun. When seen with the sun, all markings are clearly visible; when seen against the sun, some profiled markings are hardly visible and form gaps. This phenomenon can sometimes be observed when driving against the sun and changing the view between forwards and backwards by looking into the rear view mirror.

Figure A.10:
Road markings on a test
road seen with the sun



and against the sun.



Literature

CIE 144 “Road surface and road marking reflection characteristics”

EN 1436 “Road marking materials – Road marking performance for road users”

Annex B: Retroreflection of road markings and road surfaces

B.1 Introduction and summary

It is the purpose of this annex to explain the mechanisms by which road surfaces and road markings obtain retroreflection and thereby to explain:

- how the retroreflection varies with distance and with vehicle geometries
- why the 30 m standard measuring geometry is relevant
- why the retroreflection is weak
- why the retroreflection decreases strongly in wet and humid conditions.

A deeper insight into these mechanisms may serve as a basis for improvements of the retroreflection of road markings in order to improve their visibility in night driving.

Some definitions for use in the following sections are provided in B.2. These definitions include:

- the coefficient of retroreflected luminance R_L
- angles describing the geometrical situation including the observation angle α , the illumination angle ϵ and the side angle β
- the 30 m standard measuring geometry of EN 1436 “Road marking materials - Road marking performance for road users” and ASTM E 1710 “Standard Test Method for Measurement of Retroreflective Pavement Marking Materials with CEN-Prescribed Geometry Using a Portable Retroreflectometer” intended to represent a passenger car.

The discussions in B.3, B.4 and B.5 are based on Night Traffic Report No. 4 “Reflection properties of road surfaces in headlight illumination”, 1982 and Night Traffic Report No. 6 “Reflection properties of road markings in headlight illumination”, 1983. These reports were issued by a Nordic research co-operation called “Night Traffic Research”. The work is carried on by a Nordic co-operation called NMF, refer to www.nmfv.dk. The reports are out of print, but pdf copies can be downloaded from the NMF site.

The two reports are based on measured R_L values for geometries that represent systematic variations of the above-mentioned angles. The measurements were done samples of road surfaces and road markings that were cut from roads in actual states of wear. On this basis, the two reports provide models for the R_L of surfaces with and without glass beads.

The two reports are more than 25 years old, but they are still unique by the data they present and by the model explanations of R_L values.

There has been only one study with a similar aim, by Zwahlen, H T; Schnell, T ; Johnson, N ; Hodson, N ; Donahue, T and reported in “Influence of pavement marking angular systems on visibility predictions using computer models”, Transportation Research Record No. 1754, 2001. This study misses the simple interpretation of the data and uses instead a comparison to other retroreflectors.

The model for surfaces without glass beads is discussed in B.3. These surfaces include road surfaces and road markings without glass beads.

One initial model is considered in B.3.1. The basis for this model is the assumption that the surfaces are plane, but is rejected because it does not explain the level of R_L values. This model is actually intended to demonstrate that the texture of surfaces cannot be ignored.

Therefore, the actual model for surfaces without glass beads, as introduced in B.3.2, is based on the assumption of texture. This model does explain the level of R_L values and the variation of R_L values with the above-mentioned angles.

The model for road markings with glass beads is introduced in B.4. This model as well explains the level of R_L values and the variation of R_L values with the angles.

The two models predict different levels of R_L values, but the same dependence of the vehicle geometry according to a simple geometrical factor, and a fairly limited influence of distance.

Road markings with glass beads may have a significant contribution to the R_L value by reflection in the surface in addition to the contribution by glass beads. The two contributions are inseparable in a measured value, but the simple dependence of the geometrical situation still applies as it is the same for both contributions.

The two models are simplified versions of the models introduced in Night Traffic Reports No. 4 and 6 in the sense that the influence of the side angle β is ignored. Further, all the R_L values illustrated in diagrams in B.3 and B.4 are for $\beta = 0^\circ$. This matter is considered in B.5, where it is concluded that for practical purposes and for the large majority of vehicles, the influence of β can be ignored.

The 30 m geometry is a simplified representation of a passenger car in the sense that it has only one headlamp and an observer placed directly above the headlamp. This matter is considered in B.6, where it is concluded that R_L values measured in the 30 m geometry are relevant for a realistic geometry of a passenger car, for other distances than 30 m and - after conversion according to the geometrical factor - for other vehicles than the passenger car.

NOTE: In view of some variation with the distance, the 30 m distance of the standard geometry is a bit short compared to the more interesting distances of 60 to 80 m close to the cut-off of the low beam headlamp. A 50 m geometry, which was in use in the UK and the Nordic countries during a period, was more central. However, the 30 m geometry was adopted in the first edition of EN 1436 in 1997 as a compromise between the 50 m geometry and a 10 to 15 m geometry that was in use in some other countries.

The models are obviously supported by the R_L data of Night Traffic Reports No. 4 and 6. There is an indirect support also in the large amount of R_L data that has been obtained with handheld retroreflectometers, as the models support the relevance of the 30 m geometry and simultaneously explains the level of the values.

In the case of road surfaces and road markings without glass beads, it can be expected that the R_L values are low. The question is rather, why there is a useful retroreflection at all, and this explanation does appear in B.3.

In the case of road markings with glass beads, the R_L values are higher than surfaces without glass beads, but not nearly as high as could be expected by comparison to other retroreflectors and retroreflective surfaces. However, B.4 does point to losses, which do not occur for other retroreflectors and retroreflective surfaces, and which do explain why the R_L values are relatively low.

In view of this, the R_L values for the dry condition are considered in B.6. Finally, wet conditions are considered in B.7, where it is pointed out why the R_L values are reduced and often very low.

B.2 Definitions

Figure B.1 shows a small field of a surface with an area dA , which is illuminated by a lamp and viewed by an observer. The illuminance at the field, as measured on a plane perpendicular to the direction of illumination, is E_p . The field obtains a luminance L by reflection as seen by the observer.

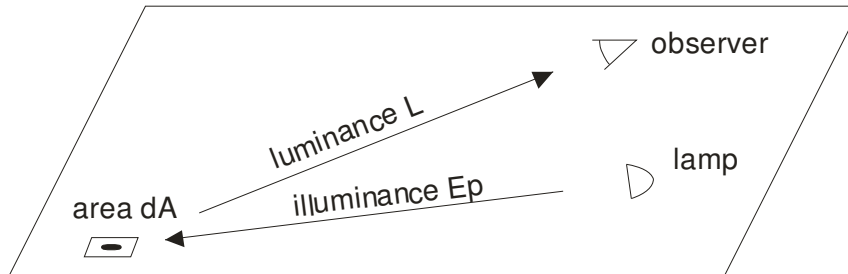


Figure B.1: A small field of a surface with an area dA , which is illuminated by a lamp and viewed by an observer.

The coefficient of retroreflected luminance R_L is defined by $R = L/E_p$. As the unit for luminance is $\text{cd}\cdot\text{m}^{-2}$ and the unit for illuminance is lx , the unit of R_L is $\text{cd}\cdot\text{m}^{-2}\cdot\text{lx}^{-1}$. However, the one thousand times smaller unit of $\text{mcd}\cdot\text{m}^{-2}\cdot\text{lx}^{-1}$ is generally used instead, in order to obtain more convenient values 1000 times higher.

The definition of the R_L is illustrated in figure B.2 by measurement of the luminance L with a luminance meter and of the illuminance E_p with a luxmeter.

Figure B.3 shows the three angles that are used to describe the geometry of observation and illumination. These are an observation angle α , an illumination angle ϵ and a side angle β .

NOTE: CIE 54.2 “Retroreflection: Definition and measurement” uses the letters a , e and b instead of the above-mentioned Greek letters α , ϵ and β , which are used for other purposes in CIE 54.2.

EN 1436 “Road marking materials - Road marking performance for road users” and ASTM E 1710 “Standard test method for measurement of retroreflective pavement marking materials with CEN-prescribed geometry using a portable retroreflectometer” define a standard measuring geometry, where $\alpha = 2,29^\circ$, $\epsilon = 1,24^\circ$ and $\beta = 0^\circ$.

This standard geometry is called the “30 m geometry” as it is intended to describe conditions for the driver of a passenger car looking at the surface 30 m ahead. Portable and vehicle mounted retroreflectometers are generally based on this geometry.

EN 1436 “Road marking materials - Road marking performance for road users” and ASTM E 1710 “Standard test method for measurement of retroreflective pavement marking materials with CEN-prescribed geometry using a portable retroreflectometer” define a standard measuring geometry, where $\alpha = 2,29^\circ$, $\epsilon = 1,24^\circ$ and $\beta = 0^\circ$.

This standard geometry is called the “30 m geometry” as it is intended to describe conditions for the driver of a passenger car looking at the surface 30 m ahead. Portable and vehicle mounted retroreflectometers are generally based on this geometry.

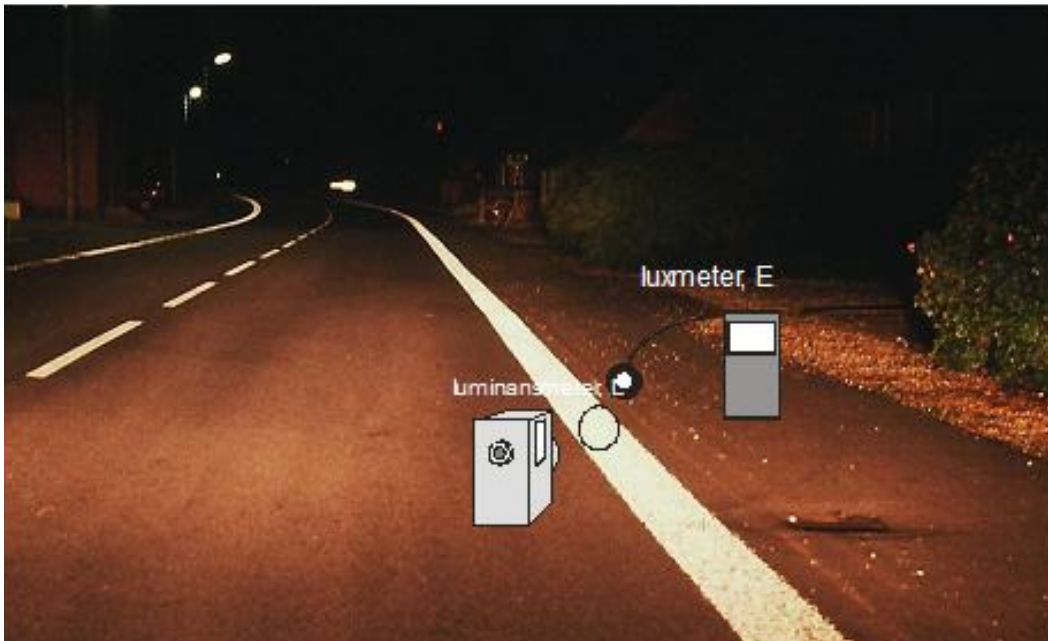


Figure B.2: Illustration of the luminance and illuminance used in the definition of the R_L .

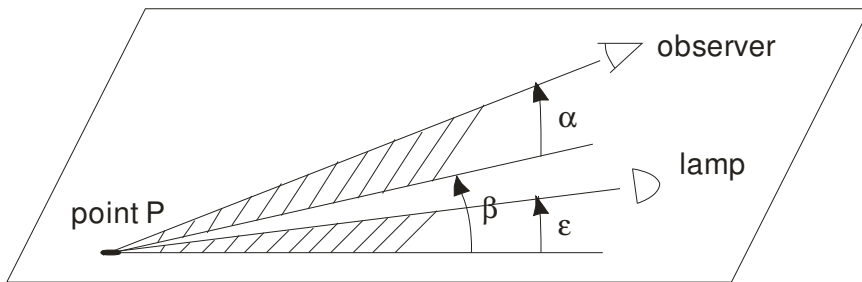


Figure B.3: Three angles that are used to describe the geometry of observation and illumination.

B.3 Model for road surfaces and markings without glass beads

B.3.1 A model assuming plane surfaces

It is tempting to consider a very simple model in which a surface is plane and has diffuse reflection. By diffuse reflection is meant that the reflected light is scattered into directions in the whole hemisphere above the plane surface in such a way that the luminance of the surface is independent of the viewing direction.

This assumption is often used in lighting calculations, for instance for room surfaces in interior lighting calculations, where it works well.

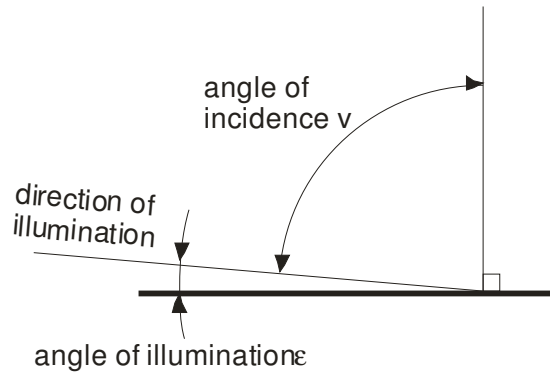
The luminance L of a plane surface with diffuse reflection is given by:

$$L = E\rho/\pi$$

where E is the illuminance on the plane of the surface
and ρ is the reflectance of the surface.

According to the cosine law of illumination, the illuminance E is given by $E = E_p \times \cos(v)$, where v is the angle of light incidence. Figure B.4 shows that the illumination angle ϵ is the complementary angle to v , i.e. $v = 90^\circ - \epsilon$. Accordingly, $\cos(v) = \cos(90^\circ - \epsilon) = \sin(\epsilon)$ and $E = E_p \times \sin(\epsilon)$.

Figure B.4: Angles of incidence v and illumination ϵ .



The following expression can then be derived for the R_L :

$$R_L = 1000 \times \sin(\epsilon) \times \rho / \pi = 6,9 \times \rho \text{ mcd} \cdot \text{m}^{-2} \cdot \text{lx}^{-1} \text{ for the 30 m geometry.}$$

The reflectance is the fraction of the incident luminous flux that is reflected; it is measured on a scale from 0 to 1. Therefore, the maximum predicted value of R_L is $6,9 \text{ mcd} \cdot \text{m}^{-2} \cdot \text{lx}^{-1}$.

This prediction is not in agreement with typical values, which are mostly higher and often much higher. One of the above-mentioned two assumptions for the surface, being plane and of diffuse reflection, must be unrealistic.

The assumption of diffuse reflection is certainly unrealistic. When a plane surface is illuminated at a grazing angle, much of the incoming light would be reflected into a forward direction. This leads to a reduction of the diffuse reflection and thereby of the R_L value. This is illustrated in figure B.5.

A more realistic assumption concerning reflection would, therefore, not solve the problem with the simple model, that predicted R_L values are unrealistic low. On the contrary, predicted R_L values would become even lower.

Such low R_L values, approaching 0, are actually observed for glossy surfaces with little texture, like some polished floor surfaces. Road surfaces and road markings covered by a film of water in wet conditions may also show very low R_L values.

But in general, the simple model fails. The assumption that the surface is plane is misleading, and a realistic model must take surface texture into account.

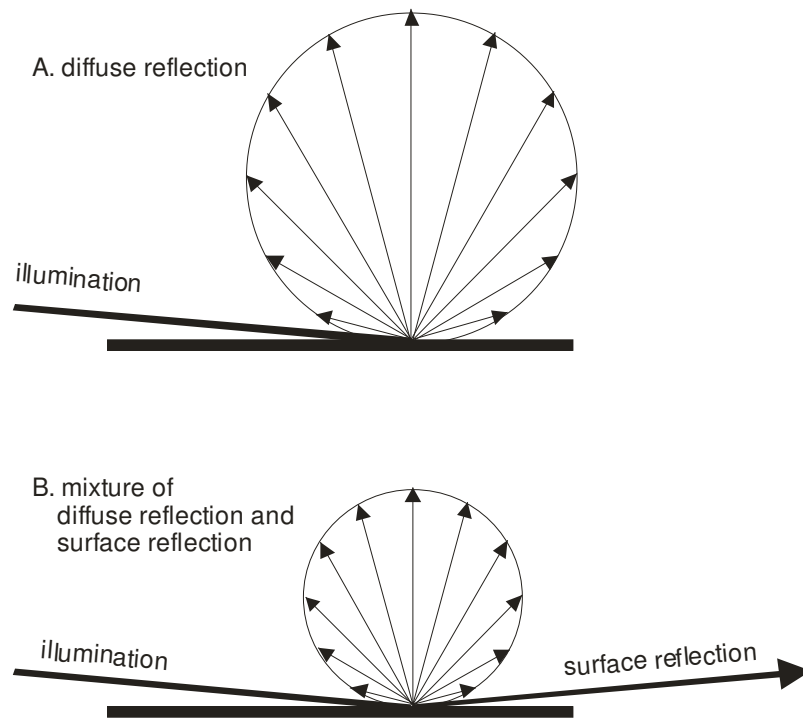


Figure B.5: Illustration of diffuse reflection (A) and of mixed reflection with both diffuse reflection and surface reflection (B).

B.3.2 A model assuming surface texture

A real surface has texture and the texture is promoted at the relevant grazing angles of illumination and observation.

Assume for instance that the texture has two small facets, one that is horizontal and the other with a strong a tilt towards the direction of illumination. Both facets are illuminated and have the same small area, and both have diffuse reflection with the same reflectance ρ .

The horizontal facet catches only a little of the incoming light at the grazing angle of illumination, therefore it obtains a low luminance and, simultaneously, it presents a small surface to the observer. The tilted facet, on the other hand, catches much more of the incoming light, obtains a correspondingly higher luminance and presents itself almost face on to the observer. This is illustrated in figure B.6.

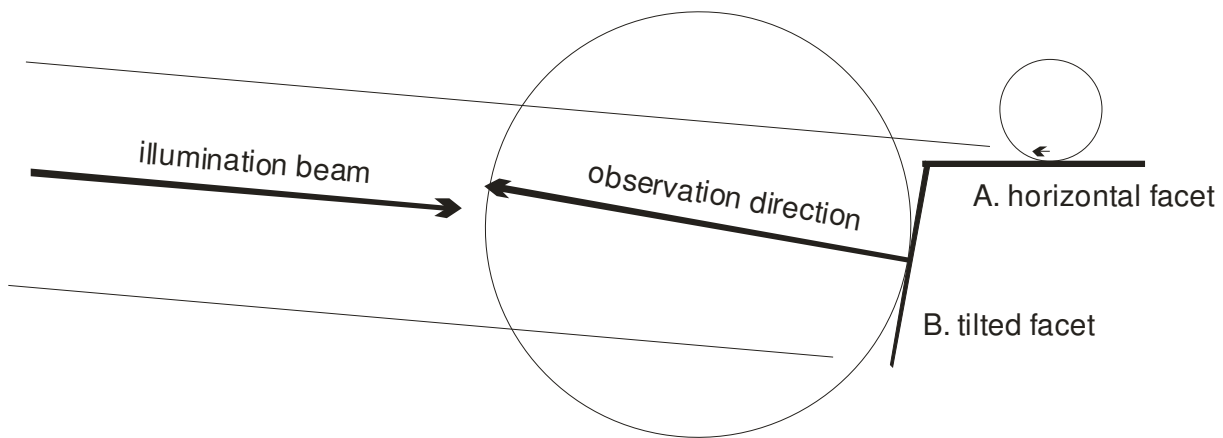


Figure B.6: Contributions to the R_L value by a horizontal facet (A) and a tilted facet (B).

The tilted facet in figure B.6 gives a dominating contribution to the R_L value compared to the horizontal facet. Therefore, it is assumed the grazing illumination singles out those facets that face the illumination direction and that these give the major contribution to the R_L value. Such facets may be called active facets.

Consider a field of the surface of an area A . This field has an apparent area as seen from the light source of $A \times \sin(\epsilon)$ and, accordingly, active facets of a total area of $A \times \sin(\epsilon)$ could catch all of the incoming light if they are perpendicular to illumination direction.

On the other hand, active facets that are perpendicular to the illumination direction are very close to being perpendicular to the observation direction as well, because the two directions are close. Therefore, the active facets also take up an apparent area of $A \times \sin(\epsilon)$ as seen by the observer.

However, the field has an apparent area as seen by the observer of $A \times \sin(\alpha)$, so that the active facets take up only a fraction of $G = (A \times \sin(\epsilon)) / (A \times \sin(\alpha)) = \sin(\epsilon) / \sin(\alpha)$ of this apparent area. The additional area seen by the observer is made up by shadows formed by the active facets.

Figure B.7 is meant to show that the geometrical factor is in fact a factor that takes account of the proportion of shadows in the area seen by the observer.

The observer is not able to distinguish between facets and shadows at a distance and, therefore, sees a luminance, which is the luminance of the active facets, but reduced by the factor G .

Active facets may not be quite perpendicular to the illumination direction and may not catch all of the incoming luminous flux. This is accounted for by adding a further factor T , which may be called a texture factor. This leads to a model expression for the R_L :

$$R_L = 1000 \times \rho \times G \times T / \pi \quad (\text{mcd} \cdot \text{m}^{-2} \cdot \text{lx}^{-1})$$

where G is the geometrical factor equal to $\sin(\epsilon) / \sin(\alpha)$
and T is the texture factor.

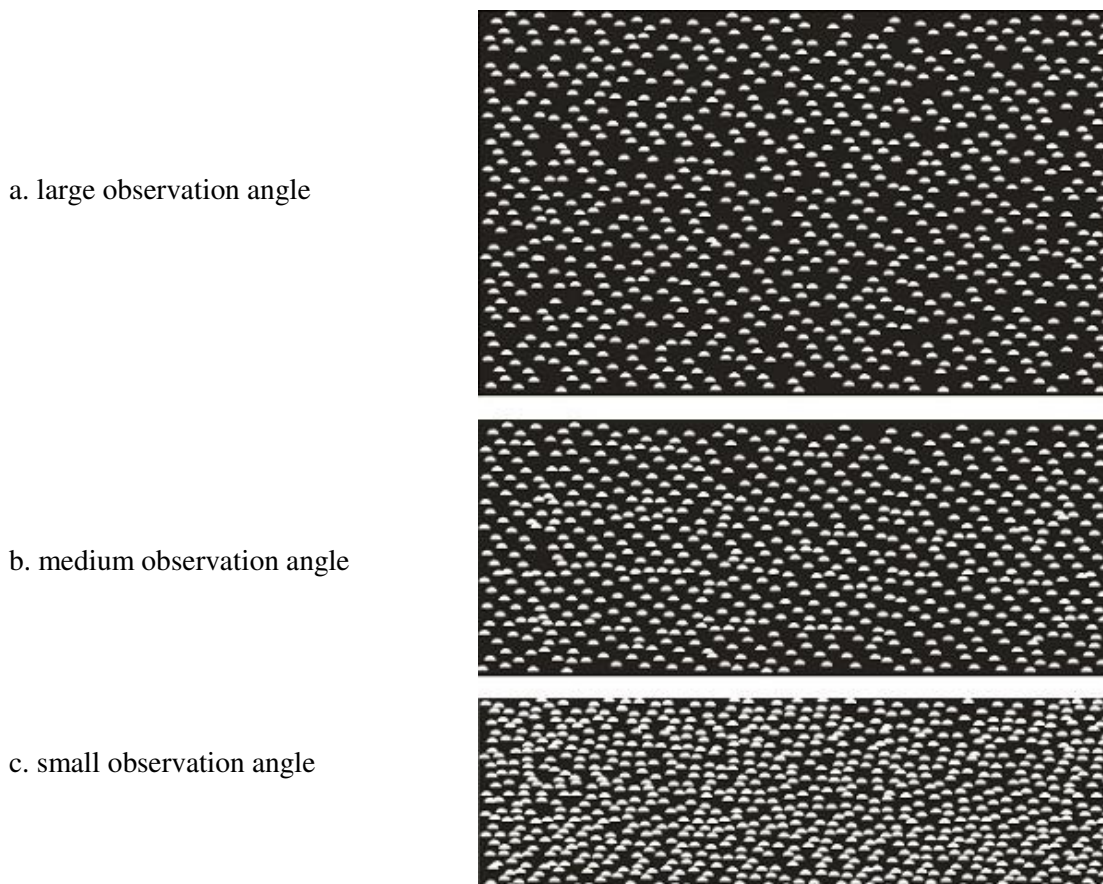


Figure B.7: An area, which is illuminated at a fixed illumination angle, but observed at three different observation angles.

B.3.3 The geometrical factor

The geometrical factor G is introduced with the intention that it might account for the influence of the observation angle α on the R_L value. If this is the case, then the ratio R_L/G should not depend on α , or at least should not vary much with α . This is the same as stating that R_L/G should not vary much with G .

Night Traffic Report No. 4 provides measured R_L values for a number of road surfaces for different combinations of α and ϵ . The combinations are arranged in such a way that for each value of ϵ there are three values of α equal to 1,54; 1,838 and 2,294 times the ϵ value. The corresponding values of G are respectively 0,544; 0,651 and 0,436. The values of ϵ are $0,5^\circ$; $0,74^\circ$; $1,24^\circ$; $2,46^\circ$ and $3,72^\circ$.

Night Traffic Report No. 6 provides measured R_L values for some road markings without glass beads for the same combinations of α and ϵ .

Figure B.8 shows curves of R_L/G as a function of G for one of the above-mentioned road markings. The different curves are for the different values of ϵ , with an additional curve for averages for the different ϵ values. It is seen from the figure that the curves are close to being horizontal. This indicates that for this particular surface, G accounts for the influence of α on the R_L value.

Figure B.9 shows curves of R_L/G for the total set of road surfaces and road markings without glass beads. In order not to get too many curves in one diagram, only the average curves for the different ϵ values are

indicated. These curves are also close to being horizontal, indicating that G might in general account for the influence of α on the R_L value.

Figure B.8: Values of R_L/G versus values of G for a road marking without glass beads.

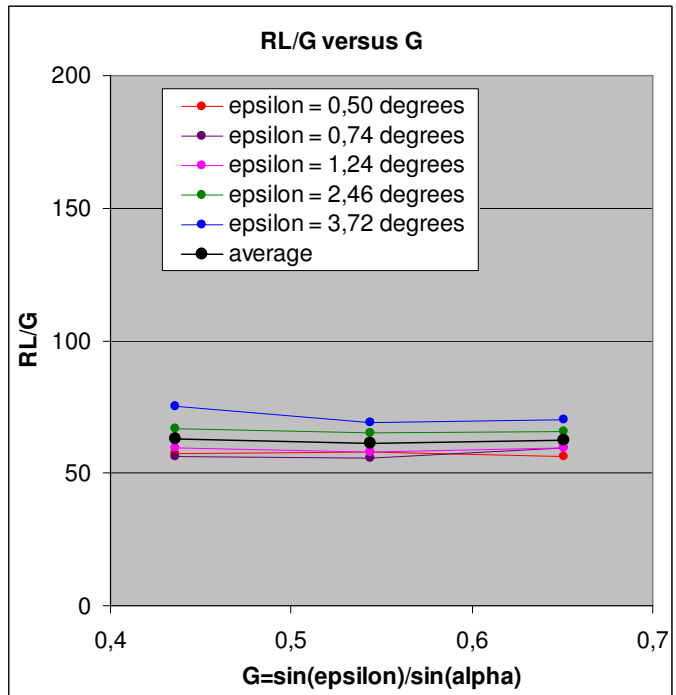
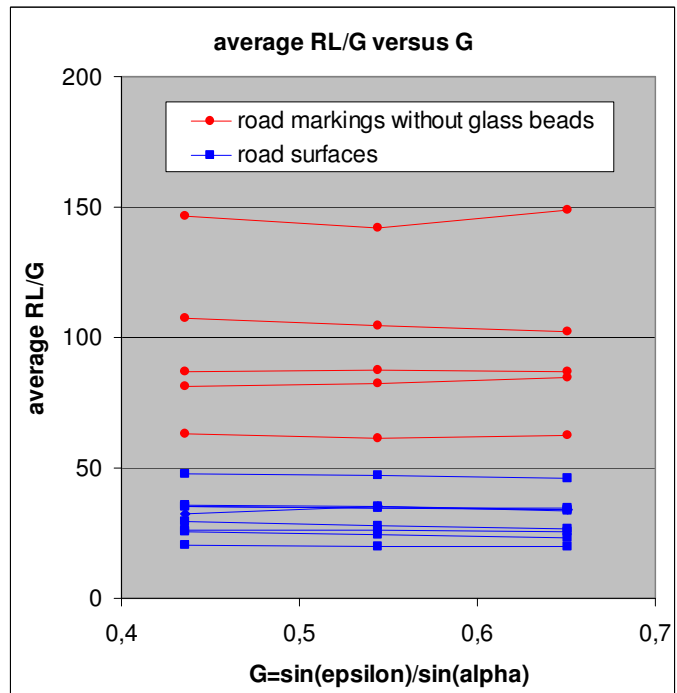


Figure B.9: Average values of R_L/G versus values of G for a number of road markings without glass beads and road surfaces.



It is concluded that the R_L value depends on the observation angle α in a simple manner - in inverse proportion to $\sin(\alpha)$ - as accounted for by the geometrical factor G . This confirms the basic assumption behind the model; that active facets with a strong tilt towards the light source provide the dominating contribution to the R_L .

Whenever the observation angle is larger than the illumination angle, the active facets are seen on the background of parts of the surface that are in the shadows of active facets - or at least has low illumination. When the observation angle increases, the background takes up a larger part of the field of view and this is the reason that the R_L value decreases.

In this sense, the geometrical factor can be considered to provide the fraction of the apparent area of the field of view that is illuminated. This fraction cannot exceed 1, and therefore the geometrical factor should be assigned the value of 1 when α is less than ϵ .

B.3.4 The texture factor

The illumination angle ϵ does influence R_L values directly in proportion to $\sin(\epsilon)$ by means of the geometrical factor G discussed in B.3.2. The reason is that when ϵ increases, the illumination penetrates deeper down into the texture of the surface and activates more facets by illuminating them.

The illumination angle ϵ might also influence the R_L value indirectly by affecting the texture factor T . This might happen if the fraction of the incoming light that falls on active facets changes with ϵ .

This is tested by means of the measured values of R_L for road surfaces and road markings without glass beads provided in Night Traffic reports 4 and 6.

Figure B.10 shows R_L values as a function of the illumination angle ϵ for one of the above-mentioned road markings. It is seen from the figure that the curves are close to being horizontal, indicating that the influence of ϵ on R_L values is relatively small in this case.

Figure B.10: Values of R_L at fixed values of the geometrical factor G versus the illumination angle ϵ for a road marking without glass beads.

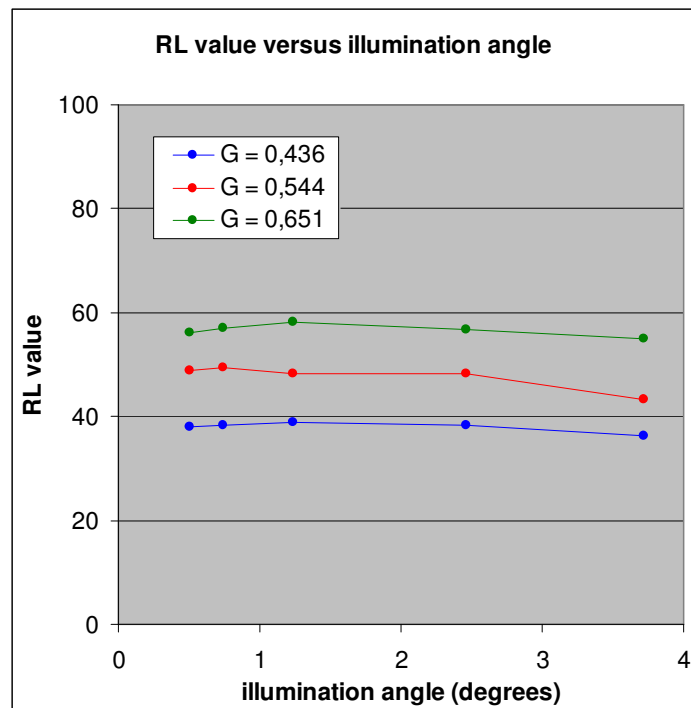
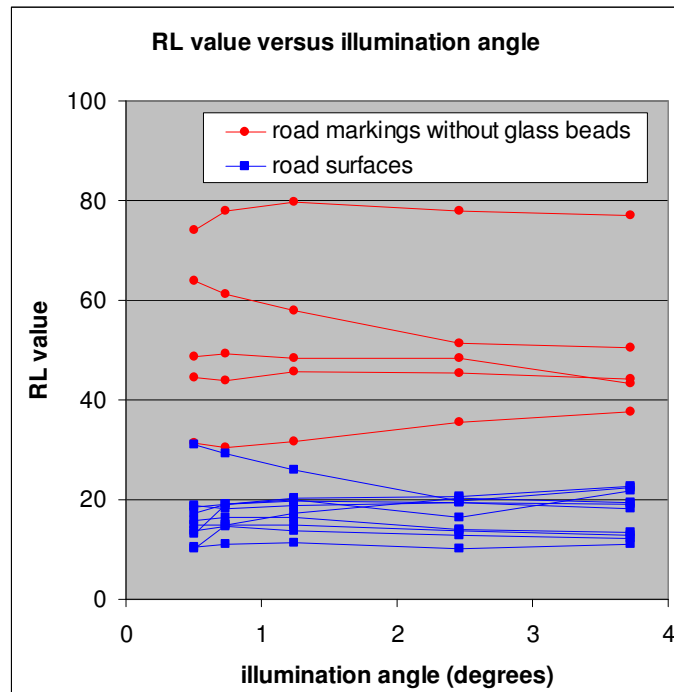


Figure B.10 has one curve for each of the values of the geometrical factor G . However, these curves are roughly parallel for the reasons accounted for in B.3.3. Therefore, it is sufficient to use one curve for one value of G . This is done in figure B.11, where one curve for the G value of 0,544 is included for each of the road surfaces and road markings without glass beads.

Figure B.11 indicates that there may be some change of the R_L value with ϵ , in particular at small values of ϵ corresponding to long distances to the road surface or road marking. However, the change is not systematic

and, accordingly, the R_L value and hence the texture factor T may be considered to be independent of ϵ to a first approximation.

Figure B.11: Values of R_L at a fixed value of the geometrical factor G of 0,544 versus the illumination angle ϵ for road surfaces and road markings without glass beads.



The R_L values of figure B.11 correspond to T values of typically 0,3 to 0,5. These values and the conclusion that T is approximately independent of ϵ , may demonstrate that texture is of a chaotic nature. Structured or profiled road markings, on the other hand, may exhibit larger values of T and show dependence on ϵ .

This is obvious for the profiled road marking shown in figure B.12. At small angles ϵ , where the light falls only on the profile sides, the value of T is constant at 1. At larger angles ϵ , where the light falls on both profile sides and bottom areas, the value of T is smaller and decreases with ϵ .

However, when the profiles are sufficiently high, the value of T may be constant within the relevant range of the angle ϵ . Values of the texture factor T are provided for some profiled road markings in figure B.13.

In cases a, b and c of figure B.13, the indicated T values are reached when the profiles are sufficiently high to catch all of the incoming light. In case d, the maximum T value is reached only in the specific geometrical situation, where all of the incoming light falls on the bars and these are illuminated over all of the height. In case e, the requirement is as in case d and probably not possible in practice.

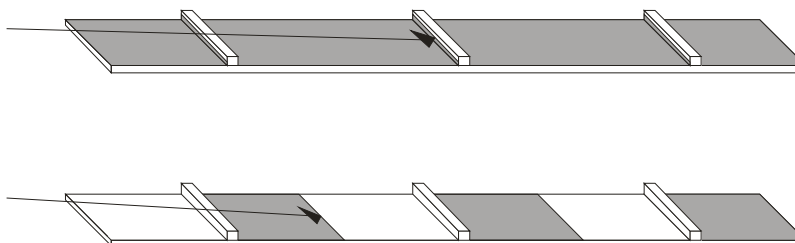


Figure B.12: Profiled road marking;
top: illuminated at a small angle ϵ , where the light falls only on the profile sides;
bottom: illuminated at a larger angle ϵ , where light falls both on profiles sides and bottom areas.

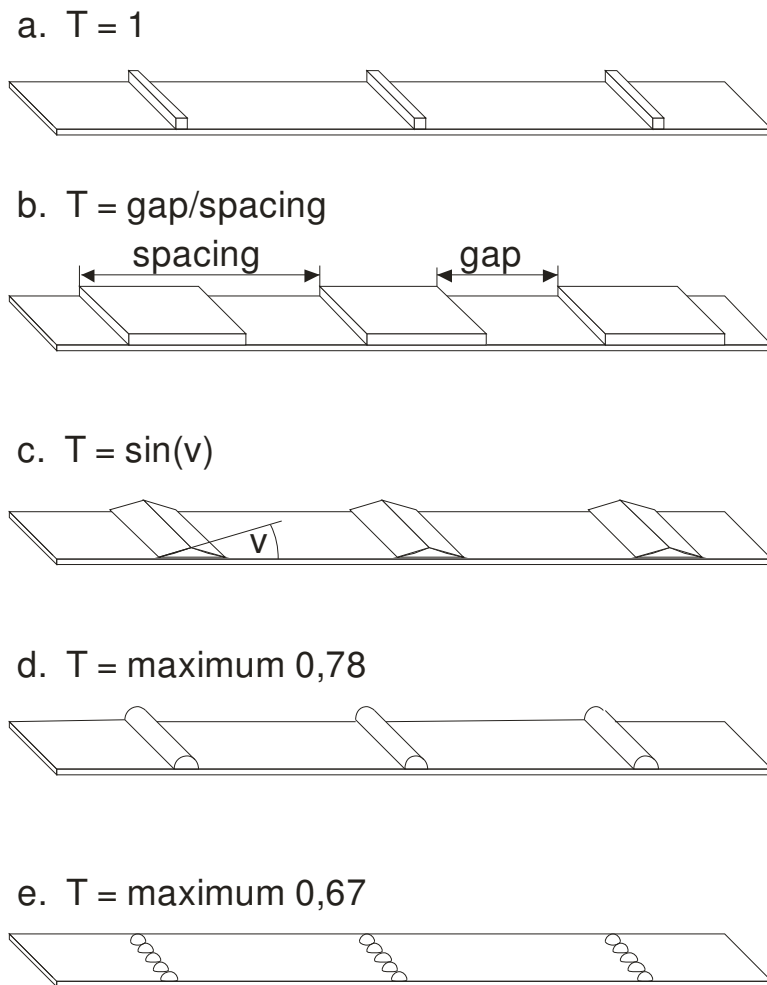


Figure B.13: Values of the texture factor T for some profiled road markings with transverse bars with vertical sides (a and b), sloping sides (c), cylindrical cross-section (d) or consisting of half spheres (e).

B.4 Model for glass beads

B.4.1 Amplification of the retroreflection by glass beads

Figure B.14 shows that a ray of parallel light falling on a glass bead becomes focussed on a relatively small field of the road marking material behind the bead. Figure B.15 shows, on the other hand, that a ray of observation directions is also focussed on a relatively small field of the road marking material behind the bead.

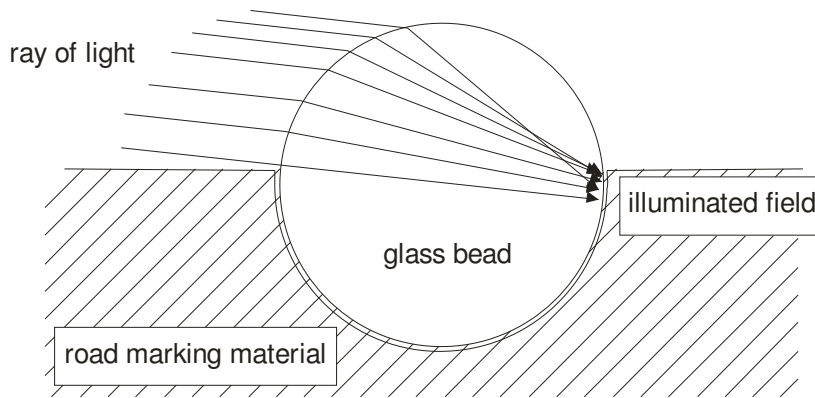


Figure B.14: A ray of parallel light entering a glass bead causes illumination of a relatively small field of the road marking material.

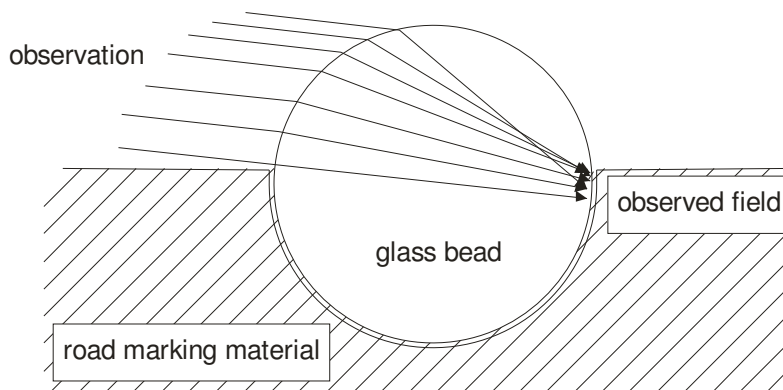


Figure B.15: Observation through a glass bead leads to viewing of a relatively small field of the road marking material.

The two fields at the back of the glass bead, illuminated and observed, do not quite coincide, but almost. The effect of the bead is then to concentrate the light on a relatively small field of the road marking material, and simultaneously let this field be viewed through the bead as if through a magnifying glass.

The reflection does occur in the road marking material, but the action of the bead is to amplify the observed luminance and thereby to amplify the contribution to the R_L value.

The drawings of figures B.14 and B.15 are based on normal and realistic conditions:

- an embedment of the glass bead to a depth of 60% of the diameter of the bead
- a refractive index of 1,55 of the glass, which is typical for ordinary glass beads
- an angular separation of the illumination and observation directions of $1,05^\circ$ as in the 30 m geometry.

Computer simulations show that the amplification is approximately by a factor of 9 for these conditions. Computer simulations also show that the retroreflected beam is so wide, approximately $\pm 10^\circ$, that the factor does not vary much within relevant vehicle geometries and distances on the road.

B.4.2 Model for the retroreflection by glass beads

According to B.4.1, the reflection from a glass bead is similar to the reflection from an active facet, except for the amplification by the glass bead. This leads to a model for the retroreflection of glass beads that is based on the model for a surface with texture introduced in B.3. Such a model is like this:

$$R_L = 1000 \times A \times \rho \times G \times B / \pi \quad (\text{mcd} \cdot \text{m}^{-2} \cdot \text{lx}^{-1})$$

where A is an amplification factor
 ρ is the reflectance of the road marking material
 G is the geometrical factor equal to $\sin(\epsilon)/\sin(\alpha)$
and B is a bead distribution factor.

In this model, as compared to the model for a surface with texture, the amplification caused by the glass beads is accounted for by the additional factor A , while the texture factor T has been replaced by a bead distribution factor B .

B.4.3 The geometrical factor

The observation angle α should have an influence only through the geometrical factor G , so that R_L/G should be independent of α . This is tested by means of figure B.16, which contains data from Night Traffic Report No. 6 in the same type of diagram as shown in figure B.9 for road surfaces and road markings without glass beads.

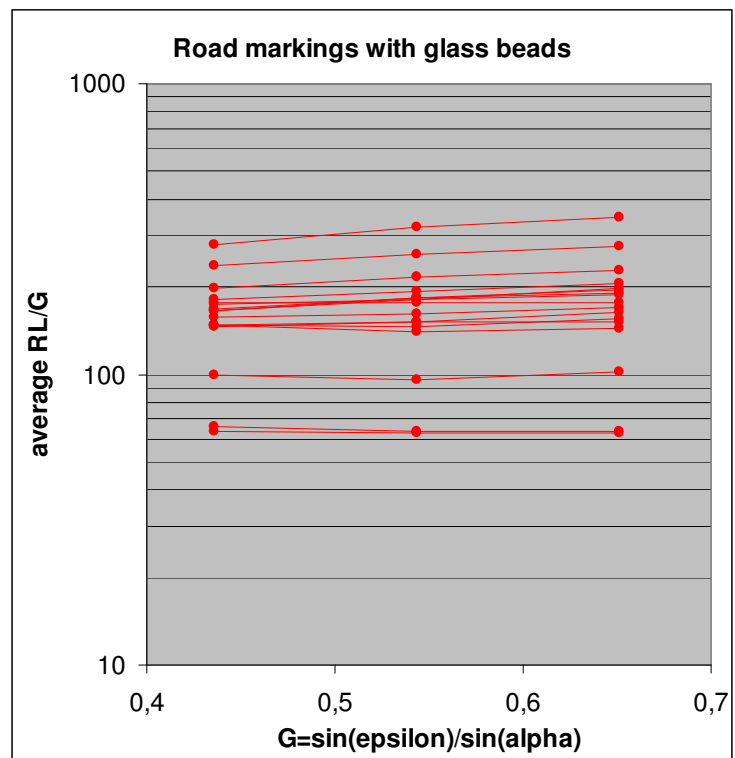


Figure B.16: Average values of R_L/G versus values of G for a number of road markings with glass beads.

Taking into consideration that the measurements were difficult, figure B.16 does verify that R_L/G is independent of G and thereby independent of α . Accordingly, the geometrical factor has the same definition and the same role in this model as in the model for road surfaces and road markings without glass beads.

B.4.4 The bead distribution factor

The bead distribution factor B has a maximum value of 1. Assuming that the value of the amplification factor A is 9, refer to B.4.1, and that the reflectance of the road marking material is 0,7, the maximum R_L value is approximately $1100 \text{ mcd} \cdot \text{m}^{-2} \cdot \text{lx}^{-1}$ for the 30 m geometry.

However, the bead distribution factor B but accounts for a couple of matters that cause a reduction of the value and thereby a reduction of the R_L value.

One of these matters is that beads are not all embedded to an optimum depth of approximately 60 % into the road marking material. Figure B.17 shows a bead in a high position, where some of the incoming light to pass through the bead. Figure B.17 also shows a bead in a deep position, where the field gets less illumination. These beads make less good use of the incoming light.

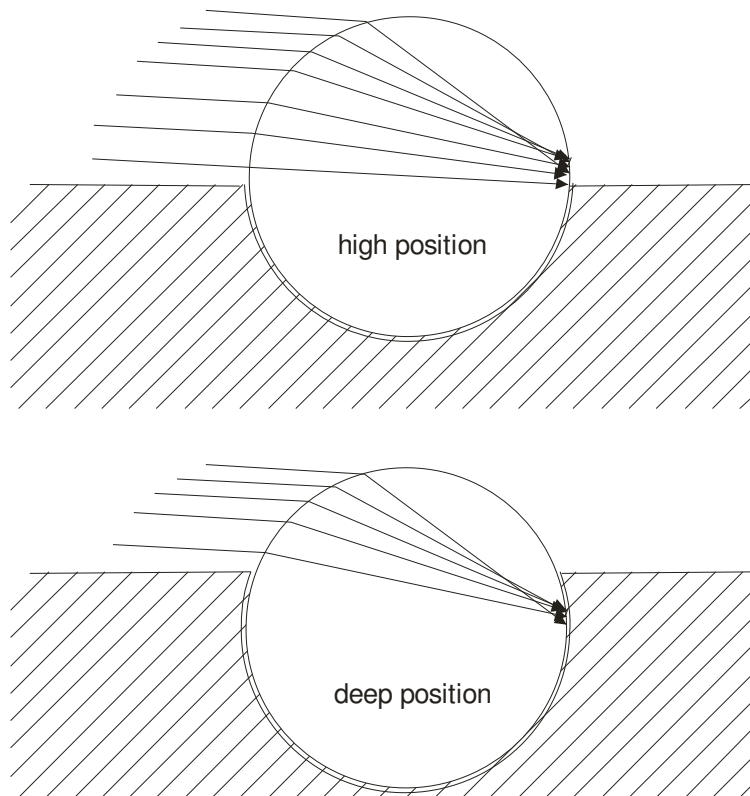


Figure B.17: Beads in high or deep positions make less good use of the incoming light compared to beads embedded at approximately 60 % of the bead diameter.

The other matter is that beads with a sparse population will not catch all of the incoming light, while beads with a dense population will cast shadows on each other and thereby prevent full illumination. There is a medium density, that is optimum, but even with the optimum density there will be some reduction of the value of B .

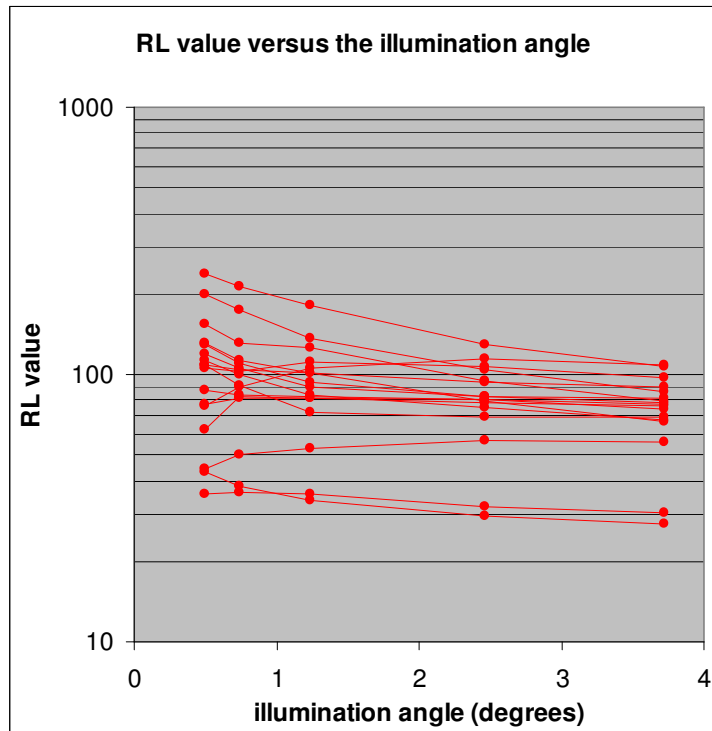
Road markings often have R_L values of 400 to 600 $\text{mcd}\cdot\text{m}^{-2}\cdot\text{lx}^{-1}$ when new, but much lower R_L values of for instance 100 $\text{mcd}\cdot\text{m}^{-2}\cdot\text{lx}^{-1}$ when some years old. This shows that the value of B may initially be as high as 0,5 and that the gradual decrease is down to for instance 0,1. These values seem reasonable.

It is easy to imagine that a certain population of glass beads may be closer to optimum at one value of the illumination angle ϵ and less than optimum at another value. Therefore, the value of B may depend on ϵ .

This is tested by means of figure B.18, which contains data from Night Traffic Report No. 6 in the same type of diagram as shown in figure B.11 for road surfaces and road markings without glass beads.

Figure B.18 does show variations of the R_L value with ϵ , in particular at the smaller values of ϵ that are the most interesting because they correspond to distances from 30 m and onwards. However, the value measured for the 30 m geometry, where ϵ equals $1,24^\circ$, does have relevance for longer distances.

Figure B.18: Values of R_L at a fixed value of the geometrical factor G of 0,544 versus the illumination angle ϵ for road markings with glass beads.



B.4.5 The amplification factor

An R_L value of for instance $300 \text{ mcd}\cdot\text{m}^{-2}\cdot\text{lx}^{-1}$ as mentioned in B.4.4 may appear to be good or even impressive, but as accounted for in B.2 the unit is per thousand. In the full unit, the value is $0,3 \text{ cd}\cdot\text{m}^{-2}\cdot\text{lx}^{-1}$, which is about the same reflection as obtained from a white wall.

R_L values of road markings are in fact small compared to R_L values of other retroreflectors.

The geometrical factor represents a loss by means of shadows by a factor of 0,54 in the 30 m geometry. This loss is an inescapable consequence of the geometrical situation.

Otherwise, the attention can be focussed on the value of the amplification factor, for which the value of 9 is provided in B.4.1 for common glass beads with a refractive index of 1,55 embedded by 60% into the road marking material. This value is actually low because of two additional losses.

The first additional loss is caused by the geometry of illumination, where the bead above the material is illuminated from the side. The bead collects less light and this results in a relatively weak illumination of the field behind the bead compared to what would be obtained, if the free part of the bead had faced the illumination direction. The loss in illumination and hence in the amplification factor and the R_L value is by approximately $2/3$.

NOTE: There is actually a loss of about $2/3$ of the light. This is the proportion of the light that falls on the non-free part of the bead after reflection in the road material.

The second additional loss is caused by poor focus of the light by a common glass bead.

Figure B.19 shows that there is no single focal point behind the bead, but a range of focal points. This indicates that a bead with its spherical shape is a poor lens with a severe spherical aberration. However, the figure also shows that the best focus is obtained at some distance behind the bead, while the focus on the material directly behind the bead is poor.

The consequence is that the amplification and hence the R_L value is low. It is in this sense that the poor focus represents a loss.

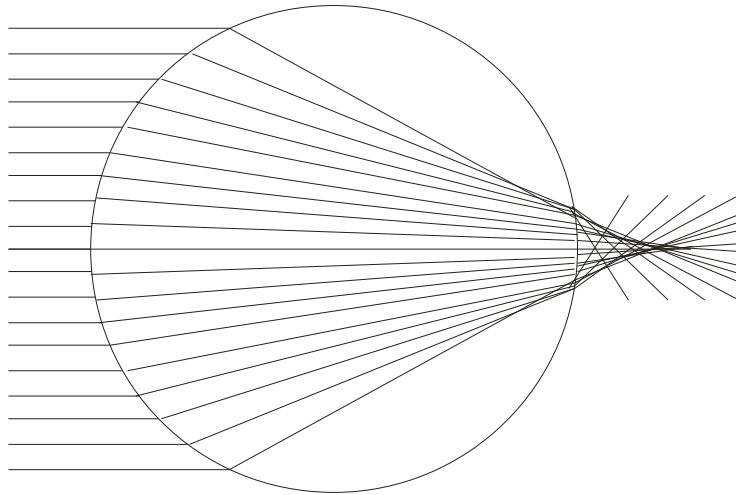


Figure B.19: A common glass bead of glass with a refractive index of 1,55 has spherical aberration and focus at some depth behind the bead.

A glass bead with a refractive index that is higher than 1,55 does provide a somewhat better focus on the material behind the bead.

There has previously been some use of beads made of flint glasses with a refractive index about 1,75. Computer simulations show that such beads may provide twice as high R_L values as the common beads made of normal glass.

So-called “ceramic” or “high index” beads with a refractive index of about 1,85 represent a more recent development. These beads may cause three times as high R_L values as common beads. However, high index beads are more costly than common beads and are used in special products only.

The refractive index of ceramic beads is optimum in the sense that beads of this refractive index cause the maximum R_L value. However, the spherical aberration gets worse, when the refractive index gets high, so that the focus on the material directly behind remains relatively poor. For this reason, even the maximum R_L value is much less than for other retroreflectors.

All the three above-mentioned losses are avoided in retroreflective sheeting materials of types using glass beads and mounted on vertical signs. A sign - and its beads - faces the illumination, so that shadows are not essential and the beads collect full illumination. Further, beads are made of normal glass, but the reflection takes place in a reflective layer at a distance behind the beads, where the focus is good.

This explains that the R_L values of road signs are easily 100 times higher than for road markings with glass beads. The associated feature is that the retroreflective beam is narrower, and in fact so narrow that the observer gets to the outskirts of the beam at short distances. Hence the observer experiences high R_L values at long distances to a road sign and lower R_L values as he approaches the road sign.

Such a variation does not occur for road markings with glass beads. These produce a much wider retroreflected beam and much lower, but relatively constant, R_L values.

NOTE: For road signs another characteristic, R_A is used instead of R_L , refer to CIE 54.2. The values of the two characteristics are roughly equal as long as the illumination is roughly perpendicular to the road sign.

B.5 Influence of the side angle β

All the R_L values illustrated in diagrams in B.3 and B.4 are for β fixed at 0° . Night Traffic Reports No. 4 and 6 do provide R_L values for β differing from 0° , the reports do describe losses of R_L values for such cases and they do include those losses into the models in an empirical manner. The losses are explained by a hiding of some illuminated facets or glass beads from view, when the observer studies the illuminated field a bit from the side.

Some of the data are illustrated in figure B.20. The geometrical situation is the one for the 30 m geometry, except that β increases in steps from 0° to 3° . The R_L values are seen to decrease with increasing β and are on the average reduced by 17% at $\beta = 3^\circ$. However, in realistic road scenarios, only side angles up to approximately 1° are relevant and for such side angles the average reduction is a couple of percent only.

Accordingly, the losses are a couple of percent only for a driver of a passenger car, whether it is the headlamp to the left or the right of the driver that is considered. The losses are even smaller for drivers of larger vehicles, where the drivers are higher above the headlamps.

The losses may be significant for drivers of very low vehicles, but for practical purposes and for the large majority of vehicles, the influence of the side angle β can be ignored.

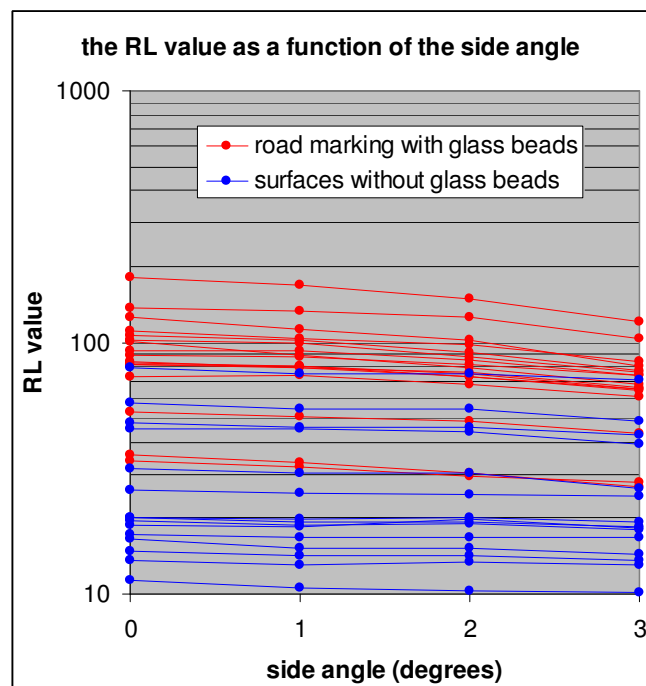


Figure B.20: The R_L value as a function of the side angle β .

B.6 Relevance of the 30 m geometry

The 30 m geometry represents a simplified vehicle with one headlamp at a height of 0,65 m above the road, and with the driver looking at a field 30 m ahead from a position directly above the headlamp at a height of 1,2 m above the road.

For this simplified vehicle, the side angle β is 0° in any road scenario. A real vehicle has two headlamps with some mutual distance and different side angles β that are rarely 0° . However, as stated in B.5, the influence of β can be ignored.

In the 30 m geometry, the observation angle α is $2,29^\circ$ and the illumination angle ϵ is $1,24^\circ$, so that the geometrical factor G equals $\sin(1,24^\circ)/\sin(2,29^\circ) = 0,54$. At the small values of α and ϵ that are relevant in driving scenarios, G can also be obtained as the ratio between the heights of the headlamp and the observer above the road; i.e. $G = 0,65 \text{ m}/1,2 \text{ m} = 0,54$.

The value of G is independent of distance for the simplified vehicle, and therefore the prediction of the models is that the R_L for the 30 m geometry applies for other distances as well. However, there is some uncertainty of this prediction, because the real R_L value may change some with distance. This applies in particular for road markings with glass beads, refer to B.4.

In a real vehicle, the driver is at some distance behind the headlamps. This makes the G value a bit higher than 0,54 at 30 m distance, but approaching 0,54 for longer and more relevant distances.

EXAMPLE: If the driver is 2 m behind the headlamps, the value of G is 0,58 at 30 m distance and 0,55 at 60 m distance.

In view of the above, the simplified 30 m geometry is relevant for a realistic geometry of a passenger car, both at 30 m and at longer distances. By relevant is meant that the R_L value measured for the 30 m geometry does apply for other distances with, however, some uncertainty.

In the same sense, the 30 m geometry is relevant for other vehicles than a passenger car, if the R_L value is first converted to the G value derived for the actual heights of the headlamps and the observer.

For a larger vehicle than a passenger car, the observer has a more high position, so that the actual G value and the converted R_L value is smaller than for the 30 m geometry.

B.7 R_L values in the dry condition

B.3 illustrates that surface reflection in ordinary surface texture can cause relatively high R_L values of $50 \text{ mcd}\cdot\text{m}^{-2}\cdot\text{lx}^{-1}$ or more and that surface reflection in profiles can cause even higher R_L values.

However, texture tends to be reduced and profiles tends to become rounded when exposed to the abrasion by wheel passages. This causes a gradual, but significant, reduction of the R_L values.

B.4 explains that the use of glass bead does lead to amplification of the R_L values and that new road markings may have R_L values measured in hundreds of $\text{cd}\cdot\text{m}^{-2}\cdot\text{lx}^{-1}$. Such values are adequate, but the glass beads are gradually lost in the abrasive action by wheels. In a couple of years, the R_L values of most road markings based on paints and thermoplastics decrease to the neighbourhood of $100 \text{ cd}\cdot\text{m}^{-2}\cdot\text{lx}^{-1}$. A significant part of such R_L values may be caused by surface reflection, so that the beads contribute by less than $100 \text{ cd}\cdot\text{m}^{-2}\cdot\text{lx}^{-1}$.

Some products using other materials or high index beads may provide higher initial R_L values, and may be more resistant to traffic. But the cost of such products prevents their widespread use. Accordingly, there is a need to develop low or average cost products with more durable R_L values.

The contribution by surface reflection is perhaps not large, but could be valuable for maintaining R_L values over extended periods of time and in wet conditions. This is a question of durable facets, structures or profiles. Neither need to be high nor to have dense populations; profiles of 1 mm height cast a 46 mm long shadow in the 30 m geometry and can be spaced with this distance.

The contribution by glass beads is larger, but more easily lost. For this contribution to be more durable, it is a requirement that the beads has a good binding to the material, or that they are replaced by premixed beads to a sufficient degree.

B.8 R_L values in wet conditions

All R_L values from Night Traffic Reports No. 4 and 6 as presented in diagrams in B.3 to B.6 are for the dry condition.

Night Traffic Reports No. 4 and 6 do provide R_L values for a slightly moist condition and conclude that the R_L values are lower than for the dry condition, but that the general variation with the angles are as described by the models.

For road surfaces and road markings without glass beads, it is assumed that a water film is present in the wet condition and that this film reflects some of the light off the surface by specular reflection and thereby prevents illumination of some of the otherwise active facets. In this assumption, the reduction of the R_L value is explained by a reduction of the texture factor T; refer to B.3.4.

This assumption is reasonable at locations where a water film is horizontal or close to horizontal. With grazing illumination, the angle of incidence to the water surface is close to 90° , and the reflectance is large. Refer to figure B.21, which shows the reflectance of a water surface as a function of the angle of incidence.

It is assumed that facets in the microtexture in particular are made inactive, while facets in the macrotexture can protrude from the water film and still be active. Therefore, some value of R_L remains in wet conditions unless the surface is completely flooded.

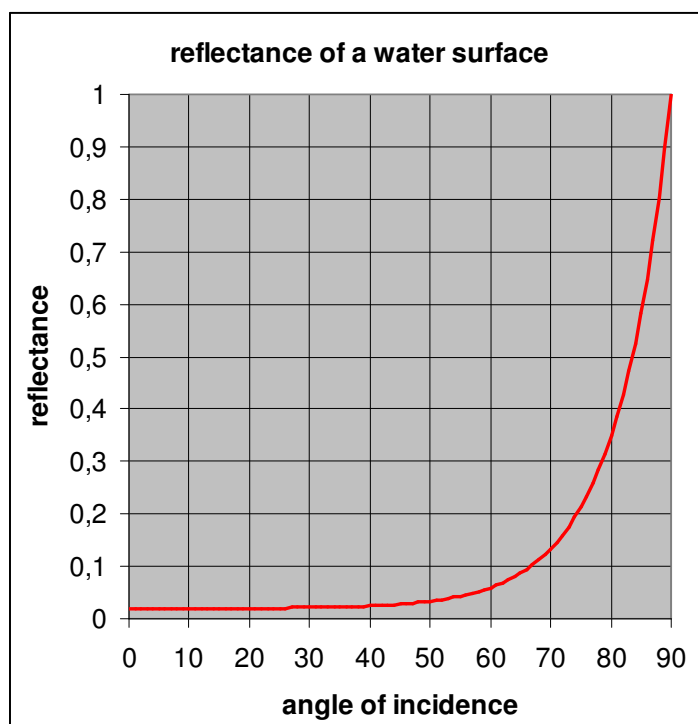


Figure B.21: Reflectance of a water surface as a function of the angle of incidence.

For road markings with glass beads, it should be considered that beads of common size distributions are small with a diameter averaging a fraction of one mm only.

A water film may cover some of the small glass beads and reduce the R_L value by reducing the bead distribution factor B. Refer to B.4.4.

Additionally, a water film may just partially cover some of the small glass beads and disturb the focus of the beads and thereby reduce the R_L value by reducing the amplification factor A. Refer to B.4.5.

EN 1436 defines a wet condition, which is obtained 60 seconds after flooding a road marking with water from a bucket. Practical experience shows that worn road markings with glass beads have a very low R_L values in this wet condition, often virtually zero.

Exceptions are profiled road markings, but even these have low R_L values in the wet condition when worn. The typical values down to $25 \text{ mcd}\cdot\text{m}^{-2}\cdot\text{lx}^{-1}$ can be assigned to reflection in the surface so that the beads are almost without effect.

Other exceptions are road markings with large drop-on beads of typical diameters of 1 mm. These glass beads are sufficiently large to break through a water film and establish some retroreflection in the wet conditions.

There are other exceptions, but these are generally expensive products of limited use.

In general, it can be stated that there is still a need to develop low or average cost products with high R_L values in wet conditions.

An obvious strategy would be to seek to improve the contribution by surface reflection by the means discussed in B.7. In the case of profiled road markings this implies that the profiles should be more durable against being rounded. Refer to figure B.20.

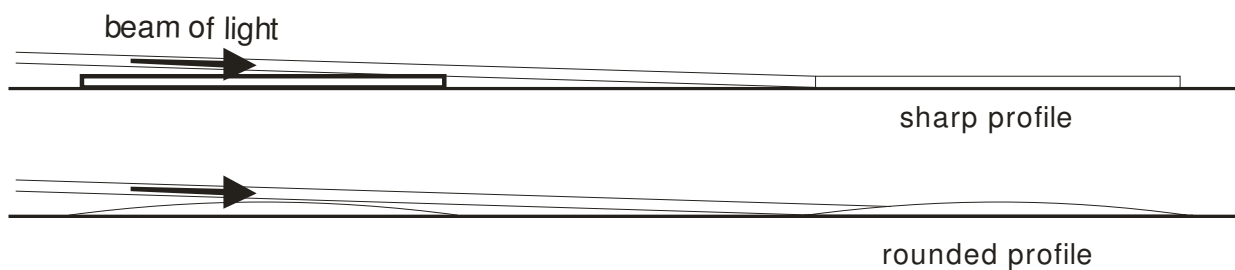


Figure B.20: A sharp profile has an edge that faces the beam of light, whereas a rounded profile does not.

B.9 Literature

Night Traffic Report No. 4 “Reflection properties of road surfaces in headlight illumination”, 1982

Night Traffic Report No. 6 “Reflection properties of road markings in headlight illumination”, 1983

EN 1436 “Road marking materials - Road marking performance for road users”

ASTM E 1710 “Standard Test Method for Measurement of Retroreflective Pavement Marking Materials with CEN-Prescribed Geometry Using a Portable Retroreflectometer”

Influence of pavement marking angular systems on visibility predictions using computer models, Zwahlen, H T; Schnell, T ; Johnson, N ; Hodson, N ; Donahue, T, Transportation Research Record No. 1754, Traffic Control Devices, Visibility, and Rail-Highway Grade Crossings 2001

CIE 54.2 Retroreflection: Definition and measurement, 2001

Annex C: Specular reflection of road markings and road surfaces

C.1 Specular reflection in general

Figure C.1 shows a road crossing at night in situations with a dry and a wet road surface. In both situations, the headlamps on vehicles provoke specular reflections in the form of bright patches stretching from the headlamps in directions towards the observer. The patches are long and narrow and they are brighter for the wet condition than for the dry condition. In the wet condition, even signal heads and tail lamps on the vehicles contribute with fairly bright reflections.

Specular reflections - as illustrated in figure C.1 - make the driver's visual task more difficult by adding to the complexity of the road scenario and by hiding road markings. This applies as well for major road works where light sources such as warning lights and luminaires for work lighting - and even retroreflectors - may cause specular reflections.

It is the purpose of this annex to provide information on specular reflection and to turn the attention towards possible adverse effects for drivers.

An account of specular reflection is given in C.2 including general observations, a physical model for the specular reflection and a test method for field measurement.

Some specular reflection values, as measured on road in Denmark, Norway and Sweden, are provided in C.3.

Finally, the possible adverse effects of specular reflection for drivers are discussed in C.4.



Figure C.1: A road crossing at night in the dry condition (top) and a wet condition (bottom).

C.2 Physical account of specular reflection

C.2.1 General observations

Specular reflection is caused by surface reflection in facets of the road surface.

Surface reflection is guided by the Fresnel law, which is illustrated in figure C.2 for a stone and a water surface. The stone surface is representative for the dry condition and is assumed to have a refractive index of 1,55 typical of glassy surfaces, while the water surface is representative for wet conditions (where facets are covered by a water film) and has a refractive index of 1,335.

Figure C.2 shows that the reflectance of surface reflection is high when the entrance angle is close to 90°. This means that strong specular reflection is reserved for geometrical situations where the incoming light is reflected through a small angle. This causes, almost like a geometrical law, that specular reflections appear to be long and narrow.

It is a further consequence that a light source that is close to the road surface, such as a headlamp on a vehicle, causes specular reflections at a short distance in front of it. The illumination is strong because of the short distance and, accordingly, the specular reflection is strong, but also of limited extension.

A light source that is high above the road surface, on the other hand, such as a road lighting luminaire, causes a specular reflection that is less strong, but of greater extension.

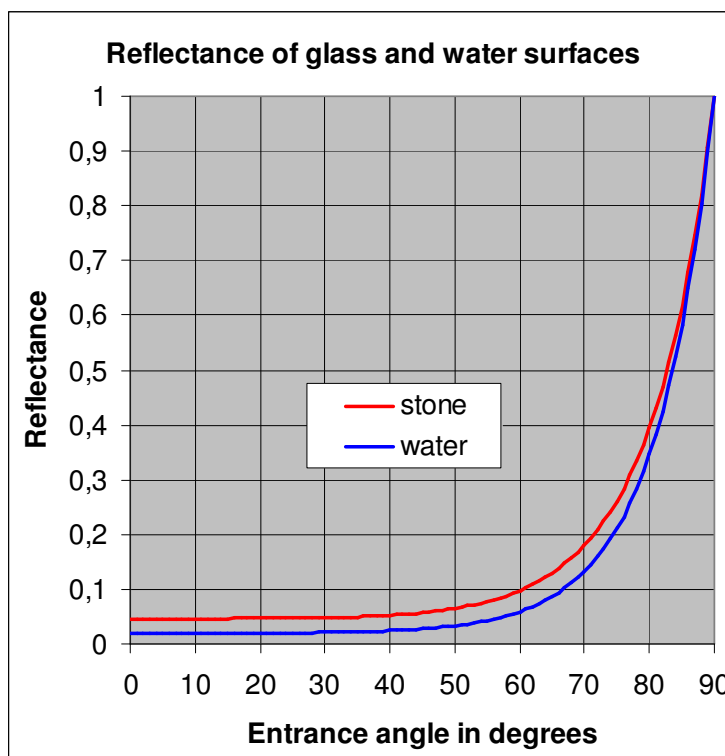


Figure C.2: Surface reflectance of stone and water surfaces.

Figure C.2 shows that the surface reflectance is actually higher for a stone surface than for a water surface and, therefore, it needs to be explained why specular reflections are stronger for wet than for dry surfaces.

The explanation is that a road surface has both microtexture and macrotexture. Even a round stone in the surface has got some microtexture that causes absorption and scattering of the incoming light. However, the microtexture is covered by a water film when the surface is wet, so that larger areas are available for reflection.

This is also the reason that the degree of wetness influences the specular reflection. A more wet the surface has a thicker water film, and a more powerful specular reflection. In the extreme case, when a surface is completely covered by a water surface, it acts like a mirror.

C.2.2 A model for the specular reflection

Light & Optics note No. 2 accounts for detailed measurements of the specular reflection of eight road surface samples in both a dry and a wet condition.

It is surprising that all 16 cases, including eight surfaces in the dry and a wet condition, can be explained by the same assumption regarding facets available for surface reflection. The assumption is that active facets within a road surface area A can form a round surface of a particular shape with a basis area a . Refer to figure C.3.

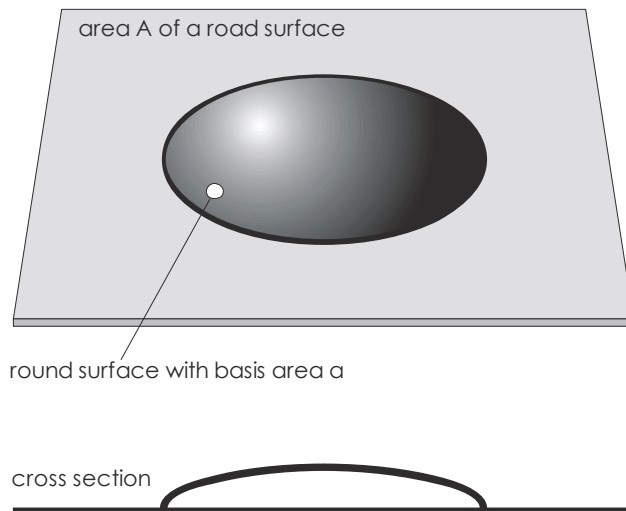


Figure C.3: Active facets within a road surface area A can form a round surface of a particular shape with a basis area a .

The proportion $f = a/A$ is characteristic for each of the above-mentioned 16 cases while the shape of the round surface is the same. This shape is the upper half of an ellipsoid with a height of 0,125 times the diameter of the base.

The reflection values are presented by means of the coefficient of reflected luminance R_L , which is the proportion between the luminance L of a field of the surface and the illuminance E at the field on a plane perpendicular to the direction of illumination.

NOTE: The symbol R_L is normally used for the coefficient of retroreflected luminance, so it may be a bit confusing to use the same symbol for situations with specular reflection. The reader is kindly asked not to become confused by this.

The unit of R_L is $\text{cd}\cdot\text{m}^{-2}\cdot\text{lx}^{-1}$. This is the full unit for a luminance coefficient. When using the luminance coefficient for other types of reflection, the one thousand times smaller unit of $\text{mcd}\cdot\text{m}^{-2}\cdot\text{lx}^{-1}$ is normally used, but specular reflection is so strong that the full unit will do. This should be kept in mind when comparing values expressed in different units.

According to the model, the reflection value is given by:

$$R_L = (f \times \rho \times \text{SRF}) / (4 \times \sin \alpha)$$

where f is the proportion a/A

ρ is the reflectance of surface reflection according to figure C.2

SRF is a value of a 'Surface Roughness Function'

and α is the observation angle measured between the observation direction and the road surface

The surface roughness function SRF is a function of the angle of tilt ν of the round surface at the location, where the reflection takes place. This function is shown in figure C.4 for the round surface of the model.

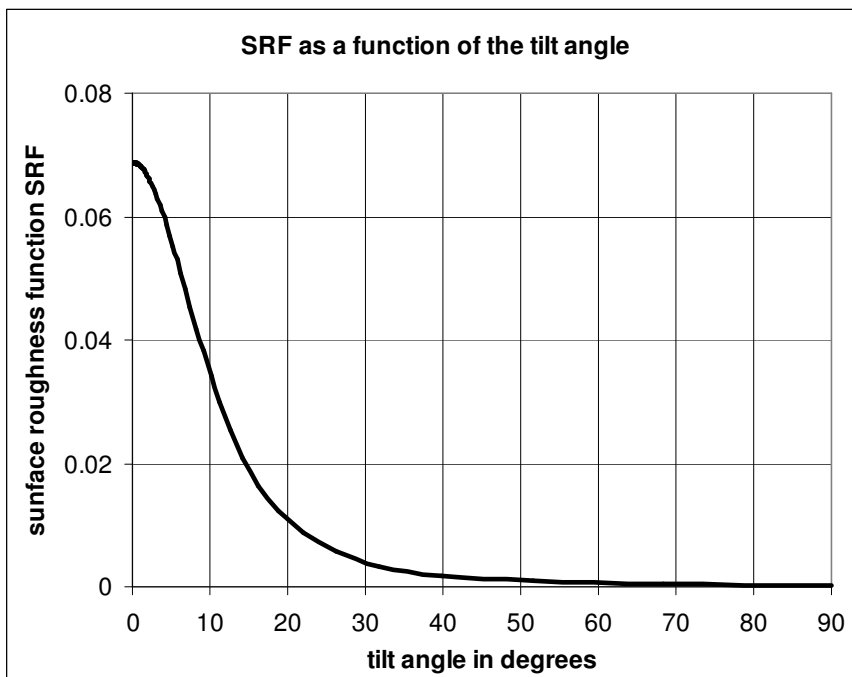


Figure C.4: The surface roughness function as a function of the tilt angle in degrees.

This model is of course not strictly accurate. Figure C.5 has been derived for one of the samples in the wet condition and illustrates the correlation between measured R_L values, and R_L values calculated in accordance with the model.

Ideally, all the points in figure C.5 should lie on a 45° line. There is significant divergence from this line for the smaller reflection values. However, for the most important higher values, and in view of the large variation of specular reflection to be considered later, the fit is acceptable for practical purposes.

Therefore, the model is used in the following; it predicts that the shape of specular reflections is approximately independent of the road surface, but that the strength of the reflection is a characteristic of the surface and may be presented by the proportion f , or by a reflection value for a single geometry.

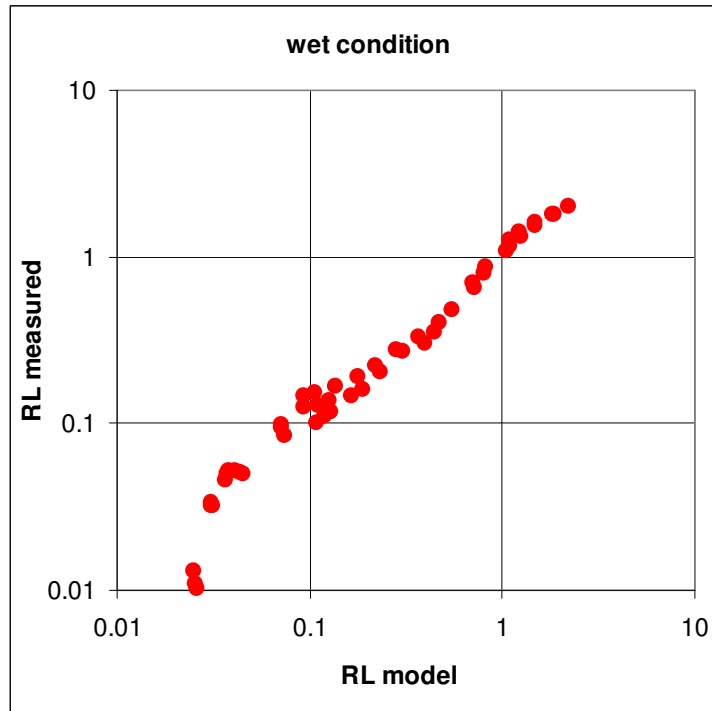


Figure C.5: Comparison of measured R_L values and model R_L values for a particular case.

C.2.3 Test method for field measurements

It is sensible that the single geometry mentioned in C.2.2 is obtained from the CEN 30 m geometry defined in EN 1436 “Road marking materials - Road marking performance for road users” by conversion from a retroreflection geometry to a specular reflection geometry. The converted geometry is shown in figure C.6, it corresponds to a central location within the reflection patch and thereby to relatively large reflection values.

observer

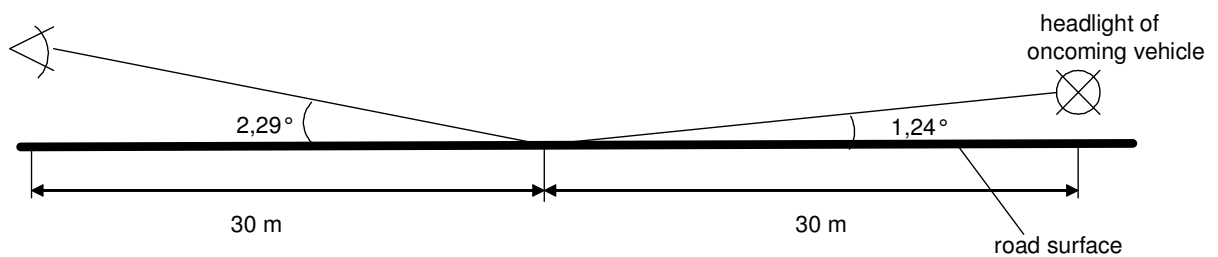


Figure C.6: A single geometry for specular reflection.

With this geometry, handheld retroreflectometers using the CEN 30 m geometry can be modified to provide the specular reflection value instead of the retroreflection value. Such an instrument is shown in figure C.7. The modification is to add a vertical, mirror surface in front of the surface, so that the observation direction is turned backwards by mirror reflection.



Figure C.7: A handheld retroreflectometer using the CEN 30 m geometry with modification to provide the specular reflection value instead of the retroreflection value.

It is a special precaution to use the front surface of a black acrylic plate as the mirror surface. The front surface has a reflectance of only 4%, so that readings are reduced by a factor of 0,04. This is in practice necessary in order to avoid saturation of the readings as specular reflection in wet road surfaces is much stronger than the retroreflection of road markings that the instrument is designed for

With this particular instrument, the measured field is so large, that the instrument includes simultaneously the retroreflection value in full and the specular reflection value reduced by the above-mentioned factor of 0,04. However, the retroreflection value of wet road surfaces is small, while the specular reflection is so high in spite of the reduction, that it is permissible to ignore the addition of the retroreflection value.

For this geometry, the relationship between the proportion $f = a/A$ defined in C.2.2 and the R_L value is:

$$R_L = 26,5 \times f \text{ (cd} \cdot \text{m}^{-2} \cdot \text{lx}^{-1}\text{) for dry road surfaces}$$

$$R_L = 26,2 \times f \text{ (cd} \cdot \text{m}^{-2} \cdot \text{lx}^{-1}\text{) for wet road surfaces.}$$

NOTE: The slight difference in the two expressions is due to different assumptions regarding the refractive indices of stone surfaces and water surfaces of respectively 1,55 and 1,335.

According to these expressions, values larger than approximately $26 \text{ cd} \cdot \text{m}^{-2} \cdot \text{lx}^{-1}$ should not occur in practical measurements. But higher values are in fact obtained in some of the measurements, refer to C.3. This is another indication that the model is an approximation.

C.2.4 Estimates of normally occurring specular reflection values

The design of road lighting installations on traffic roads involves the road surface reflection by means of tables of reflection values. Refer to CIE 144 “Road surface and road marking reflection characteristics”.

The tables used in Denmark and some other countries are labelled N2, N2, N3, N4, W1, W2, W3 and W4 and form a series of increasing degrees of specular reflection. The tables N1, N2, N3 and N4 represent dry road surfaces, while the tables W1, W2, W3 and W4 represent wet surfaces.

Some countries use tables labelled R1, R2, R3 and R3 instead of N1, N2, N3 and N4. This does not make much difference as the degrees of specular reflection are much the same.

It is possible to derive approximately the area proportion f defined in C.2.2 from these tables and thereby to estimate the specular reflection R_L values for the standard geometry of C.2.3. These are plotted in figure C.8.

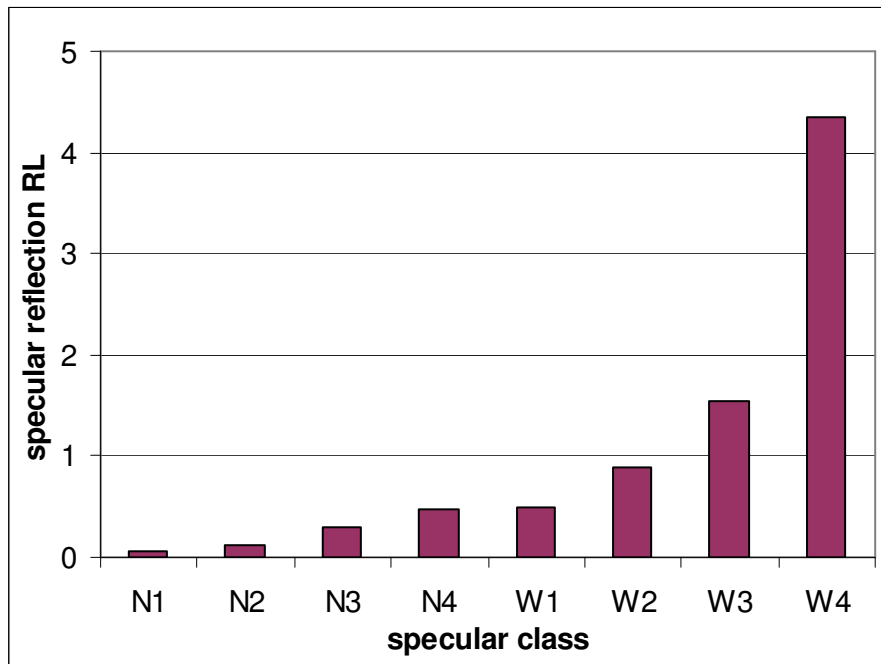


Figure C.8: Approximate specular reflection R_L values in $\text{cd}\cdot\text{m}^{-2}\cdot\text{lx}^{-1}$ for road reflection tables.

Dry road surfaces are normally represented by tables N2 and N3 (R2 and R3 in some countries) so that R_L values of a fraction of one $\text{cd}\cdot\text{m}^{-2}\cdot\text{lx}^{-1}$ should be expected. Wet road surfaces, on the other hand, are often represented by tables WG3 and WG4 so that R_L values from one to a few $\text{cd}\cdot\text{m}^{-2}\cdot\text{lx}^{-1}$ should be expected.

C.3 Measured specular reflection R_L values

C.3.1 Roads in Denmark, Norway and Sweden

The roads were selected so as to represent types of road surface normally used on major roads in the Nordic countries.

The specular reflection values were measured with the modified instrument described in C.2.3. The measurements included both the dry condition and some wet conditions occurring right after pouring water from a bucket over the location, 15 seconds later and finally 60 seconds later.

The specular reflection values are lower for the dry and for the wet conditions, and decrease quickly with time after adding water.

The wet condition after 60 seconds is thought to be the most interesting as this is the same wet condition that is used for the retroreflection of road markings according to EN 1436. This condition is known to be more

wet than those moist and wet conditions that occur in long periods in the Nordic countries and corresponds perhaps to a light rain.

The results for the wet condition after 60 seconds are provided in tables C.1, C.2 and C.3 for the roads in respectively Denmark, Norway and Sweden.

Table C.1: Specular reflection values R_L ($\text{cd}/\text{m}^2/\text{lx}^{-1}$) of some major roads in Denmark.

Specular reflection values $\text{cd}/\text{m}^2/\text{lx}^{-1}$	Major city roads in Copenhagen						Major rural roads				
	Hareskovej-Mellemvangen, south	Hareskovej-Mellemvangen, north	Åboulevarden-H.C. Ørsteds Vej	H.C. Andersens Boulevard-Vester Farimagsgade	Amager Boulevard-Artillerivej, south	Amager Boulevard-Artillerivej, north	Light asphalt concrete, 11 mm	Dark asphalt concrete, 12 mm	Dark asphalt concrete, 8 mm	Light asphalt concrete, 8 mm	Light asphalt concrete, 11 mm
Between wheel tracks	4,5	9,5	36,5	>100	23,0	19	3,2	4,0	4,2	0,8	0,9
In the right wheeltrack	25,2	3,3	>100	>100	>100	3,5	4,3	4,0	3,1	0,6	1,3

Table C.2: Specular reflection values R_L ($\text{cd}/\text{m}^2/\text{lx}^{-1}$) of some major roads in Norway.

Specular reflection values $\text{cd}/\text{m}^2/\text{lx}^{-1}$	Road surface (asphalt concretes)									
	11 mm		11 mm		16 mm		11 mm		11 mm soft	
Location	1	2	1	2	1	2	1	2	1	2
Left	1,7	0,86	2,4	64,4			1,6	2,2	6,6	5,4
Left wheeltrack	3,0	1,7	1,0	0,9			1,6	2,5	6,7	6,3
Between wheeltracks	20,5	5,5	0,9	1,0	0,7	1,4	1,2	2,3	7,0	7,3
Right wheeltrack	7,0	2,0	1,1	0,8	0,5	9,4	2,1	1,8	6,9	6,7
Right	1,9	4,0	7,5	8,3	1,3	2,0	1,4	2,8	5,6	8,1

Table C.3: Specular reflection values R_L ($\text{cd}/\text{m}^2/\text{lx}^{-1}$) of some major roads in Sweden.

Specular reflection values $\text{cd}/\text{m}^2/\text{lx}^{-1}$	Road surface										
	Asphalt concrete, 16 mm			Surface treatment, 12 mm		Asphalt concrete, 11 mm		Asphalt concrete, 16 mm		Asphalt concrete, 12 mm	
Location	1	2	3	1	2	1	2	1	2	1	2
Left	2,0	1,6	1,4	3,0	2,7	1,2	1,0	6,3	2,0	2,1	3,4
Left wheeltrack	20,6	4,1	5,1	2,7	8,0	2,5	1,4	9,1	14,8	1,7	1,5
Between wheeltracks	4,8	7,1	1,8	3,2	2,6	1,2	1,2	1,5	1,2	2,6	2,3
Right wheeltrack	2,3	1,5	75,8	2,6	3,1	1,5	3,3	1,1	1,5	1,9	2,1
Right	0,9	1,5	0,9	1,6	2,3	1,4	1,7	>100	1,7	2,2	2,2

Additional measurements were carried out using other instruments. Refer to “Spegling i våta beläggningar, Störande ljus vid vägarbeten om natten”, Sara Nygårdhs, 2005 for more details.

The major city roads in Copenhagen, refer to table C.1, show in some cases values that are very high or even marked by overflow as more than $100 \text{ cd}\cdot\text{m}^{-2}\cdot\text{lx}^{-1}$. These values are probably caused the compression and polishing actions of the road surfaces by very high traffic loads.

In other cases, the measured values are mostly within the expected range from one to a few $\text{cd}\cdot\text{m}^{-2}\cdot\text{lx}^{-1}$, refer to C.2.4.

One exception is the road surface in Norway described as “soft”. This road surface has probably been compressed by traffic loads to become fairly specular.

A few other cases stand out with high specular values. The reason is probably a high variation of the specular reflection with the local road surface conditions. Large variations can often be observed visually, refer to figure C.9.

Studded tyres are used to a much larger extent in Norway and Sweden than in Denmark and, therefore, the road surfaces often have large aggregates in order to make them durable in view of the heavy wear by studded tyres. For this reason, and because of the action of the studded tyres themselves, it was expected that the level of specular reflection would be relatively low in Norway and Sweden. This, however, is not verified by the data.



Figure C.9:
Example that a large variation of the specular variation can be observed visually.

C.3.2 Further measurements on roads in Denmark

The previous section shows that most road surfaces have specular reflection values up to a few of $\text{cd/m}^2/\text{lx}^{-1}$, while a few road surfaces have much higher values. The question is then, if surfaces with high specular reflection values can be identified by simple observation or by means of other road surface characteristics like skid resistance and texture.

In order to test this, roads were selected from the road network in the previous county of Frederiksborg so as to show a high variation of types and wear. Measurements were done for the wet condition obtained 60 seconds after adding water at 23 locations, both in the right wheel track and between wheel tracks

Initially, the skid resistance obtained by the SRT tester was used at all measuring locations. However, it turned out that there is no obvious correlation between the SRT values and the specular reflection values and, therefore, the SRT measurements were abandoned and are not considered in the following. Close up photographs of all the road surfaces are available, but seem to be of little help in predicting cases of strong specular reflection.

At a later point in time, measurements of the mean profile depths were done at the locations by the Danish Road Institute using a laser profilometer.

Figure C.10 shows that there is some correlation between the specular reflection values (provided as averages for the two transverse locations) and the mean profile depth.

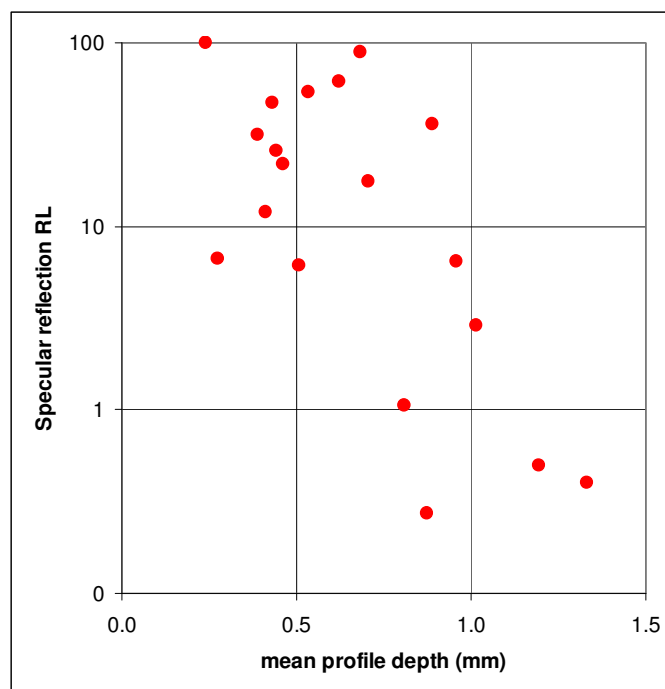


Figure C.10: Correlation between the mean profile depth (mm) and the specular reflection value R_L ($\text{cd/m}^2/\text{lx}^{-1}$).

It is obvious that specular reflection should have some correlation with texture, and therefore one might speculate about reasons why figure C.10 does not show a stronger correlation.

One reason might be that the mean profile depth is not the relevant measure of texture in this connection, as the specular reflection is perhaps more affected by the shape of the texture than by the size. Another reason might be a mismatch between the locations where the two characteristics were measured (the mean profile depths were obtained as averages over a certain length of road at a transverse location that did not match any of the two transverse locations at which the specular reflection values were obtained).

In any case, road surfaces with little texture as reflected by a low mean profile depth may be expected to show a strong specular reflection.

General observations may be helpful. Figure C.11 shows strong specular reflection of vehicle headlamps and is indeed a surface for which high values were measured. Figure C.12 shows strong specular reflection of the sky, and is also a surface for which high values were measured.

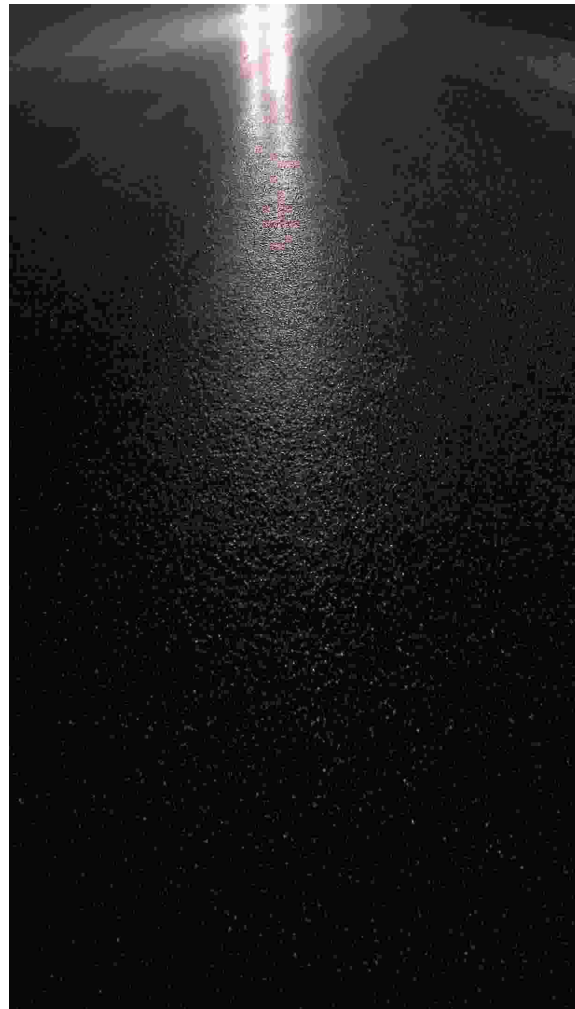


Figure C.11: Strong specular reflections of headlamps.



Figure C.12: Strong specular reflection of the sky.

C.4 Possible adverse effects of specular reflections for drivers

Headlamps on vehicles are a strong source of specular reflections because they are powerful light sources and sit low.

Opposing traffic streams are often directed close to each other at road works so that opposing headlamps become a strong source of direct glare. However, the question in this connection is if headlamps can cause substantial additional glare by specular reflection in the road surface.

According to the reflection model introduced in C.2.2, the total luminous intensity of the reflection in front of a headlamp with a luminous intensity of 10 000 cd in directions towards the road surface can become no higher than approximately 100 cd. This is to be compared to the direct luminous intensity in directions towards other drivers that is typically 200 cd.

Therefore, it should be concluded that headlamps cannot cause serious glare by reflections in addition to the glare they cause directly. This should apply for other light sources in the road environment as well.

NOTE: The completely flooded road surface is of course a particular case that is not covered by the model. A water surface is able to reflect almost the full intensity of headlamps and other light sources.

The next question is if headlamps and other light sources can cause reflections with enough luminance to disturb the visibility of road markings. To answer this question, it is sufficient to compare R_L values of road markings in retroreflection to R_L values of road surfaces in specular reflection.

For the dry situation, these R_L values typically match each other being of the order of $0,1 \text{ cd}\cdot\text{m}^{-2}\cdot\text{lx}^{-1}$ give and take. For wet conditions, on the other hand, the R_L values of road markings are mostly a small fraction of a unit, while the R_L values of road surfaces are easily a full unit or several units.

This shows that, at least for wet conditions, specular reflections of opposing headlamps can easily make it difficult to see the road markings. Other light sources in the environment may well be able to do the same.

The third question is if specular reflections can add so much to the visual complexity that drivers may find it difficult to interpret complex road scenes such as at road crossings and road works. General experience leads to the conclusion that this is the case.

Literature:

Light & Optics note No. 2, 1990, "A model for the specular reflection of road surfaces"

Sara Nygårdhs, 2005, "Spegling i våta beläggningar, Störande ljus vid vägarbeten om natten"

EN 1436:2007, "Road marking materials - Road marking performance for road users"

CIE 144:2001, "Road surface and road marking reflection characteristics"

Annex D: Measurement of the retroreflection of road markings and road surfaces

D.1 Introduction and summary

This annex relates to measurement of the coefficient of retroreflected luminance R_L in the 30 m standard measuring geometry. The 30 m geometry is defined in annex B of EN 1436 “Road marking materials - Road marking performance for road users” and in ASTM E 1710 “Standard Test Method for Measurement of Retroreflective Pavement Marking Materials with CEN-Prescribed Geometry Using a Portable Retroreflectometer”.

The R_L value for the 30 m geometry is relevant for driving at night in a passenger car, when observing a road marking in the illumination of the headlamps of the vehicle. The R_L value is the luminance of the road marking at 30 m distance in proportion to the illuminance at the road marking. The illuminance is measured on a plane perpendicular to the illumination direction.

As luminance has the unit of cd/m^2 (candela per square meter) and illuminance has the unit of lx (lux), the unit of R_L is $\text{cd}\cdot\text{m}^{-2}\cdot\text{lx}^{-1}$. However, with this unit R_L values are normally small fractions only, so in order to obtain more convenient values, the 1000 times smaller unit of $\text{mcd}\cdot\text{m}^{-2}\cdot\text{lx}^{-1}$ is used by convention (mcd means millicandela).

In the 30 m standard measuring geometry, measurement and illumination take place in directions lying above each other in the same vertical plane, and with the measurement and illumination directions forming angles of respectively $2,29^\circ$ and $1,24^\circ$ to the road marking surface. These angles are called respectively α and ϵ in EN 1436. ASTM E 1710 uses a different angular system.

The specifications in the two standards include several other matters, like the permissible angular spreads (also called aperture angles or just apertures) and overall spectral response. The specifications of EN 1436 are considered in the various sections of this annex. The specifications in ASTM E 1710 are identical or at least similar.

It is fortunate that an R_L value obtained in a single geometry is sufficient to express the retroreflectivity of a road marking for relevant geometrical situations. The reasons for this are explained in detail in annex B. One of these reasons is that the retroreflection from a road marking is in a wide beam, which makes most of the geometrical complexity known from other retroreflectors go away. The width of the beam also causes the intensity of the retroreflection to be weak, which explains the above-mentioned use of a small unit.

When measuring values of a characteristic parameter, it is always a problem if there is no way to obtain true values. As an example, the SRT skid resistance of a road marking or road surface depends of the properties of the pendulum and the quality of the rubber glider in contact with the surface. In a way, the truth is in the pendulum, and true values can only be obtained with the pendulum. The problem is that it is difficult to introduce more convenient methods, even if they could be as relevant as the SRT value.

It should be possible to obtain true R_L values, as the R_L has a simple physical definition. It does not matter much if the methods are inconvenient, as long as they can be used to provide true values that can be used to test or calibrate more convenient methods.

The obvious idea would be to obtain true R_L values by full scale measurement according to the definition of the R_L . In principle this requires use of a suitable lamp, a luminance meter and a luxmeter; and darkness so that measurements are not disturbed by daylight.

Full scale measurements are indeed inconvenient, but have been attempted by among else the German BAST (Bundeanstalt für Strassenwesen) and DELTA in connection with investigations by the “Expert Panel” of the CEN/TC 226 WG2 “Horizontal signalisation” in the early 90’s.

Full scale measurements are discussed in D.2, where it is concluded that they require expensive equipment and that it is difficult to obtain accuracy. Full scale measurements are actually not used in practice and, accordingly, cannot be used to provide true values. An exception might be the calibration of road marking panels in the controlled indoor environment, as done by the French road laboratory LCPC (Laboratoire Central des Ponts et Chaussées)

It is then obvious to turn to laboratory measurement in search of a source of true values. As discussed in D.3, a laboratory method is defined in ASTM D 4061 “Standard Test Method for Retroreflectance of Horizontal Coatings”. This method was in use at some laboratories in the USA and it was used to provide “true” values in a couple of tests of handheld retroreflectometers in the 90’s.

This method had been derived directly from similar methods of measuring other retroreflectors, like panels of retroreflective sheeting materials, and was inaccurate for use with road marking panels. It is amusing that at least some of the handheld retroreflectometers provided more accurate values than the “true” laboratory values they were tested against.

Road markings are not really retroreflectors, they are surfaces with texture that are measured and illuminated at grazing angles and with some enhancement of the reflection only. With this in view, a much more accurate laboratory method was developed and offered to the ASTM E12.10 committee.

This work was for some reason not carried to a successful conclusion involving the completion of an inter-comparison test, but the USA institute NIST (National Institute of Standards and Technology) did introduce a version of the laboratory method and is able to supply panels with true values determined this way.

There is no European specification for laboratory measurements, and in fact NIST is probably the only institute that has introduced a satisfactory method. So it is fair to state that trueness cannot be supplied by laboratory measurements on panels in general.

Handheld retroreflectometers are discussed in D.4.

Early types of retroreflectometers used down-scaled versions of the measuring geometry so that a realistic geometry is compressed into the small space within the retroreflectometer volume. It is explained that this that leads to poor accuracy in terms of repeatability and reproducibility, when placing a retroreflectometer on a real road marking. Additionally, calibration had to be by means of panels measured in the laboratory and therefore include the uncertainty of laboratory measurements.

The major problem with the early types is poor control of the measuring distance and non-uniformity of the fields of illumination and measurement. It is much better to use a particular type of optics, the collimating optics, which provides a virtually infinite distance by optical means, and also uniform fields. This leads to heavy improvement of repeatability and reproducibility, and allows calibration by means of white tilted surfaces, which can easily be calibrated with good accuracy in the laboratory.

Additionally, it is explained how the repeatability is improved by the use of a particular mutual arrangement of the fields of illumination and measurement – where the field of measurement is the smaller of the two and enclosed by the illuminated field. This is the opposite of the natural arrangement according to the definition of the R_L , but has the effect that a geometrical factor that is inherent in the R_L is not included in the measurement.

Other requirements to handheld retroreflectometers – and methods of simple tests in accordance with these requirements - are accounted for.

Handheld retroreflectometers with this kind of optics and calibration that also meet the other requirements have gained so much faith by users that they are considered to supply the true values. As an example, portable instruments for use in Germany have to be approved by BASt “Bundesanstalt für Straßenwesen” by comparison to an LTL-2000 as the reference instrument. As another example, several states in the USA had a point in time made the use of the LTL-2000 mandatory and would not allow use of a later version, the LTL-X, without proof of good reproducibility between the two.

This development did take a number of years. The forerunner for the LTL-2000 and the LTL-X, which is the LTL-800, emerged already in 1982. These types have all been supplied by DELTA and have been similar in terms of optics and calibration. The LTL-2000's are no longer produced, but a large number of those and even some LTL 800's are still in use. There are other types by other producers on the market, in particular the Stripemaster by Road Vista and the ZRM 6013 by Zehntner.

The availability of reliable handheld retroreflectometers has spurred development and practical application in the road marking area.

Development includes road marking materials and application methods with the aim of improving the R_L values of road markings, or at least providing predictable R_L values. This development relies on application on road trial sites and testing with handheld retroreflectometers. The testing includes other performance characteristics than the R_L , but the R_L gets the larger attention.

In some countries, type approval of materials requires testing on road trial sites or in wear simulators.

Practical application is reflected by national road standards or tender specifications involving minimum requirements for the R_L in periods as specified in contracts and assuming verification measurements on the roads.

It is of course a problem with handheld instruments that roads are very long, so that the road markings can only be spot-checked. Various schemes for doing this have been devised, but even spot-checking is tedious work. It is also a problem to use a handheld instrument on roads with busy traffic, and it is a particular problem to close such roads.

For these reasons, it is probably often avoided to carry out the road measurements that are implied in contracts. The availability of the handheld instruments may still have an effect in the sense that the measurements can be carried out, if necessary, but this may be on rare occasions only.

The option is to use vehicle based retroreflectometers that can do the measurements when driving at normal speed and thus cover long stretches of road without significant disturbance of the traffic. A few types that have existed and been in use for several years are discussed in D.5 together with a new development by DELTA, the LTL-M.

A few of the tests of the accuracy of measurement that have been carried out in various connections are considered in D.6. The purpose is to give an impression of the accuracy that can be obtained in laboratory measurements and with retroreflectometers, either handheld or vehicle based.

It is indicated that an LTL 2000 may perhaps be as accurate as the above-mentioned laboratory method adopted by NIST.

It is also indicated that a sufficient accuracy has not been demonstrated for the older types of vehicle based retroreflectometers although the accuracy can be reduced, when having good procedures of calibration and alignment and experienced operators.

Further, it is indicated that the LTL-M has a much improved accuracy compared to the older types of vehicle based retroreflectometers. The real accuracy is difficult to establish, but may be as good as for handheld instruments.

In the long run, mobile retroreflectometers with properties like the LTL-M may gain the confidence that would give them the role of the reference instruments. If so, this could spur a further development in the field road markings.

D.2 Full scale measurement

It is possible to measure the R_L value of a road marking according to the definition; as the proportion between the luminance L of a field of the road marking and the illuminance E at the field.

This requires the use of a lamp directed to illuminate a field of the road marking at the desired location, a luminance meter with the measuring field aimed at the field and a luxmeter placed at the location and directed towards the lamp. Refer to figure D.1.

In practice, a set-up as shown in figure D.2 has been used in some cases to measure R_L values in the 30 m geometry. However, the requirements to the equipment turned out to be high and problematic.

Figure D.3 shows typical apertures in full scale measurements and the maximum permissible apertures defined in EN 1436 and ASTM E 1710. The maximum permissible apertures are large, and can be large, because the retroreflected beam from road markings is wide. It is for the same reason that the retroreflection is weak and large apertures are needed.

The figure shows that full scale measurements are at a disadvantage compared to dedicated equipment, as the aperture of a luminance meter is small while dedicated equipment can be made to use the full aperture. Accordingly, the lamp must be powerful, but in spite of that the signal is weak.

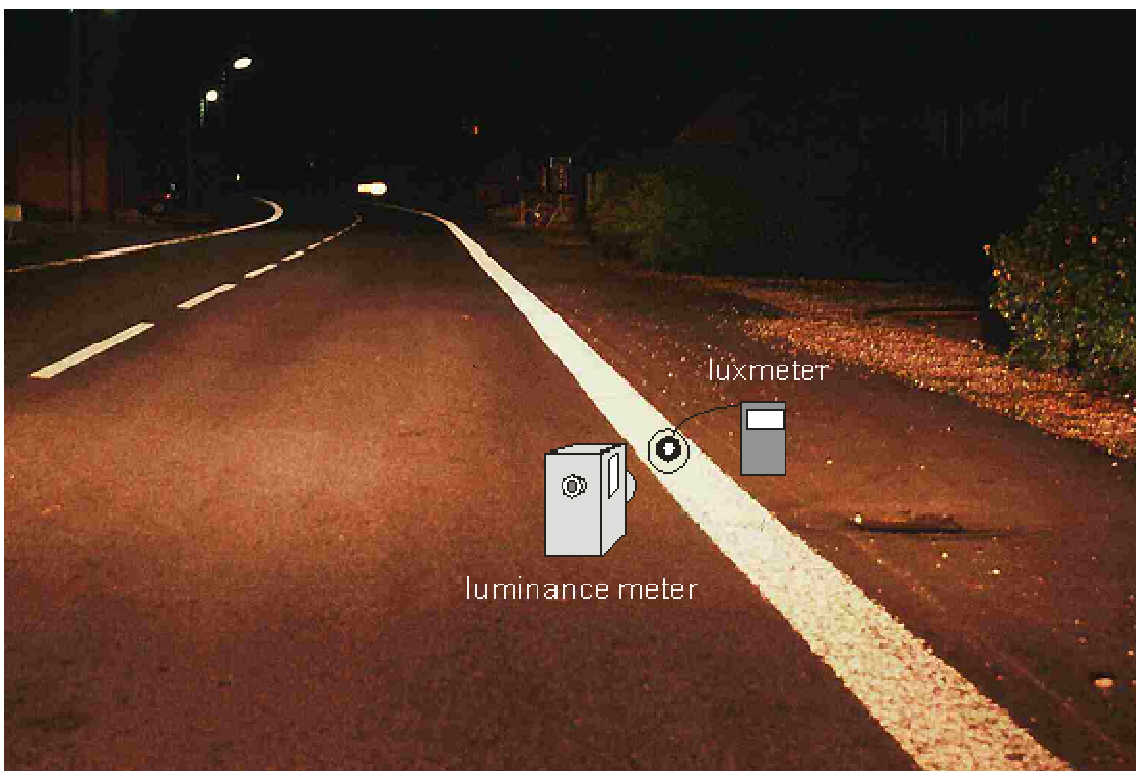


Figure D.1: Principle of full scale measurements of R_L values.

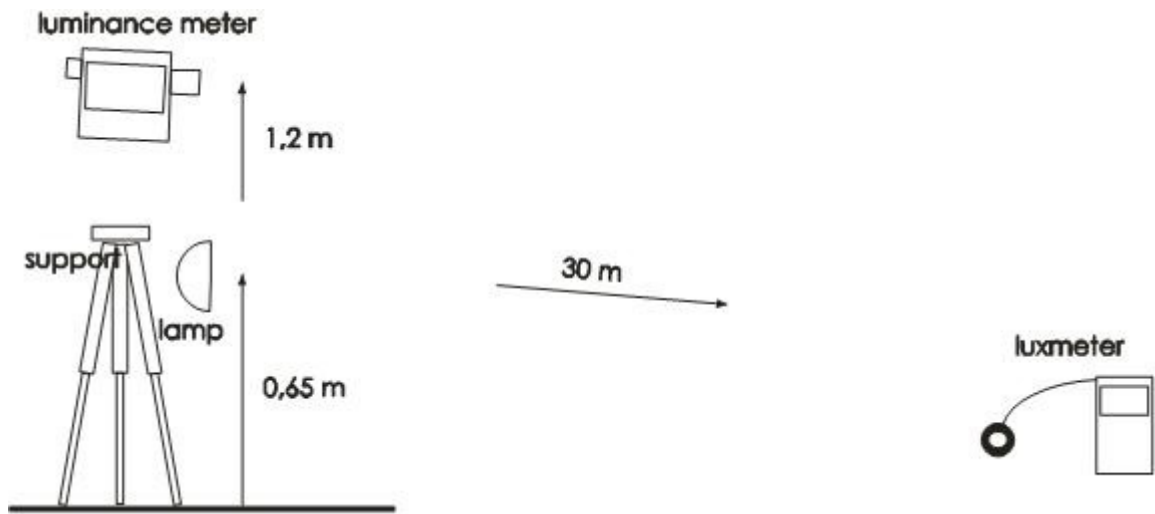


Figure D.2: A set-up for use for the 30 m geometry.

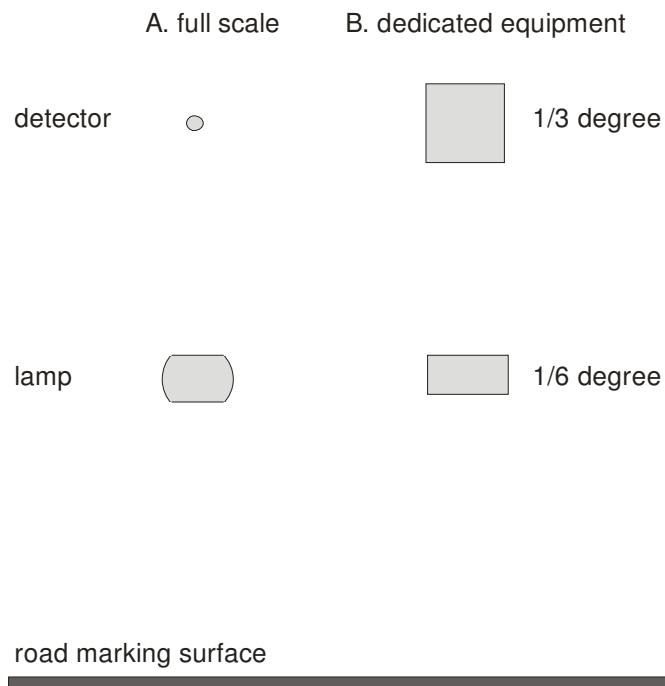


Figure D.3: Typical apertures in full scale measurements (A) and the apertures used in dedicated equipment (B).

EXAMPLE: If the lamp has a luminous intensity of 100.000 cd in the central direction, the illuminance at 30 m is $100.000/30^2 = 111$ lx.

In order to be able to resolve one unit of $\text{mcd}\cdot\text{m}^{-2}\cdot\text{lx}^{-1}$, the luminance meter must have a sensitivity of 111 lx times $0,001 \text{ cd}\cdot\text{m}^{-2}\cdot\text{lx}^{-1} = 0,111 \text{ cd}\cdot\text{m}^{-2}$. At the same time the measuring field of the luminance meter must be small, so that it can be contained within a 10 cm wide road marking at the distance of 30 m. The maximum measuring field is then approximately 11 minutes of arc, but should in practice be smaller, for instance 6 minutes of arc. Luminance meters with such properties can probably not be found on the market, at least they would be expensive.

Other difficulties emerge in practice, like intrusion of foreign light, reflections from bright surfaces ahead, curve of the road etc. Additionally, the measurements are inconvenient as they have to be carried out at night and traffic on the road has to be stopped.

For these reasons, full scale measurements have never proved to be accurate, and they have only been used on an experimental basis. An exception is a full scale method used in laboratory measurements in indoor conditions; refer to D.3.

D.3 Laboratory measurement

As full scale measurement cannot be used as the reference method providing “true” R_L values, it is natural to turn to laboratory measurement for that purpose.

One such method is defined in ASTM D 4061 “Standard Test Method for Retroreflectance of Horizontal Coatings”. A panel with the road marking is placed horizontally in a dark room, see figure D.4. A projector lamp with a liberally wide beam is used to illuminate the panel and a luxmeter type of photometer is used measure the total reflected luminous intensity. The projector lamp and the detector is placed at a fairly long distance, for instance 20 m, at the heights that provide the correct angles.



Figure D.4: Test panel with a road marking seen at a small angle.

The luminance of the road marking L is determined as I/A_p , where I is the measured total reflected luminous intensity and A_p is the area of the road marking surface A as projected onto the measuring direction by multiplication with $\sin\alpha$. The illuminance E is measured at the centre of the road marking and the R_L value is determined as L/E .

The method provides a small signal only for a number of reasons. The R_L of road markings is low compared to other retroreflectors, the projected area of a road marking on a panel is small, and the detector is placed at a long distance and collects light in a small aperture only.

Simultaneously, because of wide beam illumination and wide field detection by a luxmeter, the ambient signal from light reflected in the room may be strong.

Therefore, a low signal has to be determined even when overlaid with a strong ambient signal. In itself, this sets a limit to the accuracy that can be obtained.

But there is a more fundamental source of error, that the method has the inherent assumption that the road marking surface is plane. This is not quite true as real road marking surfaces have at least some texture and in some cases large deviations from planeness by curve, structure or profile.

Illumination at a the very low angle of 1,29° goes deep into the texture at the front end of the panel – because there is nothing in front to cause shadows – and high up in the texture at the back end – because whatever is high up will catch light. Accordingly, the surface catches more light than a plane surface would do, and therefore reflects with a higher luminous intensity. The results is a bias towards higher R_L values to a degree depending on the surface.

EXAMPLE: A 500 mm long plane surface collects light in proportion to a projected height of $500 \times \sin 1,29^\circ$ mm = 11,2 mm. A surface with a 1 mm texture might catch light as if the projected height is $11,2 + 1 = 12,2$ mm, which is an increase of 9 %.

For these reasons, the method is not accurate.

The method has been derived from a similar method used for retroreflective sign panels and other retroreflectors. For such retroreflectors the method is accurate, because the retroreflection is much higher, and because such panels and retroreflectors are measured at angles, where texture has no influence.

This shows that road markings are not really plane retroreflectors, they are not plane and they are hardly retroreflectors. Road markings are more comparable to road surfaces and it is in fact better to apply the methods and conventions that are applied for road surfaces, than those applied for retroreflectors.

An improved method needs to have more suppression of ambient light, and more control with the amount of light falling on the road marking surface. Figure D.5 illustrates such a method, which has been called the “band method”.

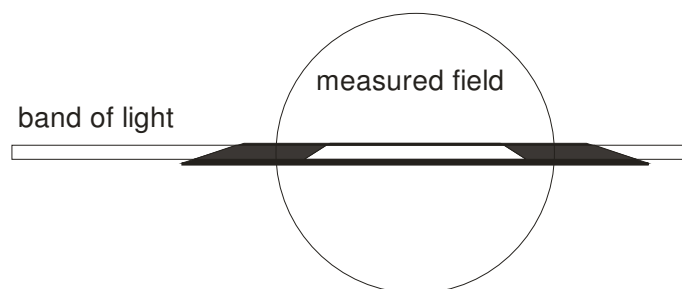


Figure D.5: Illustration of the “band method”.

The road marking is illuminated by a narrow band of light that covers part of the length only, but all of the width. The luminous intensity of reflected light is measured with a luminance meter type of detector that has a relatively small measured field.

This reduces the ambient signal to the degree that it can be ignored, because much less light is emitted into the room, and because most of the room is excluded from the measurement.

The remaining matter is to provide calibration. This is done by means of a tilted white reflection standard that is high enough to contain a part of the band of light. The R_L of the road marking is obtained as

$$R_L(\text{road marking}) = R_L(\text{standard}) \times W(\text{standard}) \times S(\text{road marking}) / (S(\text{standard}) \times W(\text{road marking}))$$

where $W(\text{standard})$ is the width of the standard
 $W(\text{road marking})$ is the width of the road marking
 $S(\text{standard})$ is the signal provided by the standard
and $S(\text{road marking})$ is the signal provided by the road marking.

The value of $R_L(\text{standard})$ has to be obtained by fundamental methods.

This method was first developed by DELTA and offered to the ASTM E12.10 committee in charge of ASTM D 4061. It was proved to be sufficiently accurate to serve as a reference method.

A version of the method has been adopted by the National Institute of Standards and Technology, NIST (USA). ASTM D 4061 is under revision in order to make it reflect the method. This method can also be applied as DELTA, but is probably not in use anywhere else for the time being.

The only competitor to this method is probably to use full scale measurements in the more controlled indoor environment. At least the French road laboratory LCPC (Laboratoire Central des Ponts et Chaussées) uses such a method to calibrate road marking panels.

D.4 Portable retroreflectometers

D.4.1 Introduction

Early types of retroreflectometers were in use already in the 1970's. There was several of those, of which two are shown in figures D.6 and D.7.



Figure D.6: An early type of retroreflectometer.



Figure D.7: Another early type of retroreflectometer.

These and other early types used the same kind of arrangement, simulating a driving situation by means of a lamp and a detector on a small scale. A housing serves to reduce the ambient daylight.

Refer to figure D.8, which shows such an arrangement. The lamp and the detector need not be placed physically at the indicated location, but can be placed as images created by suitable optics in order to make the components fit into the limited space.

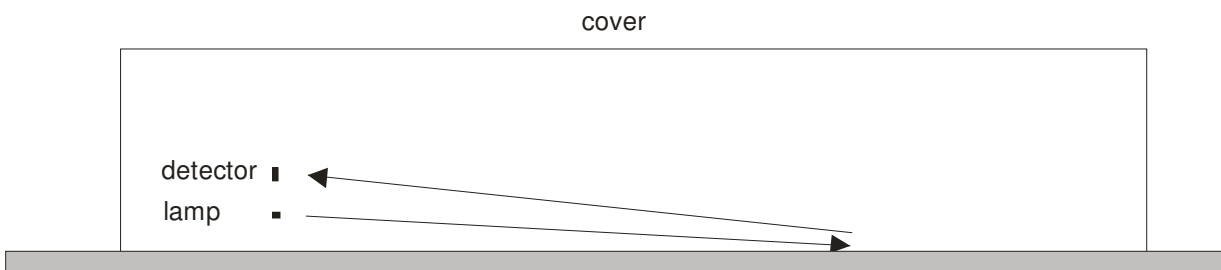


Figure D.8 Principle of early portable retroreflectometers.

A problem with these early types is that a retroreflectometer, when placed on a real road marking surface, may sit a bit high or low, or may be tilted a bit. This changes the actual measuring distance and affects the reading because of the distance law of illumination. Another problem is that the fields of illumination and measurement are not uniform, and that they move relative to each other when placing a retroreflectometer on a real road marking. This also affects the reading.

For these reasons, probably, the early types used larger angles than defined in the 30 m geometry corresponding to distances in the range of 10 to 15 m. This does counteract the above-mentioned influences on the readings, but not to a sufficient degree, and it makes the measurement less relevant for driving situations.

The first instrument to demonstrate solutions to these problems was the LTL 800 by DELTA, which emerged in 1984, see figure D.9. This instrument uses the collimating optics, which is ideal for simulating long distances within limited space.

The simulated situations were similar for the early types, but not quite the same, so that the measured values were not directly comparable. The LTL 800's were adjusted to a 50 m geometry, in which the angles are correspondingly smaller than in the 30 m geometry.

However, in the middle of the 90's the WG2 of CEN/TC 226, when drafting the first version of EN 1436, defined the 30 m geometry as a compromise between the different geometries. After this, the LTL 800 was adjusted to the 30 m geometry. Later retroreflectometers were all built for this geometry. The early types were not redesigned or adjusted, and gradually disappeared.

The main argument for short simulated geometries is that they allow larger signals and less critical adjustment of the angles. The main argument for longer distances is that they are more relevant for drivers. However, the LTL 800's worked well and proved that the 50 m geometry is viable, so in a way it was a pity that the compromise settled on 30 m.

The success of the LTL 800 was largely based on use of the collimating optics, which introduces so many advantages that it is useful to understand how it works. Therefore, collimating optics are explained in D.4.2, advantages regarding suppression of variation in D.4.3 and D.4.4, and advantages regarding calibration in D.4.5.

On this basis, a summary of reasonable requirements to handheld retroreflectometers is given in D.4.6.



Figure D.9: One of the first LTL 800's.

D.4.2 Collimating optics

The solution to the major problems with the early types of retroreflectometers is to raise the distance by optical means. This can be done by means of a collimating lens as shown in figure D.10.

A small lamp and a small detector (or images of the physical lamp and detector) are placed in the focal plane of a lens.

When seen through the lens, as illustrated in figure D.11, it looks as if the lamp and the detector is at a very long distance, actually at the virtual infinite. The lens serves to create these infinitely remote images, and serves simultaneously as the window that gives a look to the images. Accordingly, the images of the lamp and the detector appear to be of constant angular sizes regardless of the distance and location from which the lens is observed.

This means that the apertures of illumination and measurement are constant; they are actually those that would be seen directly at a distance equal to the focal width of the lens and they can be given the desired values. Those are in practice the maximum permissible apertures of the 30 m geometry.

The angular separation between the centres of the lamp and the detector also remains constant and can be given the desired value. This is in practice the $1,05^\circ$ of the 30 m geometry.

As the images of the lamp and the detector are at the virtual infinite distance, the illuminance as well as the sensitivity of detection is independent of the distance from the lens. In total, the collimated principle is

perfect for portable equipment, but it must be adapted for the particular purpose as considered in the following.

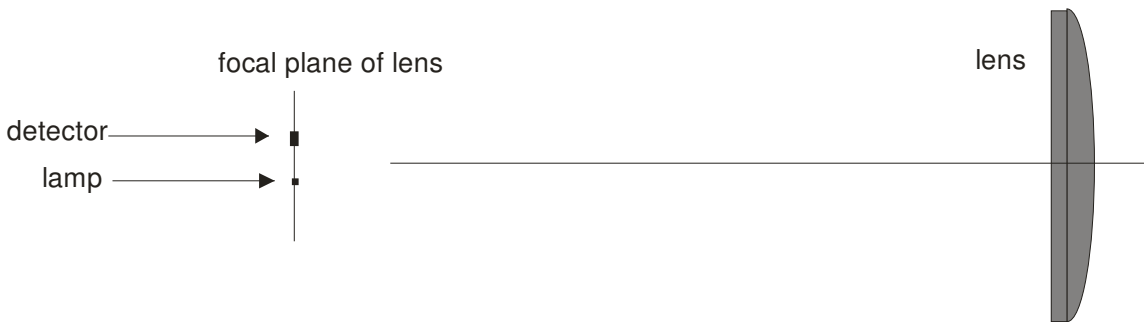


Figure D.10 A lamp and a detector placed in the focal plane of a lens.

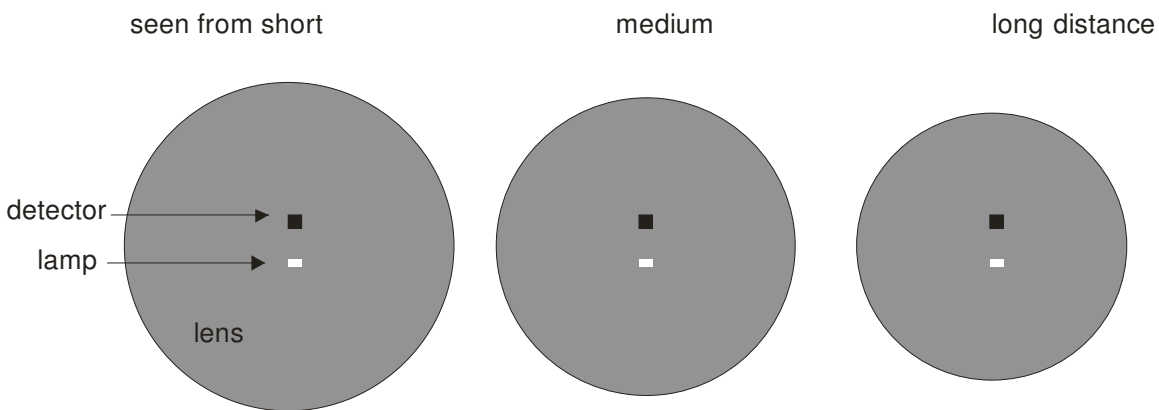


Figure D.11 Lamp and detector seen through a lens at different distances.

Because the lens is the window to the images of the lamp and the detector, the illuminated and detected fields created by the images can only be as wide as the lens. It is desirable that the fields have widths of at least 40 to 50 mm, so that the lens diameter must be minimum 50 mm.

A second matter to consider is that the lens does not find room close to the ground or road marking surface. Instead, a mirror is placed close to the ground, allowing that the lens, lamp and detector can be placed upright; see figure D.12.

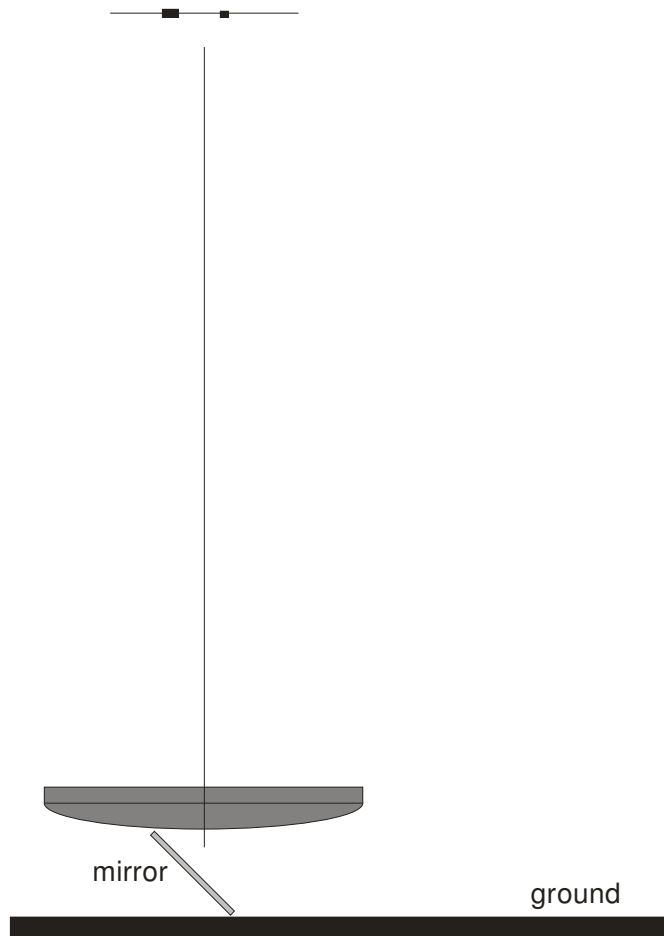


Figure D.12: Use of a mirror close above the ground level.

Figure D.13 shows the view to the lens, and further on to the lamp and the detector, through the mirror. It is obvious that the mirror now serves as the window that confines the view and thereby also the fields on the road marking surface.

The third matter is that one of the fields, illuminated or measured, must be fully enclosed in a uniform part of the other field. This is a general requirement for reflection measurements and serves to provide easy calibration and robustness to the precise locations of the fields.

Therefore, the view to the lamp is reduced as shown in figure D.14, so that the illuminated field becomes fully contained within the measured field. As an alternative, the view to the detector could have been reduced, but the actual choice has some advantage as discussed later.

Such a reduction of the view can be introduced in different ways; here it is sufficient to note that it can be done.

EXAMPLE: In the LTL 800's by DELTA, there were actually two mirrors behind each other, one for the lamp and one for the detector. The mirror in the front was semitransparent and thus allowed for a view to the mirror in the back, and to the lamp through a diaphragm, which reduced the view.

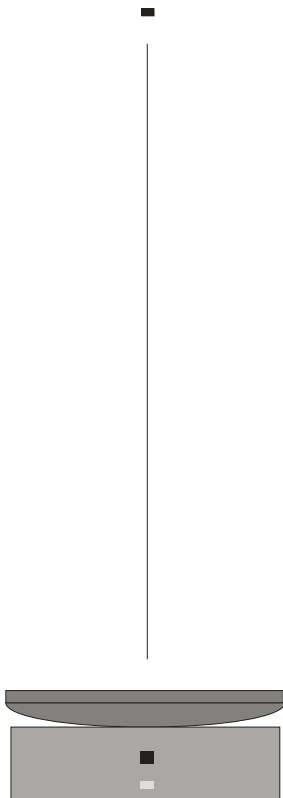


Figure D.13: View through a mirror to the lens, and further on to the lamp and the detector.

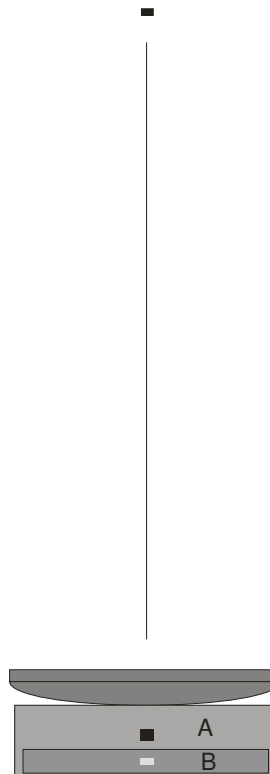


Figure D.14 Reduction of the view to the lamp.

When a retroreflectometer with such optics is placed on a plane surface, the fields are as illustrated in figure D.15. Both of the fields are uniform except that the edges are un-sharp. All of the illuminated field, including un-sharp edges, is enclosed within the uniform part of the larger measuring field. The measured area is defined by the smaller of the two field; in this case the illuminated field.



Figure D.15: Example of placement of the illuminated field (I) and the measured field (II).

D.4.3 Tolerance to tilts

EN 1436 mentions two different arrangements of the illuminated and the measured field:

- A: the measured field is enclosed within the illuminated field
- B: the illuminated field is enclosed within the measured field.

It is arrangement B that is illustrated in figure D.15. However, an illustration of arrangement A would look the same, just interchanging the labels I and II.

In arrangement A, the measurement relates to the luminance L . Further, as the illuminance E is monitored, the measurement relates to luminance in proportion to illuminance, which is R_L . Accordingly, arrangement A leads to direct measurement of the R_L .

It is explained in annex B that the R_L value varies with a geometrical factor G equal to $\sin\varepsilon/\sin\alpha$. The correct value of G is $G_0 = \sin\varepsilon_0/\sin\alpha_0 = \sin 1,24^\circ/\sin 2,29^\circ = 0,542$. If the retroreflectometer is tilted by a small angle δ , the illumination and observation angles change away from the intended values of ε_0 and α_0 to $\varepsilon = \varepsilon_0 + \delta$ and $\alpha = \alpha_0 + \delta$. This means that the geometrical factor G changes to $\sin(\varepsilon_0 + \delta)/\sin(\alpha_0 + \delta)$ and the measured R_L value changes accordingly.

Therefore, when arrangement A is used, tilts affect the measured R_L value directly by means of the geometrical factor G . Even small tilts lead to significant change of the measured R_L value.

EXAMPLE: Assume that a retroreflectometer has feet spaced 400 mm apart and that the back feet are lifted 1 mm relative to the front feet. The instrument is then tilted by $0,143^\circ$. The geometrical factor G changes from 0,542 to 0,568 implying a change of the R_L value of 5 %.

In arrangement B, the measurement relates to luminous intensity. Further, as the light output is monitored, the measurement relates to intensity in proportion to luminous flux, which is a characteristic that differs from the R_L and may be called R_L^* . It can be shown that the two are related by $R_L^* = R_L/G$.

In this way, the geometrical factor G is omitted from the measurement of the R_L^* value. The R_L value is obtained as the product of the measured R_L^* value and the correct value of G for the 30 m geometry ($G_0 = 0,542$), so that tilts do not directly affect the R_L value. There may still be some variation with tilts caused by other factors (refer to annex B), but in an overall sense the variation with tilts is strongly reduced. This is a valuable feature, that helps to improve the accuracy of the measurement.

In conclusion, arrangement B is preferable to arrangement A.

D.4.4 Tolerance to lifts

When a retroreflectometer is lifted, the illuminated field and the measured field both move forwards. For the 30 m geometry, the movements are by respectively 46 mm and 25 mm for each mm of lift.

This is illustrated in figure D.16 for lifts that increase in uniform steps. For these lifts, the illuminated field remains fully within the constant part of the measured field so that the signal remains at a maximum and does not change from step to step.

Accordingly, a retroreflectometer using collimating optics can have a tolerance against lifts provided that the larger of the two fields has some reserve. There is a limit to this tolerance, as further lifts make the illuminated field move gradually out in front of the measured field so that the signal decreases.

A tolerance to lifts is a valuable feature in terms of accuracy of measurement. It will be discussed later what tolerance is needed.



Figure D.16: Movements of the illuminated and the measured fields with lift of the retroreflector in uniform steps.

D.4.5 Calibration of retroreflectometers

Before calibration, a retroreflectorometer must be zero-adjusted in order to compensate for any zero-signal generated by the detector or by the optics.

For this purpose a black surface is used. An extremely black surface is created as the aperture of a wedge of two black acrylic plates, see figure D.17.

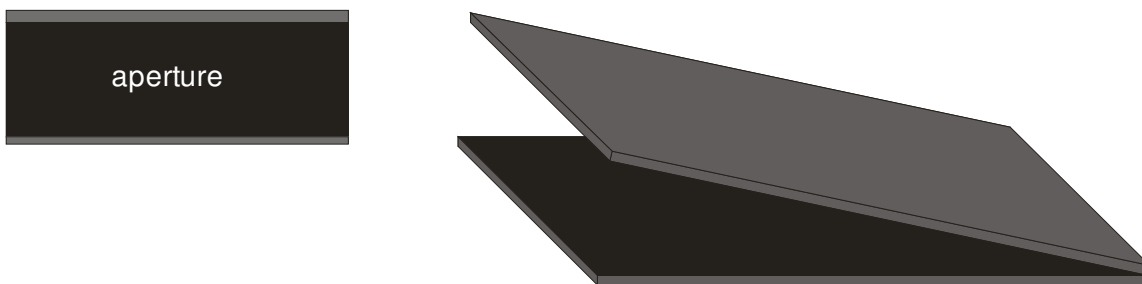


Figure D.17: An extremely black surface formed as the aperture of a wedge of two black acrylic plates.

NOTE 1: DELTA retroreflectorometers are provided with a black surface in the form of a wedge as shown in figure D.17. The wedge is either in a protective bottom supplied with the instrument or it forms a unit together with a calibration block. The instruments provide guided instructions on how to perform the procedure of zero-adjustment and calibration.

It may seem that the most simple calibration standard is a panel with a pavement marking, whose R_L value has been obtained in laboratory measurement. A panel can be used by any type of retroreflector regardless of its optical design and arrangement.

However, it is not easy to obtain panels that are uniform, and it is not easy to do accurate measurement of R_L values of panels. Additionally, panels are not convenient in terms of transport and maintenance.

Therefore, it is more attractive to use calibration blocks with white tilted surfaces. These are more easy to measure in the laboratory, they are small and handy, and the surface can be created by a robust material like a white ceramic plate. Such plates can have high reflectance values of 0,9 that vary a few percent among plates only. Further, white ceramic plates can be cleaned by washing.

A calibration block is shown in figure D.18. Such blocks can probably be used only for retroreflectometers with collimating optics.

NOTE 2: DELTA retroreflectometers are supplied with such blocks, which are calibrated at DELTA with accreditation and traceability to NIST.

The standard R_L value to assign to a calibration block is in principle the value that has been measured in the laboratory. However, for a calibration block that is to be used to calibrate a retroreflector with arrangement B, refer to D.4.3, it is convenient to assign the value of $G_0 \times R_L$ so as to introduce the multiplication with the factor G_0 that is needed according to D.4.3. The value of G_0 for the 30 m geometry is 0,542.

The purpose of tilting the white surface of a calibration block is to avoid that specular reflection from the surface influences the calibration. A tilted white surface with a high reflectance has an R_L value that approaches the theoretical maximum value for diffuse reflection of $1000/\pi = 318 \text{ mcd}\cdot\text{m}^{-2}\cdot\text{lx}^{-1}$. After multiplication with G_0 , the maximum R_L value for diffuse reflection is $172 \text{ mcd}\cdot\text{m}^{-2}\cdot\text{lx}^{-1}$. White ceramic plates typically have values of $160 \text{ mcd}\cdot\text{m}^{-2}\cdot\text{lx}^{-1}$ (after multiplication with G_0), which are suitable central values.

During calibration, the block is placed at a location relative to the retroreflector, where the white surface contains the smaller of the two fields of measurement, and where the larger of the two fields contains the smaller. For a particular retroreflector, the intended location will be obvious or fixed by design.



Figure D.18: Calibration block with a white tilted surface.

D.4.6 Requirements to portable retroreflectometers

It is not directly a requirement in neither EN 1436 nor ASTM E 1710 that a portable retroreflector is based on the collimating principle, but in practice this should be requested because of the advantages in terms of accuracy of measurement and easy calibration. Refer to D.4.2.

Additionally, it is not a requirement that a portable retroreflector has the arrangement B of the fields of illumination and measurement, but in practice this should also be requested because of the improved repeatability. Refer to D.4.3.

It is a requirement in EN 1436 that a portable retroreflectometer has a minimum tolerance to lifts, refer to D.4.4 and see also item f in the list of requirements provided below. However, it is an advantage if the tolerance is larger than the minimum, as this is necessary when measuring profiled road marking with profiles higher than the minimum tolerance (2 mm).

Finally; it is not a requirement either that a calibration block with a white tilted surface is used for calibration, but this is preferable for the reasons mentioned in D.4.5.

Both ASTM E 1710 and EN 1436 provide a number of direct requirements. Those of the EN 1436 are the most complete and are listed below:

- a. angles and aperture angles are in accordance with the 30 m geometry and the measured area is minimum 50 cm²
- b. the spectral match has a quality that ensures a maximum error of ± 5 % for yellow road markings
- c. the range of R_L values that can be measured is from 1 up to at least 2000 mcd·m⁻²·lx⁻¹
- d. daylight, in particular direct sun, does not influence the readings
- e. there is no offset by surface reflections on the road markings (in particular on wet road markings)
- f. the R_L values measured at lifts of -1 mm, 1 mm, and 2 mm deviate maximum ± 10 % from the R_L value measured at 0 mm
- g. calibration is by means of a traceable standard sample for which independent calibration is possible.

Test methods for these requirements are provided or at least mentioned in EN 1436:

- a. observe the patch of light from the illumination on a screen at a long distance and check that it agrees with the requirements for illumination
- b. place yellow long pass absorption filters with known transmittance values for standard illuminant A illumination in front of a white standard and verify that the reading drops by a factor that is within ± 5 % the transmittance values
- c. use panels with R_L values ranging from very low to very high
- d. repeat measurements in direct sun with and without additional cover by for instance black cloth
- e. use a panel in the form of a black acrylic plate and observe that the reading is virtually zero (reflections in the internal surfaces of the retroreflectometer might cause a reading)
- f. use a panel placed at different heights as and observe that the reading complies with the requirements
- g. refer to the documentation provided by the supplier of the retroreflectometer.

Most of the tests are simple and do not require much equipment or expertise. The test of the illumination mentioned in item a can in principle also be carried out for the measurement by sending light through the measurement optics. However, this requires some expertise and dismantling of the retroreflectometer.

Concerning the test of spectral match mentioned in item b, filters of the types OG 515, OG 530 and OG 550 by Schott are suitable as they are simple and have pure yellow colours that span the interesting range.

When these filters are 1 mm thick and placed so that both the incoming light and the reflected light passes through the filters, the transmittance values are approximately as indicated in table D.1. The chromaticity values are shown in figure D.19 for information.

Table D.1: Transmittance values of 1 mm thick filters passed twice.

Schott filter type	Transmittance
OG 515	0,73
OG 530	0,66
OG 550	0,52

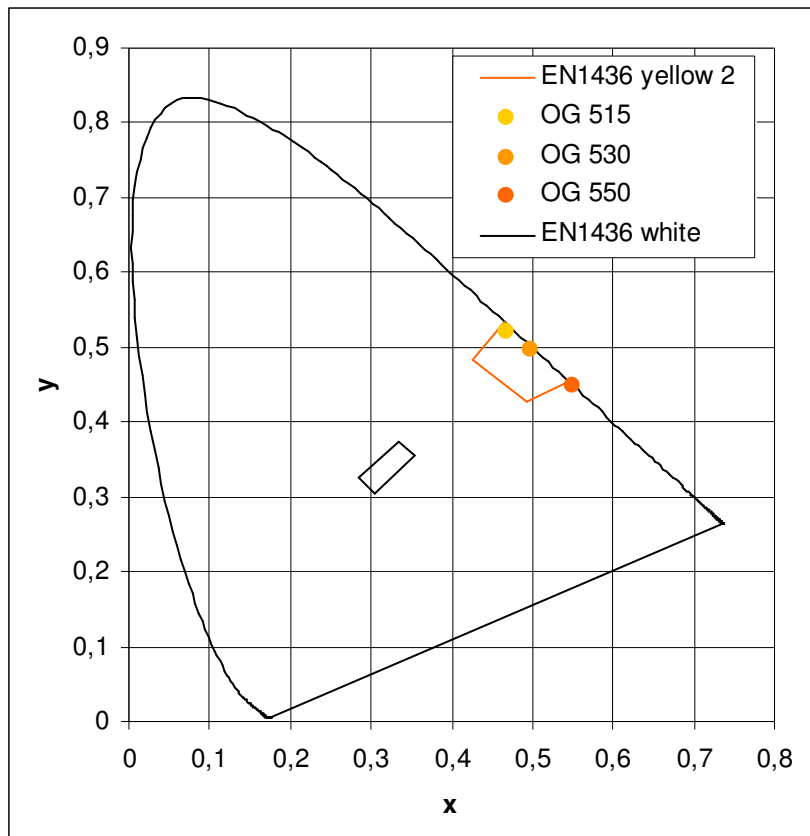
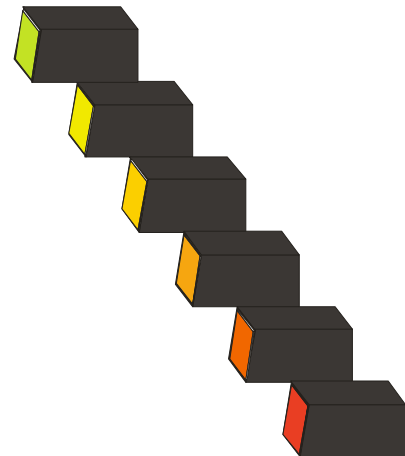


Figure D.19: Chromaticity of 1 mm thick Schott filters passed twice shown together with the chromaticity boxes for white road markings (EN 1436 white) and new yellow road markings (EN 1436 yellow class 2).

NOTE 1: For the internal quality assurance, DELTA uses calibration blocks with a range of colours created by coloured filters mounted in front of the white surfaces.



The lift test mentioned in item f is illustrated in figure D.20. The lifts can be obtained by putting coins or other thin items under the feet of the retroreflectometer, or under the panel in the case of a negative lift (the panel must be small enough to fit between the feet of the retroreflectometer).

The movement of the panel in proportion to the lift H ensures that the same patch of the panel is measured for the different lifts, so that non-uniformity of the panel does not interfere.

The retroreflectometer shown in the figure D.20 is an LTL 2000, which is no longer in production. In this case, the R_L value drops by more than 10 % when the lift is 5 mm. This means that the tolerance to lift is 4 mm, but can be set somewhat higher to 4,5 mm. As the LTL 2000's use arrangement B, the panel has been moved by $4,5 \times 46 \text{ mm} = 207 \text{ mm}$ when the lift is 4,5 mm.

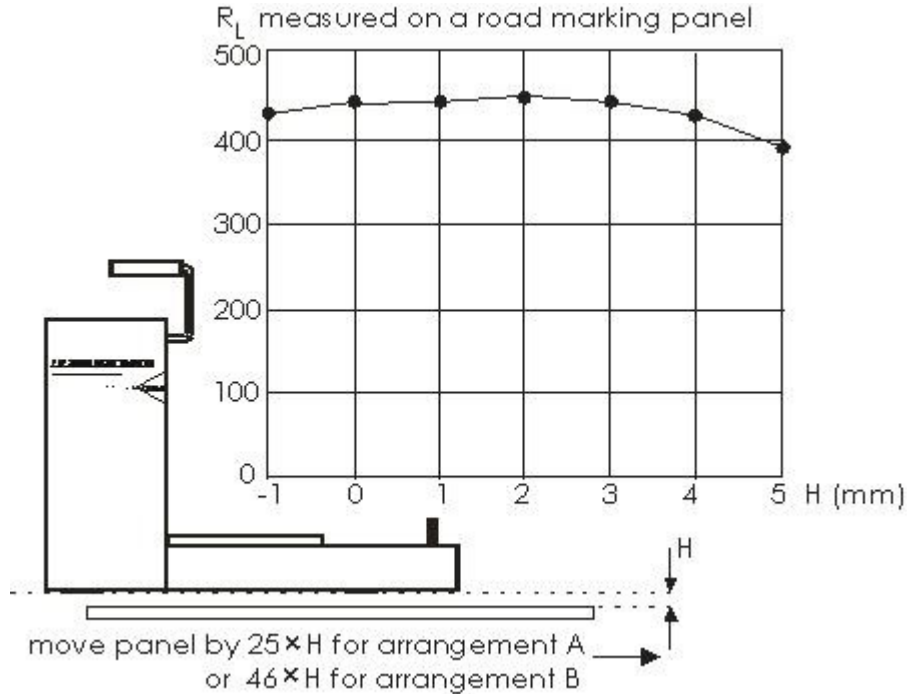
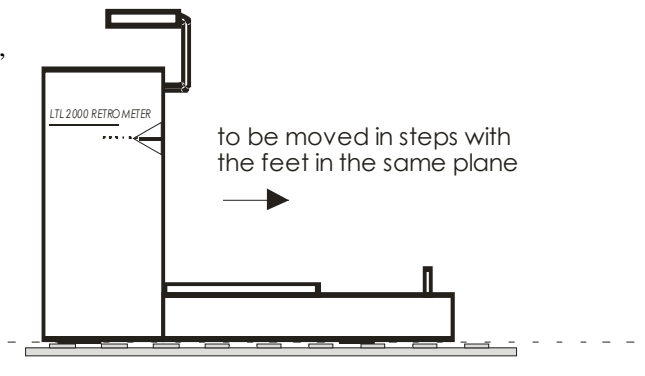


Figure D.20: Example of a lift test.

This means than an LTL 2000 can measure profiled road markings correctly, when the height of the profiles is maximum 4,5 mm, or the gap between profiles is maximum 207 mm.

NOTE 2: An LTL-X has a much higher tolerance to lifts.

NOTE 3: Depending on the profile spacing, it may be necessary to move the retroreflectometer in steps and form the average of the individual readings. If so, the retroreflectometer must be moved with the feet in the same plane.



D.5 Vehicle based retroreflectometers

D.5.1 The Ecodyn 30

Figure D.21 shows the Ecodyn, which was developed at the French road laboratory LCPC (Laboratoire Central des Ponts et Chaussées) during the 80's and is now supplied by a French company named Vectra. In an initial period, the measuring geometry corresponded to a relatively short distance on the road, but the instrument was converted to the 30 m geometry – in a 1:5 scale - during the mid 90's and was accordingly named Ecodyn 30. Ecodyn 30's are in widespread use in Europe and some are in use elsewhere.

The working principle of the Ecodyn 30 is that several measurement areas, located side by side, are enclosed within a larger illuminated area, refer to figure D.22. Measurements are initiated at intervals with a fairly low frequency and result - each of them - in a vector of values for different positions transverse to the road. Only those of the values that are deemed to represent positions within a road marking are used to derive the R_L value representing the road marking.

This means that there is some reserve in the width of the total field covered by the measurement fields, and this provides for some tolerance in steering the vehicle while driving along a longitudinal marking. In a particular version of the Ecodyn 30, that has been supplied over several years, the frequency of measurement is 10 per second, the number of measurements fields is 14 and the fields are spaced approximately 4 cm apart, so that the total width is approximately 56 cm.

The total width of the field seems to be small, but apparently allows for practical driving with the Ecodyn 30.

At least some of the Ecodyn 30's use software that use only one of the 14 values – the maximum – to derive the R_L value. This implies some approximation, and it illustrates that the Ecodyn 30 cannot distinguish double lines. The Ecodyn 30 involves some additional approximation in the case of broken lines – the smallest measured R_L values are assumed to correspond to fields outside of the lines, or fields that are not fully placed on a line, and these are eliminated on a statistical basis.

In the 1:5 scale, the measured fields are placed 6 m in front of the retroreflectometer, where it cannot for practical reasons be protected from ambient light by physical means like covers or shades. Instead, the influence of the ambient light is suppressed by means of modulation of the illumination and selective amplification of the signals at the modulation frequency.

This suppression is not sufficient in direct sunlight. Therefore, the influence of ambient light is measured and subtracted.

Concerning accuracy, the primary observation is that the Ecodyn 30 uses a scaled version of the 30 m geometry so that changes of the geometry influence the R_L value. The geometry is not really controlled in practical driving; random changes are caused by bumpiness of the road and systematic changes by changes of the load of the vehicle or transverse curve of the road.

The situation is much like with early types of handheld retroreflectometers that were also based on down-scaled geometries. Offsets from the desired geometry affect the readings, even through the sources of the offsets are different. Refer to D.4.

Offsets from the desired geometry can be divided into two kinds, offset of distance without offset of the height position as illustrated in figure D.23, and offset of height position without offset of distance as illustrated in figure D.24. The two kinds of offset are called respectively offset of distance and offset of height in the following.

Offset of the distance affects the reading by means of the distance law of illumination, so that an offset of 10 % causes a change of the reading of 20 %. A 10 % offset of the distance corresponds to a tilt of the vehicle of 0,229°.

Offset of the height position affects the reading by means of a change of the geometrical factor, so that an offset of 10 % affects the reading by 6 %. An offset of the height position of 10 % corresponds to 2,4 cm for the 1:5 scale used by the Ecodyn 30.

The Ecodyn 30 must be calibrated by means of panels, and this carries additional uncertainty in view of the difficulty of calibrating panels in the laboratory. Refer to D.3.



Figure D.21: The Ecodyn 30.

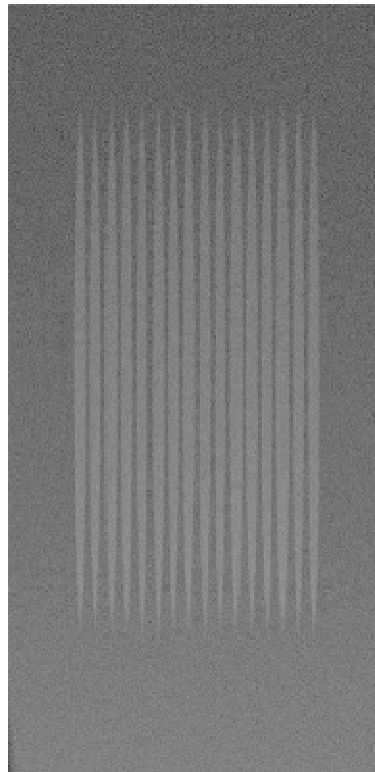


Figure D.22: The Ecodyn 30 uses several measurement areas enclosed within a larger illuminated area.

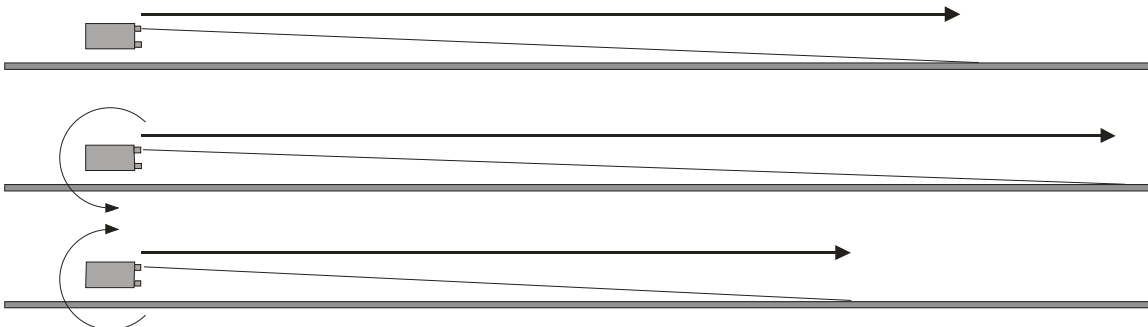


Figure D.23: Offset of the distance of measurement.

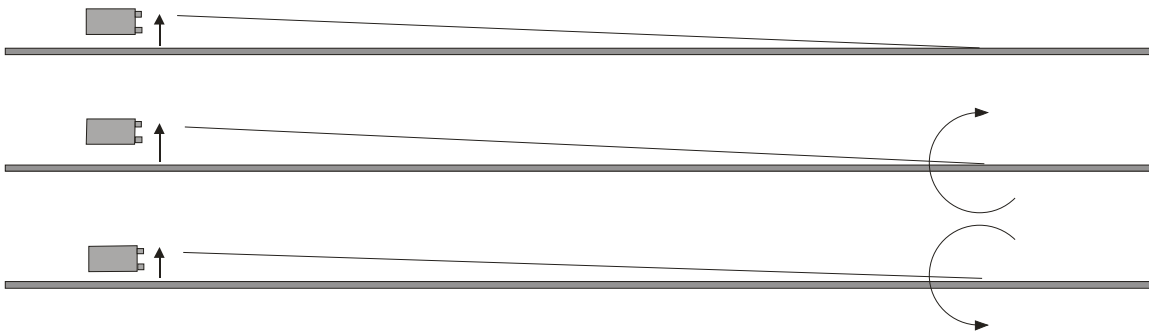


Figure D.24: Offset of the height position of the measuring aperture.

D.5.2 The Laserlux

Figure D.25 shows the Laserlux, which was developed by Gamma Scientific during the early 90's and is now supplied by an American company named Road Vista. The measuring geometry corresponds to the 30 m geometry in a 1:3 scale. Laserlux has a widespread use in the USA and some are used elsewhere.

The working principle of the Laserlux is that a rather small illuminated area is contained within a measured area, and that both of these sweep together in a transverse direction across the road marking, refer to figure D.26. During a sweep, measurements are initiated with a fairly high frequency so that a vector of values for different positions transverse to the road is derived. As with the Ecodyn 30, only those of the values that are deemed to represent positions within a road marking are used to derive the R_L value representing the road marking.

In a particular version of the Laserlux that has been supplied over several years, the frequency of the sweeps is 20 per second, the number of values within a sweep is 200 and the locations are spaced approximately 0,55 cm apart, so that the total width is approximately 110 cm.

The relatively wide field covered by the Laserlux allows probably for ease of steering the vehicle. The spacing of the data-points allows that double lines can be separated and that the R_L value is based on an average of several data-point over the width of the road marking.

The name Laserlux refers to the use of a HeNe laser with red light at a wavelength of 633 nm for illumination. The intention is not only to obtain a concentrated beam, but also to suppress the influence of ambient light by the use of a narrow band pass filter at the laser wavelength in front of the detector.

This method of suppressing the ambient light is quite efficient, but not sufficient in itself in direct sunlight. Therefore, the influence of ambient light is measured and subtracted. This happens at intervals only, so that errors occur when driving in and out of shadows.

It is to be noted that the use of a laser causes disadvantages, when measuring road markings of different colours. To understand that, it is first necessary to understand that an R_L value is to be derived as if the incoming light has a well-defined broad spectral distribution and that a particular colour is created by absorption of a characteristic part of this distribution. This means that road markings of different colours are associated with different levels of R_L values. The levels depend not only on the hue of the colour but also on its saturation.

The use of red laser light of a single wavelength does not lead to the right levels for the colours. In particular, the cold colours of blue and green will appear to be very dark, while the warm colours of yellow orange and red will appear to be almost as bright as white.

The supplier of the Laserlux recommends the use of different calibrations for white and yellow road markings by means of a white and a yellow calibration panel. However, yellow road markings have colours with so much variation, that they cannot all be represented by a single yellow calibration panel. Refer to the colour box for yellow class 2 shown in figure D.19 and to the transmittance values of yellow filters provided in table D.1.

It might not be quite obvious how the R_L values provided by the Laserlux varies with distance as the small laser-spot itself might not change much. However, the size of the measured field does change with distance and, therefore, the average illumination of the measured field changes. This is precisely what is measured by the detector and therefore the Laserlux has the same dependence on distance as the Ecodyne.

In D.5.1 it is stated that the Ecodyn 30 readings are affected by offsets of the height position as well as by offsets of distance. This however, is not the case for Laserlux, as the illuminated field is smaller than the measured field so that the geometrical factor is not included in the measurement. Refer to D.4 for some explanation of this.

As with the Ecodyn 30, the Laserlux must be calibrated by means of panels, which can be expected to introduce additional uncertainty.



Figure D.25: The Laserlux.

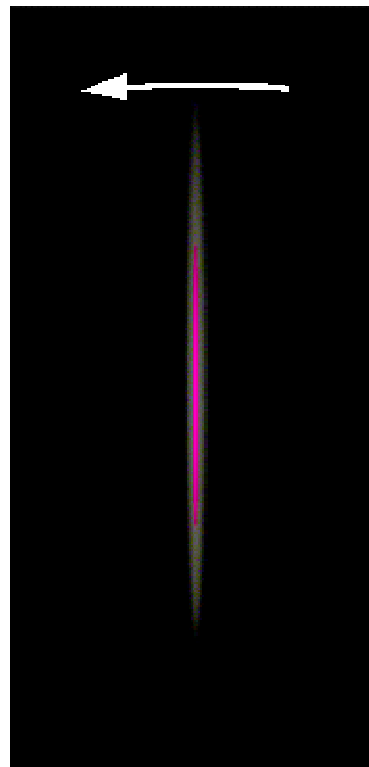


Figure D.26: The Laserlux sweeps its fields in the transverse direction across the road marking .

D.5.3 The ZDR 6020

An additional retroreflectometer, the ZDR 6020 Dynamic retroreflectometer has become available on the market by Zehntner GmbH. The producer states that it is based on the same principles as the Ecodyn 30

except that it uses 16 measuring fields instead of 14, and performs some operation on the resulting 16 values to provide the average R_L value for the entire width of the road marking.

D.5.4 The MR

DELTA will start supplying a vehicle based retroreflectometer, the LTL-M, early 2011. Figure D.27 shows a prototype of the LTL-M.



Figure D.27: The LTL-M prototype.

The measuring geometry is the 30 m geometry in a 1:5 scale, meaning for instance that the nominal measuring distance D_0 is 6 m. The locations of the detector and the light source are interchanged.

The light source is a xenon flash lamp that emits flashes with a duration of typically 10 microseconds. By means of suitable optics the flash lamp illuminates a field on the road that is approximately 1 m long and 1 m wide. The detector is a digital camera used with a fixed exposure time set typically to 10 microseconds.

The flashes of the flash lamp and the exposures of the camera are synchronized. The current rate is 25 flashes and exposures per second.

A field of the road is shown in a part of the image that has a width of more than 1000 pixels and a height of typically 100 pixels. This field is a bit wider than the illuminated field but much longer, covering a distance range from approximately 4 to 8 m. The width of the road area covered by an image is more than 100 cm and allows for easy steering.

If driving with a speed of 90 km/h, the distance moved between two flashes/exposures is actually 1 m equal to the length of the illuminated field. This means that the measured areas approximately fit together along the road marking and that all, or almost all of the road marking area, is covered. If driving at a higher speed, there will be gaps between the measurement areas, but the amount of surface included is still very high. The exposure time is so short that blurring of the image because of speed is insignificant at any practical driving speed.

Suitable software analyses this part of the image and determines if it contains a longitudinal road marking. If so, the software determines the sides enclosing the road marking surface and also possible fronts and ends of road markings in broken lines. The software also identifies those parts of the road marking surface that are illuminated by the flash lamp. Additionally, the software determines the actual distances D to locations on the surface that correspond to each of the pixels.

Figure D.28 shows a typical image with a 30 cm edge line.

By means of suitable optics another part of the image is made to show the light source itself in such a way that it represents the distribution of the illuminance E_0 on a vertical surface at the distance D_0 . The software uses this distribution to determine the illuminance E created by the flash lamp at locations on the road marking surface by $E = E_0 \times (D_0/D)^2$. The term $(D_0/D)^2$ represents the distance law of illumination.

In this way the influence of offsets of distance is eliminated. The influence of offsets of the height position is eliminated by the above-mentioned interchange of the locations of the detector and the light source.

Figure D.28 contains also a typical image of the light source.

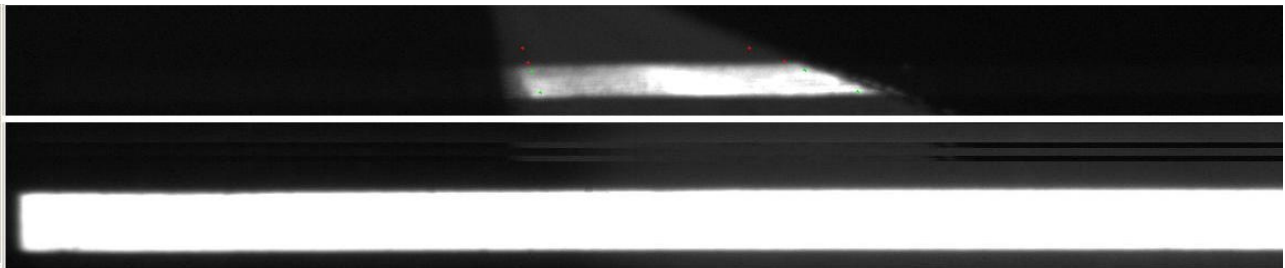


Figure D.28: The illuminated part of a 30 cm edge line (upper image) and the flash lamp (lower image).

NOTE: The images are actually wider than shown in figure D.28 and other similar figures.

On this basis, the R_L value at a location is derived by:

$$R_L = C_0 \times C \times (P-D)/E$$

where C_0 is a correction factor

C is a calibration factor

P is the value of the pixel corresponding to the location

and D is a residual level of daylight.

The result is expressed as the average R_L value for a field on the illuminated part of the road marking surface.

Two such fields are indicated in figure D.29. The upper field corresponds to a 5 cm wide lane in the middle of the marking surface, while the lower field includes almost the entire width of the road marking. The LTL-M can be made to provide the R_L value for either of the two fields, or both, and in fact a transverse distribution if needed.

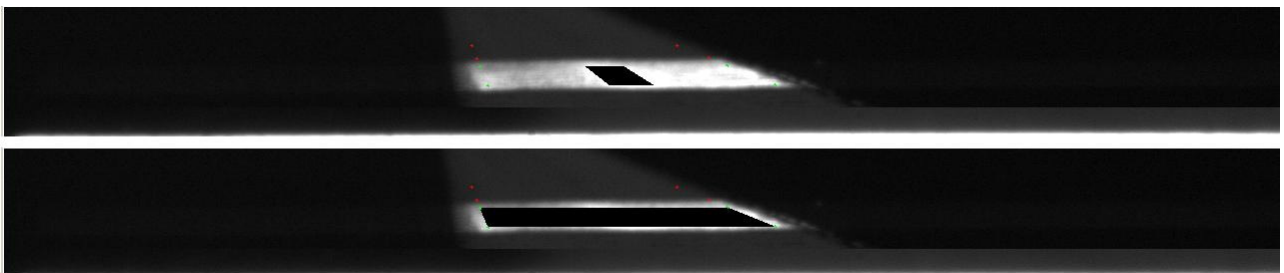


Figure D.29: Two fields for integrating the R_L value.

The retroreflected luminance of the road marking surface dominates over daylight during the brief period of the flash. However, in bright daylight there is a residual level of daylight, which is determined for a field on a part of the road marking surface that is not illuminated by the flash lamp.

The residual level of daylight that is used in the current image is actually one that has been determined from a previous image, while the level determined from the current image is saved for use with the next image. In this way, the residual level of daylight is determined at the correct location and just a short time before it is used, typically 1/25 of a second earlier.

Linearity and uniformity of the response of the camera pixels is ensured on the basis of an initial procedure carried out in laboratory conditions.

The LTL-M by its construction and way of working ensures an almost constant sensitivity over the width of the illuminated field. However, a global calibration is carried out in order to eliminate a possible small variation. To this purpose, the LTL-M is aimed to illuminate a uniform white surface placed at the distance D_0 and additional software is initiated. This software determines an array of the above-mentioned correction factors C_0 as an average of a large number of exposures and stores the values. The software also derives some geometrical measures that are used for the above-mentioned analyses of road images during driving.

The value of the above-mentioned calibration factor C is derived in a calibration procedure using a calibration standard of one of the types used for handheld retroreflectometers. The calibration standard is placed at the distance D_0 , the LTL-M is aimed to illuminate the ceramic front surface of the standard and additional software is initiated. This software determines C as an average for a large number of exposures and stores the value.

The software used during driving determines not only the R_L values as described in the above, but also:

- the geometry of the road marking including the width and gaps in broken lines
- the geometry of measurement including the height position of the equipment, the measuring distance and three angles relating to the orientation of the equipment relative to the road marking surface.

The software derives all the above-mentioned values for one or two lines (for instance double centre lines) simultaneously.

D.6 Accuracy of measurement

D.6.1 Accuracy of laboratory methods

An intercomparison test was initiated by the ASTM 12.10 committee in 2002 in order to determine the accuracy of laboratory methods. For this purpose, a set of 12 panels with widely different properties and R_L values ranging from virtually 0 to more than $1000 \text{ mcd}\cdot\text{m}^{-2}\cdot\text{lx}^{-1}$ was prepared.

DELTA determined the repeatability of the band method to be 3,5 % measured as the standard deviation between two sets of values.

DELTA also compared the R_L values obtained with the band method to R_L values obtained with an LTL 2000 by averaging over the panel surfaces. The two methods are in good agreement, refer to figure D.30, which shows that the two methods confirm the accuracy of each other. As the standard deviation is about the same as the above-mentioned repeatability of the band method, it can be claimed that the LTL 2000 may probably be as accurate as the band method.

Additionally; the French road laboratory LCPC (Laboratoire Central des Ponts et Chaussées) measured the set of panels with its full scale laboratory method in two versions. The R_L values obtained with the two versions of the LCPC laboratory method agrees well with each other. Further, the average LCPC values

show an extremely good correlation to those of the band method (and the LTL 2000) with a Pearson coefficient of 0,999. However, there is a systematic deviation of 20% with the LCPC values being the higher.

The cause of this systematic difference was never located, and the inter-comparison test was never completed.

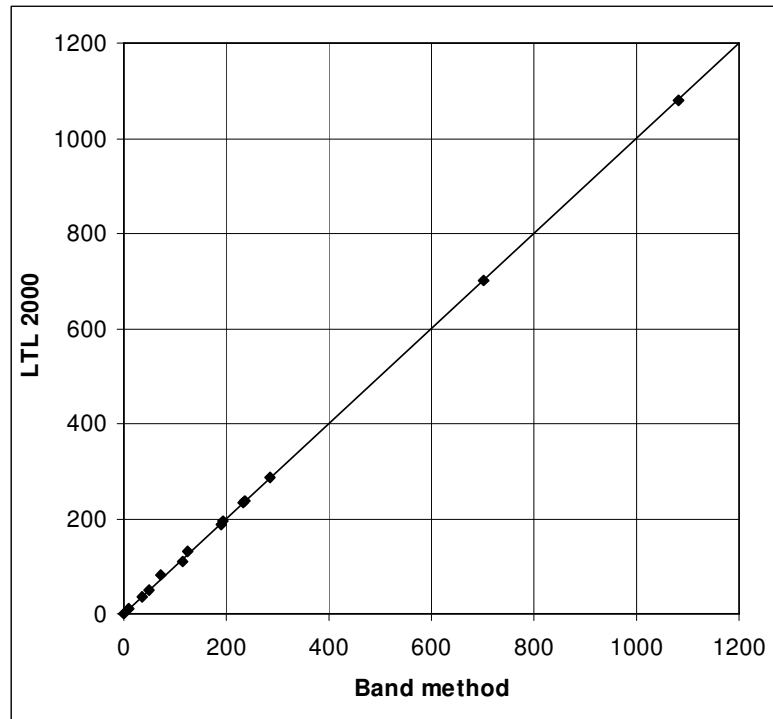


Figure D.30: Comparison of R_L values obtained with the band method and an LTL 2000.

D.6.2 Accuracy of handheld retroreflectometers

Handheld retroreflectometers have been subjected to studies involving repeatability, reproducibility and inter-comparison at some occasions by the “Expert Panel” of the CEN/TC 226 WG2, by the HITEC organisation in the USA, by the NMF and by others.

Some of the studies by the “Expert Panel” were carried out during the early 90’s and involved a number of the early retroreflectometers working with 10 to 15 m geometries and also an early version of the LTL 800 adjusted to a 50 m geometry. It became clear that the R_L values did not agree well between the different types. Some of the differences were thought to be caused by differences in the measuring geometries, including angles and aperture sizes.

It was on this basis that the CEN/TC 226 WG2 agreed on the 30 m geometry as a compromise solution, and on some of the principles presently established in annex B of the EN 1436. The geometry and the principles were later adopted by the ASTM in the standard E 1710.

The LTL 800’s were readjusted to the 30 m geometry, but were gradually replaced by LTL 2000’s and later LTL-X’s in different versions. The early retroreflectometers disappeared from the market, and gradually from use. A few other types of retroreflectometers have emerged since then, all with the 30 m geometry and all more or less adapted to the requirements of the standards.

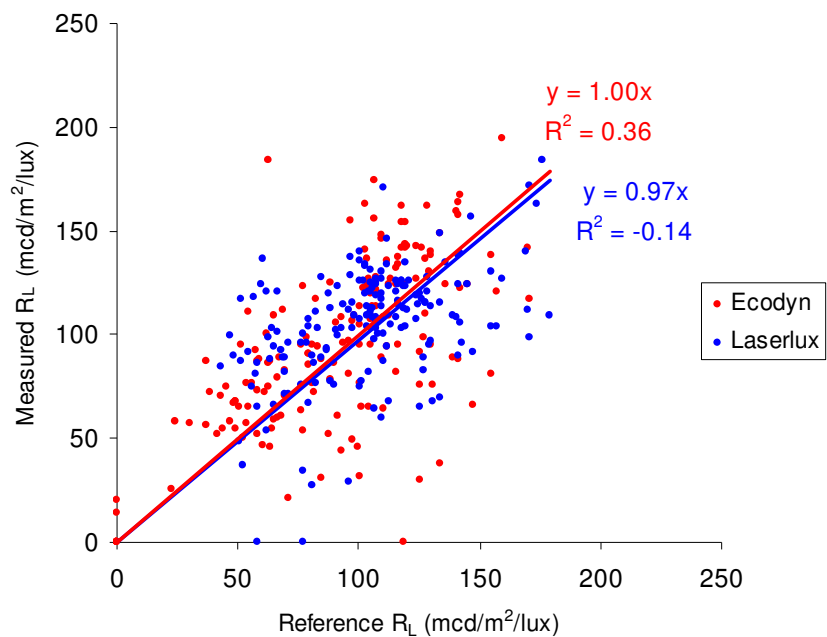
The real improvement in the accuracy of handheld retroreflectometers can be attributed to the standards. Those handheld retroreflectometers that meet the requirements of these standards, such as listed in D.4.6 for EN 1436, have in general obtained good marks in studies. Therefore, the individual studies are not listed nor discussed.

D.6.3 Accuracy of vehicle based retroreflectometers

D.6.3.1 A UK study

The accuracy of the Ecodyn 30 and the Laserlux has been investigated by the TRL (Transport Research Laboratory, UK), and is reported in a power point presentation “TRL’s current understanding of HSMs and associated correction factors”, Stuart McRobbie, 2006. The total amount of data is shown in figure D.31, and does show a large scatter of the data indicating a large uncertainty of measurement.

Figure D.31: Some results from a TRL investigation.



D.6.3.2 A study in the Nordic countries

The Ecodyn 30 is used extensively in the Nordic countries and, therefore, the NMF has organised a couple of studies. These also indicate a relatively large uncertainty of measurement, but not as large as in the above-mentioned study. The best results were obtained in the most recent study reported in VTI report 675, “Mobile measurement of road marking”, Sven-Olof Lundkvist, 2010.

This study included comparison of measurements with an LTL 2000 and an Ecodyn 30 on 200 m long stretches of road markings in Denmark and Sweden, including plane and profiled road markings, continuous and broke lines, and different types, widths, conditions of wear and levels of R_L .

The results given as averages for the 200 m stretches are shown in figure D.32. It may be concluded that the uncertainty of measurement of a retroreflectometer like the Ecodyn 30 can be reduced, when having good procedures of calibration and alignment and experienced operators.

The study included an early prototype of the LTL-M prototype as well. The results are given in figure D.33 and indicate less than half the uncertainty of measurement as compared to the Ecodyn 30. The report includes other comparisons and laboratory testing; refer to the report itself.

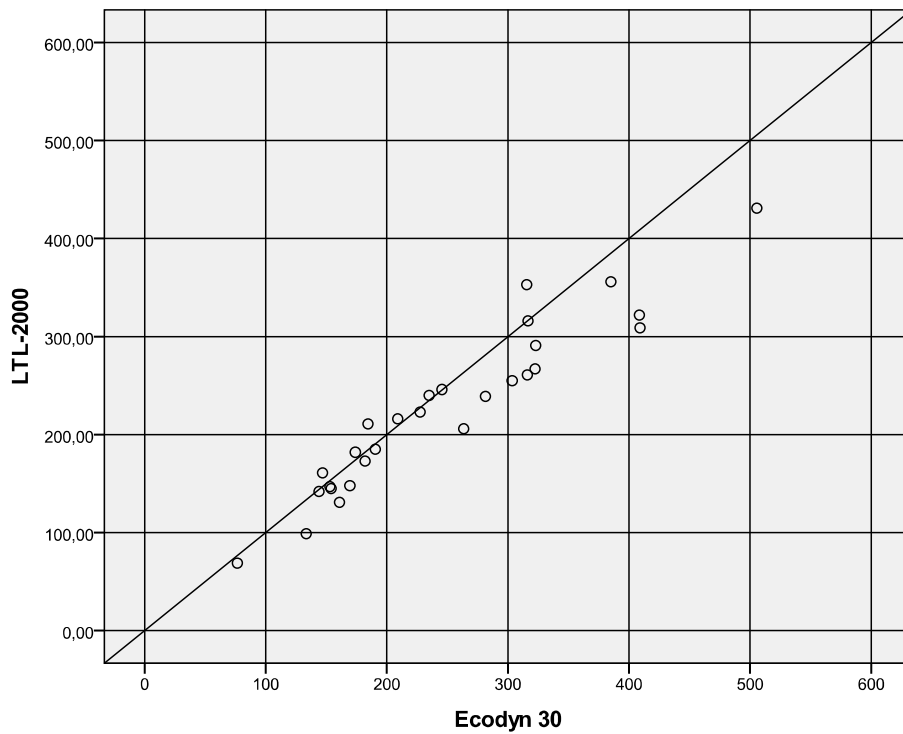


Figure D.32: Comparison between average R_L values for 200 m stretches of road markings obtained with an LTL 2000 and an Ecodyn 30.

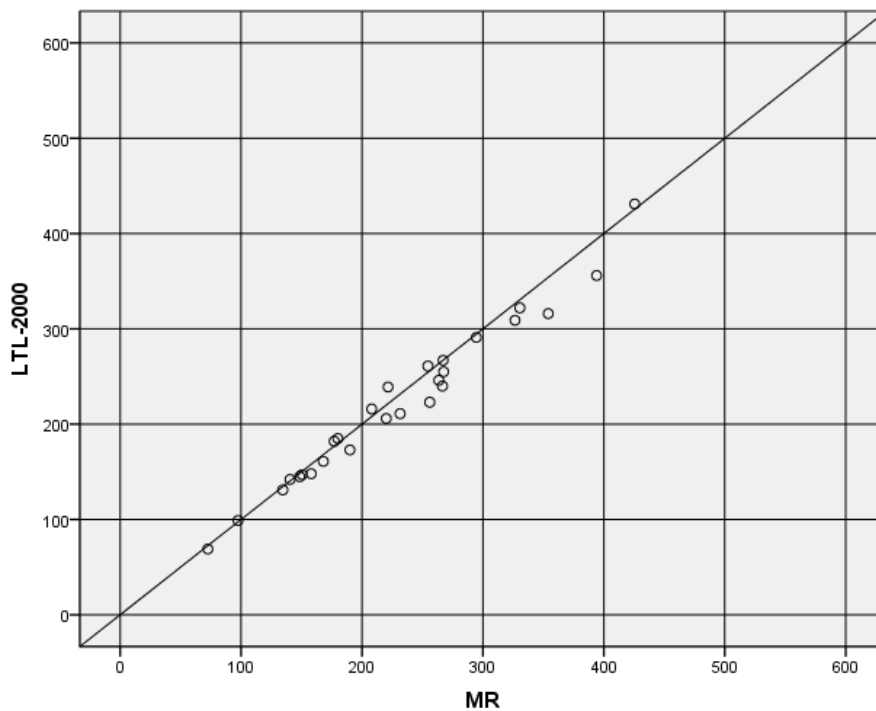


Figure D.33: Comparison between average R_L values for 200 m stretches of road markings obtained with an LTL 2000 an early LTL-M prototype.

D.6.3.2 A test by the “Expert Panel” of the CEN/TC 226 WG2

The test was conducted by Luc Goubert (BRRC, Belgian Road Research Centre) and Sven-Olof Lundkvist (VTI, Swedish National Road and Transport Research Institute) in September 2010. At present (March 2011) a “Draft report of the first round robin test for mobile reflectometers” is available for participants in the test.

A total of 21 test sites were measured by 5 retroreflectometers, a handheld LTL-2000 and four mobile instruments. Two test sites are broken lane lines, while the rest are continuous edge lines.

During the test it became clear to the participants that most of the road markings have strong transverse non-uniformity and that this would affect intercomparisons in view of the different methods of dealing with the width of the road markings:

- a. the LTL 2000 with a 4-5 cm wide measuring field was placed approximately in the middle of the road markings
- b. two mobile instruments select the 4 cm wide lane with the largest R_L
- c. one mobile instrument provides the average R_L value for the entire width
- d. one mobile instrument provides the average R_L value for the entire width or for a 5 cm wide lane placed accurately in the middle.

The mobile instrument mentioned under d. in the list was the LTL-M prototype with upgrading concerning the software analysis of the images and the stability in terms of constant monitoring of the dark level of the camera.

The two sets of R_L values supplied by the LTL-M illustrate the influence of the transverse non-uniformity. The two sets are compared in figure D.34, which does show a considerable scatter. This is in spite of the fact that both sets are derived from the same images and, therefore, not affected by uncertainty of measurement.

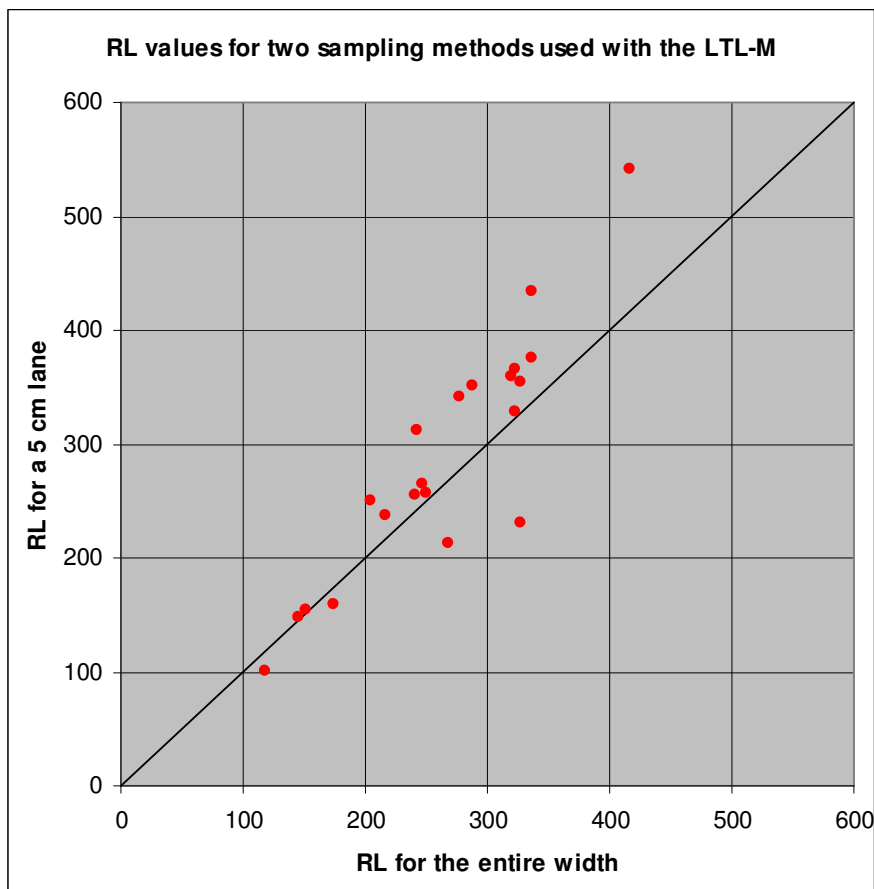


Figure D.34: Comparison of the two sets of R_L values provided by the LTL-M.

A closer study of the images supplied by the LTL-M shows:

- a. most of the road markings have the highest level of retroreflection along the middle and, therefore, higher R_L values for the 5 cm lane than for the entire width
- b. two road markings have peculiar lacks of retroreflection along the middle and, therefore, lower R_L values for the 5 cm lane than for the entire width
- c. the rest of the road markings are fairly uniform in the transverse direction and, therefore, have little difference between the two R_L values.

These observations indicate which of the values that should be used for intercomparison in specific cases. However this may be described in the report, or not, the LTL-M stands out among the mobile instruments. Refer to the final report when available.

A fair comparison to the LTL 2000 is shown in figure D.35, which indicates good agreement.

It is reasonable that LTL-M has a small uncertainty of measurement as it has the same abilities to suppress variation and the same easy calibration with ceramic calibration blocks as an LTL 2000. Because of this, the LTL-M may be the break-through in mobile measurement in the same way as the LTL-2000 was for handheld measurement.

It may well be that the LTL-M is as accurate as the LTL-2000 and that the uncertainties of the two instruments add equally to the small scatter observed in figure D.35. The first observation will be proven or disproven by events, the second observation can perhaps not be neither proven nor disproven.

It is pointed out that averaging over the entire width is the method that is relevant for drivers and that this is the method that is expected to be commonly used with the LTL-M. The second method was added mainly to provide R_L values that can be compared with the R_L values of the LTL-2000.

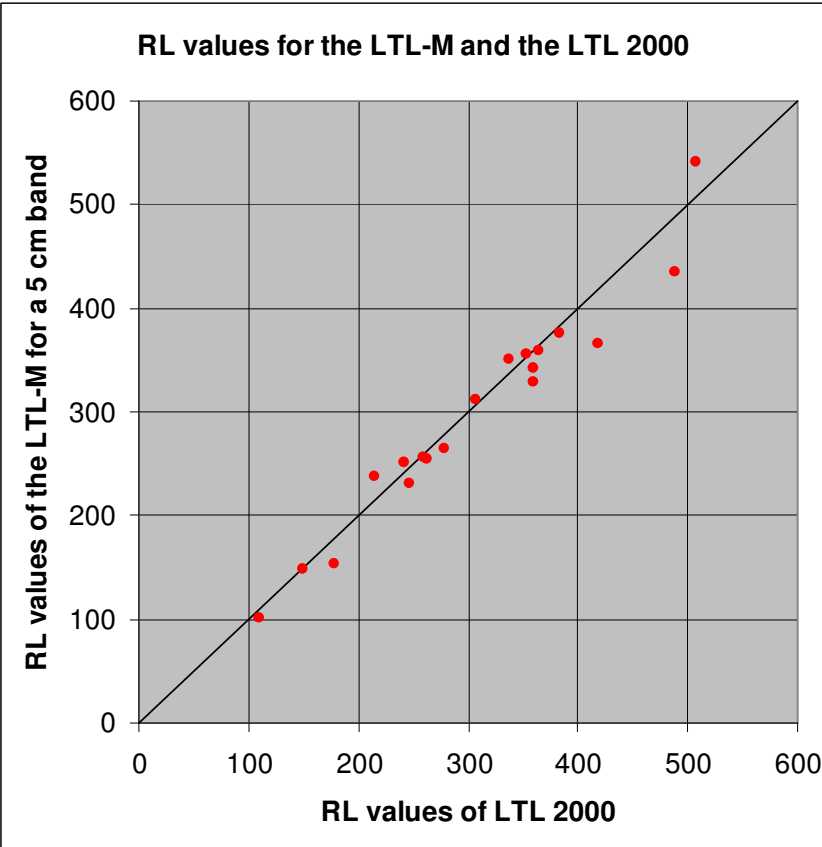


Figure D.35: Comparison of the R_L values for the LTL-M to those of the LTL-2000.

Literature

EN 1436 “Road marking materials - Road marking performance for road users”

ASTM E 1710 “Standard Test Method for Measurement of Retroreflective Pavement Marking Materials with CEN-Prescribed Geometry Using a Portable Retroreflectometer”.

ASTM D 4061 “Standard Test Method for Retroreflectance of Horizontal Coatings”.

Annex E: Measurement of the reflection in diffuse illumination of road markings and road surfaces

E.1 Introduction and summary

This annex relates to measurement of the luminance coefficient in diffuse illumination Q_d in the 30 m standard measuring geometry. The 30 m geometry is defined in annex A of EN 1436 “Road marking materials - Road marking performance for road users” and in ASTM E 2302 “Standard Test Method for Measurement of the Luminance Coefficient Under Diffuse Illumination of Pavement Marking Materials Using a Portable Reflectometer”.

The Q_d value in the 30 m geometry is intended to represent reflection in daylight or under road lighting as observed by the driver of a passenger car.

The Q_d value is the luminance of the road surface or marking (or rather a field of the road surface or marking at 30 m distance) in proportion to the illuminance on the road surface or marking (at the field). The illuminance is measured on the plane of the road surface or marking.

As luminance has the unit of cd/m^2 (candela per square meter) and illuminance has the unit of lx (lux), the unit of Q_d is $\text{cd}\cdot\text{m}^{-2}\cdot\text{lx}^{-1}$. However, in order to obtain more convenient values, the 1000 times smaller unit of $\text{mcd}\cdot\text{m}^{-2}\cdot\text{lx}^{-1}$ is used by convention (mcd means millicandela).

The 30 m geometry used for Q_d is in family with the 30 m geometry used for the coefficient of retroreflected luminance R_L in the sense that the measuring angle α is $2,29^\circ$ in both and that the requirements regarding angular apertures of measurements are the same. For both, the photometer shall have a spectral response according to the $V(\lambda)$ distribution (the standard distribution for photopic vision).

The difference lies in the illumination, which is diffuse and according to CIE illuminant D65 (simulating daylight) as defined in CIE 15.2 “Colorimetry” for Q_d and directional and according to standard illuminant A (simulating a headlamp with an incandescent light source) for R_L .

The Q_d value measured for a surface does not have the property of the R_L value, that the single Q_d value is sufficient to account for the reflectivity of the surface for all relevant conditions. The Q_d value can at most be assumed to account for the reflectivity for typical or average conditions of illumination. Refer to annex A.

The overcast sky gives a reasonably good approximation to diffuse illumination and, therefore, it has been attempted to do full scale measurement of Q_d values in overcast sky conditions. These attempts have not been successful as reported in E.2.

As full scale measurement cannot supply true Q_d values, attention is turned towards laboratory measurement on road marking panels as a source of trueness. Diffuse illumination is intimately connected to the use of photometric spheres and, therefore, laboratory measurement with illumination in a photometric sphere is considered in E.3.

It is reported that laboratory measurements performed at DELTA with a high quality 3 m sphere and a specially designed photometer represent a very good approximation to “trueness”. However, laboratory measurement of Q_d has probably been used only at DELTA and only in the process of developing the handheld Q_d30 reflectometer. Further, the equipment is no longer in service. Therefore, the source of “trueness” might have been laboratory measurement, but this is not the case in practice.

The handheld Q_d30 reflectometer appeared in the middle of the 90’s; it is described in E.4. This instrument also provides diffuse illumination from a photometric sphere, but through an aperture in the bottom of the sphere so that the reflectometer can be placed on the surface to be measured. The various arrangements of the Q_d30 are accounted for with the aim of explaining that:

- the readings are insensitive to any direct effect of lifts and tilts
- white and yellow road markings are measured correctly
- the calibration method is based on diffuse illumination and generally sound.

In practice it has become accepted that the Qd30 represents the accepted trueness in Qd measurements.

In view of the familiarity of the 30 m geometries used for the Qd and the R_L it is tempting to add the Qd function to a retroreflectometer that is primarily intended for R_L measurement. All that it requires is the additional illumination system, and it gives the user the benefit of doing two measurements, while handling only one instrument. Handheld retroreflectometers with the Qd function are called “combination instruments”. Such are discussed in E.5.

The first combination instrument was the ZRM 1013 by the Zehntner company that appeared during the late 1990’s. It is explained that the illumination system for Qd needs to be big in order to cover the fairly big measuring field needed for R_L with reserves. The illumination system for the ZRM 1013 is actually small and it is truncated at the bottom in order not to generate false R_L signals.

Because of this, and because of the general design of the illumination system, the Qd function of the ZRM 1013 is inaccurate and show deviations by comparison to the Qd30 that are larger than the width of the Qd classes defined in EN 1436.

This Qd function was actually useless, but nevertheless forced DELTA to provide a combination instrument for reasons of competition. This was a version of the LTL 2000 called the LTL 2000 SQ. The Qd illumination system of the LTL 200 SQ was also small, but provided a somewhat better approximation to diffuse illumination.

The ZRM 1013 has been replaced by the ZRM 6013 and the LTL 2000 SQ by the LTL-XL. The more recent combination instruments have bigger illumination systems and probably more accurate Qd functions. There has, however, not been any independent test of the accuracy.

It is a particular matter that the Qd function does not really measure Qd because of truncation of the illumination system. This makes calibration difficult by reducing the usefulness of fundamental methods. There is probably no other way than to set the calibration value so that the measured values deviate as little as possible from those of a Qd30.

The combination instruments became so popular that the production of the Qd30 stopped. However, a number of Qd30’s are still in use at road trial sites and elsewhere. It is ironic that the combination instruments rely on the Qd30 for calibration, while the Qd30 is no longer produced because of the combination instruments.

The requirements for portable Qd measurement, as described in EN 1436, are accounted for in E.6. The account is brief because the above-mentioned combination instruments fail to meet the most fundamental requirement, which is to provide a good representation of diffuse illumination.

There is no discussion of mobile Qd measurement, as it is impossible to design a vehicle mounted illumination system that would not be in danger of colliding with obstructions like kerbstones and rail guards.

E.2 Use of daylight illumination

The Expert Panel of the CEN/TC 226 WG2 “Horizontal signalisation” has at a couple of occasions used daylight illumination in attempts to do full scale measurements of Qd on road trial sites. The equipment

needed is a luminance meter to measure the luminance of a field of a surface and a luxmeter to measure the illuminance at the field on the plane of the surface.

The aim was to do these measurements in clouded daylight conditions as the overcast sky provides an illumination that is a reasonably good approximation of diffuse illumination.

However, a good representation of the overcast sky is not found very often except perhaps when it rains, which in itself prevents measurements. Additionally, the location must have a view to the horizon that is unobscured by vegetation and buildings. For these reasons, the attempts by the Expert Panel did not provide reliable data.

It is concluded that daylight is too variable to be used in connection with good measurements of Q_d .

This applies also for the Ecodyn vehicle based retroreflectometer, which includes a “daylight factor” measurement. The luminance of the road markings is measured as part of the R_L measurement, while the illuminance is measured by a luxmeter that is mounted high on the vehicle. The daylight factor does not correlate well with the Q_d value for the reasons given above.

E.3 Laboratory measurement with illumination in a photometric sphere

DELTA has performed Q_d measurement of panels with indirect illumination from a photometric sphere with equipment as shown in figure E.1.

The direct illumination covers only the lower half of the sphere, but some of the light is reflected up onto the upper half of the sphere and gives it an almost uniform luminance by indirect illumination. The measuring optics were placed below the panel surface with a view through a mirror placed above the surface, so as to cause as little obstruction of the illumination of the road marking panel as possible.

A photometric sphere has an inner surface with a matt white coating that approximates diffuse reflection. Such a sphere has the property that light reflected from one location on the sphere is placed almost uniformly over the inner surface. Additionally, the light within the sphere is reflected several times because of a high reflectance of the coating, and this makes the distribution of reflected light even more uniform.

Diffuse illumination is intimately connected to the use of photometric spheres and is used in several types of measurements of reflection, transmission and colorimetry. This applies also for the opposite process, collection of light from a surface. Refer to CIE 15.2, “Colorimetry”.

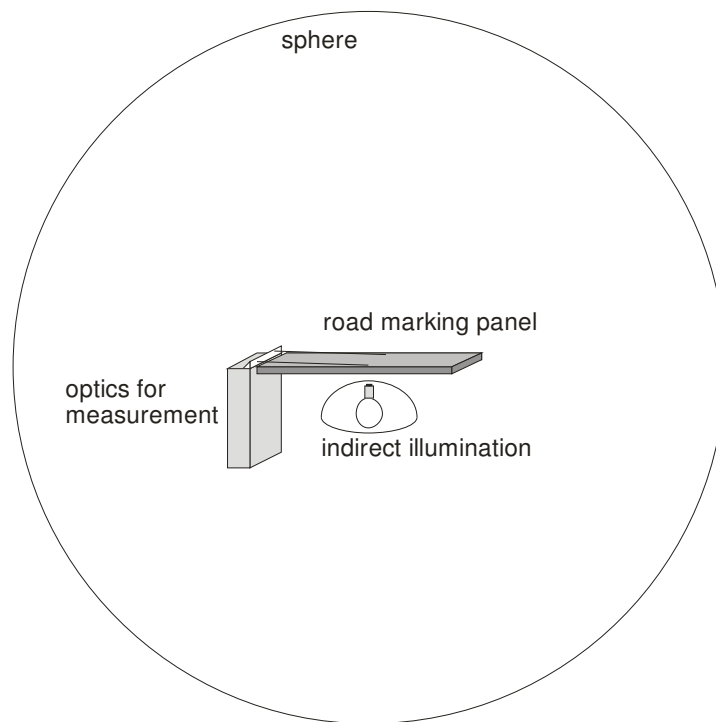


Figure E.1: Laboratory measurement of Qd values of road marking panels.

The particular sphere used in this case was a 3 m sphere of high quality. It provided a close approximation to uniform luminance and thereby to diffuse illumination. Because of this, and because of a high quality of the optics for measurement, these laboratory measurements represented undoubtedly a very good approximation to “trueness”.

As far as it is known, laboratory measurement of Qd is not described in any standard, and has probably been done only at DELTA. The equipment was used in the process of developing the handheld Qd30 retroreflectometer, and is no longer in service. Therefore, the source of “trueness” might have been laboratory measurement, but this source is not used in practice.

E.4 The Qd30 handheld reflectometer

The first handheld reflectometer for the measurement of Qd, the Qd30, was developed by DELTA and appeared in the early 1990’s. The principles of the Qd30 are shown in figure E.2.

The Qd30 has a photometric sphere that is closed at the bottom by a bottom surface with an opening. The sphere is illuminated by an incandescent lamp that is placed at the centre of the sphere and is equipped with a shade, that prevents direct illumination of the opening in the bottom surface.

This illumination of the sphere surface might not be quite uniform, but several reflections within the space enclosed by the sphere surface and the bottom surface provide for a high degree of uniformity of the total illumination.

The illumination falls on a road marking through the bottom opening. Measurement takes place through another opening, which is small. The optical arrangement is of the collimating type with a mirror above the ground, as discussed in annex D.

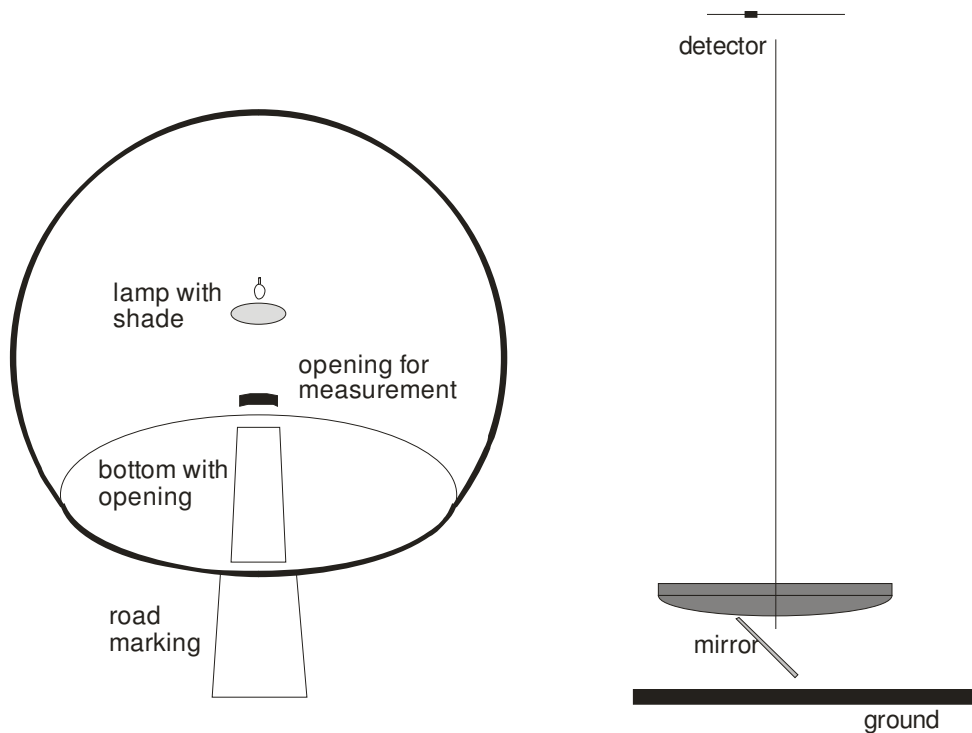


Figure E.2: The illumination system (left) and the measurement optics (right) of the Qd30.

It may be noted that the lamp is an incandescent lamp with a fairly low colour temperature, and that this seems in conflict with a requirement that the spectral distribution is according to the CIE standard illuminant D65 in order to represent daylight with a high colour temperature.

However, there is a correction filter in front of the detector, which makes the overall spectral response of the Qd30 correct. The filter is placed at the detector, instead of the lamp, in order to achieve a better reduction of ambient light (this is like putting sunglasses in front of the detector).

Because of this correction, the Qd30 is able measure road markings of yellow and some other colours correctly.

The fields of illumination and measurement are illustrated in figure E.3. It can be noted that the measured field is smaller than the illuminated field and enclosed within that field with a good reserve.



Figure E.3: Fields of measurement (I) and illumination (II) in the Qd30.

The matter that the measured field is the smaller of the two fields shows that the measurement is of the nature of luminance and that the Qd value, after suitable calibration for illuminance, is measured directly according to its definition as the ratio between luminance and illuminance.

This arrangement of the fields is called arrangement A in annex D. The other possible arrangement, with the illuminated field enclosed in a larger measured field is called arrangement B.

The reason that the choice is arrangement A is that the Q_d value does not change much with the observation angle, so that the measured value does not vary much with the unavoidable tilts, when placing a handheld reflectometer on a road marking in real conditions. Refer to annex A for an explanation why the Q_d value does not change much with the observation angle.

NOTE: When measuring the coefficient of retroreflected luminance R_L , it is the other arrangement B that is preferable, refer to annex D. The reason is that the illumination is in a direction that is lower than the measurement direction, introducing shadows into the illuminated field as seen in the measurement direction. This makes the R_L value depend on tilts of the retroreflectometer, if measured directly with arrangement A. Use of arrangement B provides better repeatability by eliminating this dependence.

When measuring the Q_d value, there are no shadows and therefore no variation to counteract. On the contrary, if arrangement B is used, the measured value is in direct proportion to the actual value of the observation angle, and the repeatability is less good.

The reason for providing the reserve in the illuminated field is that lifts are unavoidable, when placing a handheld reflectometer on a road marking, and that this makes the measured field move forwards (to the right in figure C.3). The movement is by 25 mm for each mm lift of the reflectometer, but there is no direct influence on the measured value as long as the measured field stays fully within the illuminated field.

The reserve is needed in particular when measuring the Q_d of profiled road markings. The reason is that the measurement beam needs to pass some length in order to reach to the bottom of the surface between profiles, or to pass over one profile onto the next profile. The capability of a retroreflectometer in this sense is described as tolerance to lifts in annex D, and applies equally well for a reflectometer. The tolerance of the Q_{d30} is 4 mm.

The Q_{d30} is calibrated by means of a calibration unit, which is illustrated in figure E.4. The unit has an opal plastic plate and a reflecting prism. When the opal plastic plate is illuminated from above, its bottom face, as seen through a reflecting prism obtains a luminance that is in proportion to the illuminance on the opal plastic plate.

Accordingly, the calibration unit has a Q_d value, and this value is measured in the laboratory. This Q_d value does not depend much on the directionality of illumination because of the diffusing property of the opal plastic plate. However, in order to eliminate any such dependence, the laboratory measurement is done with diffuse illumination from a photometric sphere.

In order to compensate for variation of the illumination by the lamp, the illumination is monitored by feed back from a small photodetector placed next to the illuminated field on the bottom plate.

This feed back also accounts for additional illumination caused by reflection from the road marking surface up into the sphere. If not accounted for, this additional illumination would cause bias.

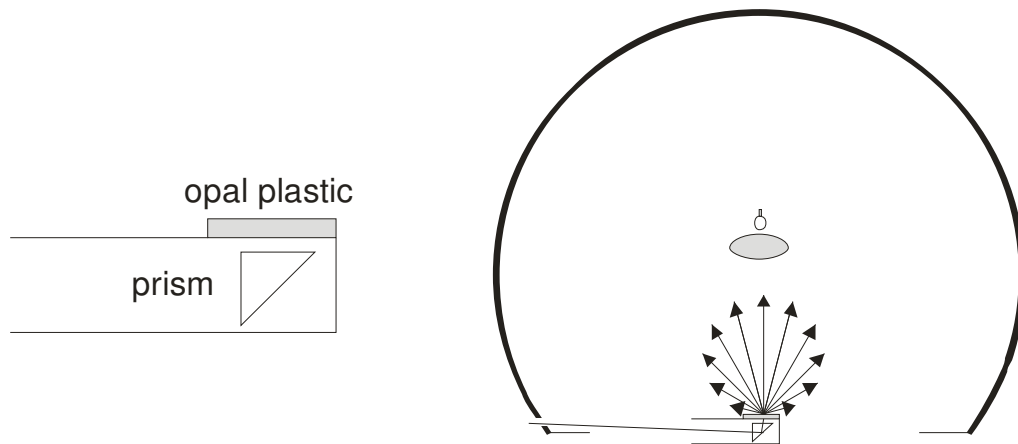


Figure E.4: A calibration unit (left) and its placement in a Qd30 reflectometer (right).

The first version of the Qd30 used a 50 cm sphere with a very un-ergonomic ring structure just at the knee of the operator when carrying the reflectometer. A later version had a slightly smaller sphere without this ring structure.

The Qd30 shows good agreement with laboratory measurements on panels as described in E.3. The repeatability is also good as illustrated in figure E.5 for measurements of test markings at a road trial site. The Qd30 on the road trial site is shown in figure E.6.

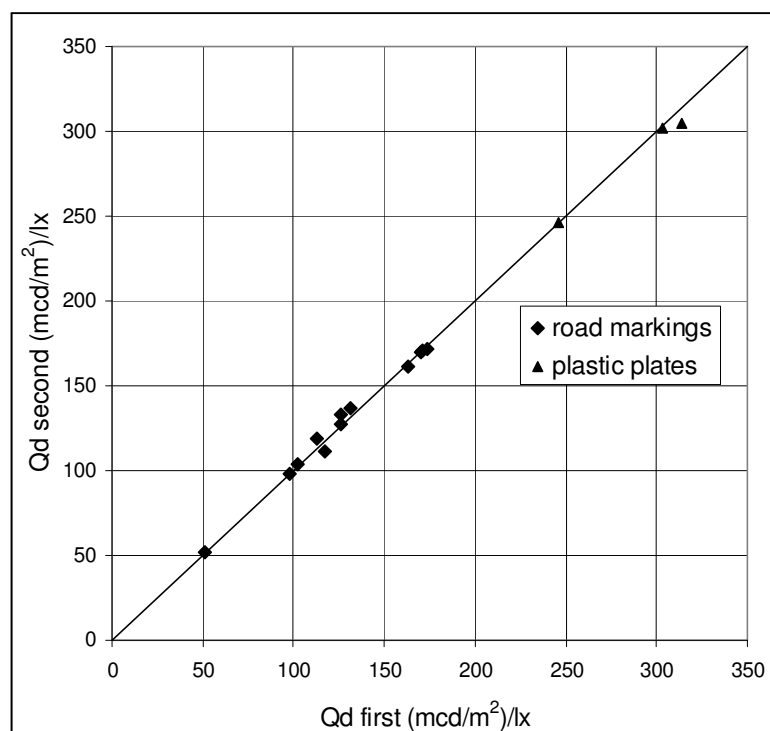


Figure E.5: Repeatability of the Qd30.

Figure E.6:
A Qd30 in use during a meeting
of the Expert Panel on a road
trial site.



It has become accepted that the Qd30 represents trueness in Qd measurement. Unfortunately, the Qd30 is no longer in production, and it has not been replaced with any instrument of comparable accuracy. A number of Qd30's are still in use at road trial sites and elsewhere.

E.5 Handheld combination instruments

A combination instrument is a retroreflectometer for the measurement of the R_L in the 30 m geometry that has an additional illumination system for the measurement of Qd, so that the instrument can measure either the R_L , the Qd or both in a sequence. The first such instrument was the ZRM 1013 by the Zehntner company that appeared during the late 1990's. This instrument is shown in figure E.7.

It is of cause tempting to add the Qd function to a retroreflectometer. All that it requires is the additional illumination system, and it gives the user the benefit to do two measurements, while handling only one instrument.

However, there is a difficulty. For the R_L measurement, the measured field should be relatively large, because it should be larger than the illuminated field and enclose that field with reserves. For the Qd measurement, on the other hand, the illuminated field should be even larger than the measured field and enclose that field with reserves.

The illumination system for the Qd measurement has, therefore, in principle to be large, which would make the combination instrument bulky and unhandy.



Figure E.7: The ZRM 1013 combination instrument.

The idea represented by the ZRM 1013 is the opposite, to keep the typical compactness of an R_L instrument and add only a small illumination system for the Q_d . The ZRM 1013 shown in figure E.7 does not have any bulge to make room for the illumination system, which is only a small cylinder of the size of a typical tin can.

When the illumination system is small, it is not possible to use the best arrangements of the fields, and it is unavoidable that the repeatability of measurement and the ability to measure profiled markings suffer.

Another difficulty is illustrated in figure E.8, which the incident beam for the measurement of R_L and a white wall that is part of the Q_d illumination system.

A significant part of the incident beam is reflected in the road marking surface in forward directions by specular reflection and falls on the lower part of the white wall. The same happens actually with the measuring beam, so that two reflected beams meet on the lower part of the white wall and create a false signal.

This signal can lead to quite large measuring errors. The errors would be particularly large, when measuring wet road markings, for which the real signal is small and the false signal is large because of strong specular reflection.

The false signal is avoided in the ZRM 1013 by leaving a gap in the Q_d illumination system at the surface, so that most of the reflected light can escape. This is also illustrated in figure E.8.

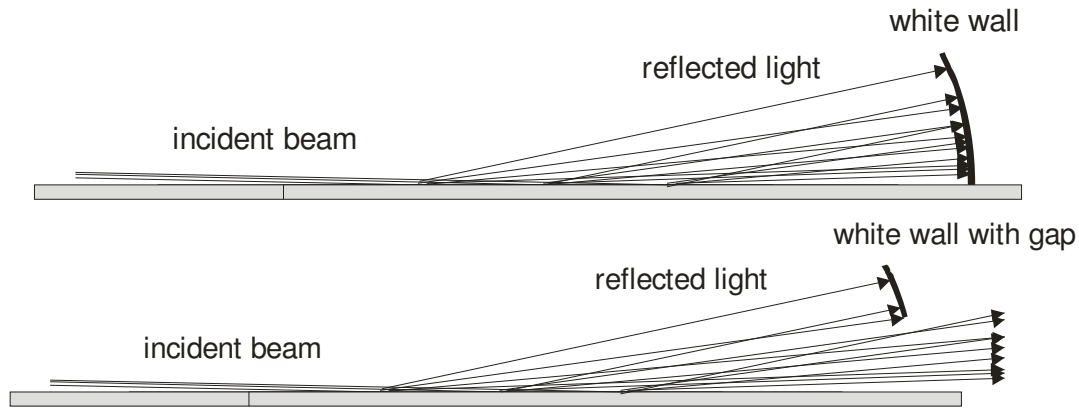


Figure E.8: Reflected light hitting a white wall in the Qd illumination system (top) or passing through a gap in the wall (bottom).

However, this means that the Qd illumination system does not provide full illumination in specular directions. Accordingly, it is not the Qd value, that is measured, but another average of individual q values.

Figure E.9 illustrates an illumination system, which provides a constant luminance down to an illumination angle. When the angle is 90°, there is full diffuse illumination and no gap from the illumination system to the surface, while smaller values of the illumination angles correspond to larger gaps to the surface.

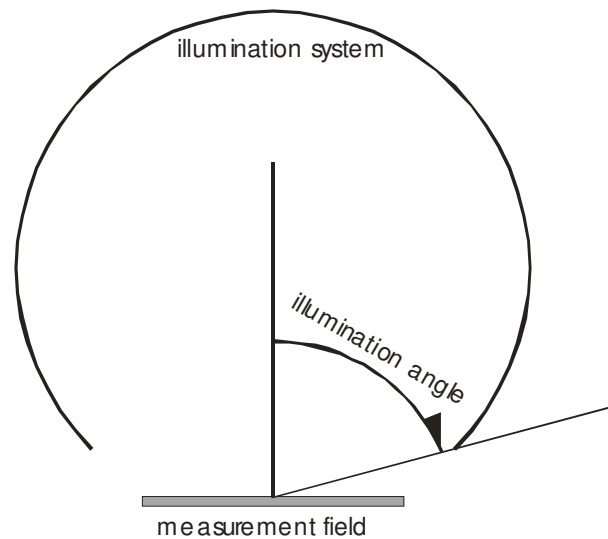


Figure E.9: A truncated illumination system may be described by an illumination angle.

Figure E.10 shows the average q value as the percentage of Qd for the reflection tables N1, N2, N3 and N4. These average q values are derived by calculations on basis of the N tables that are introduced in annex A.

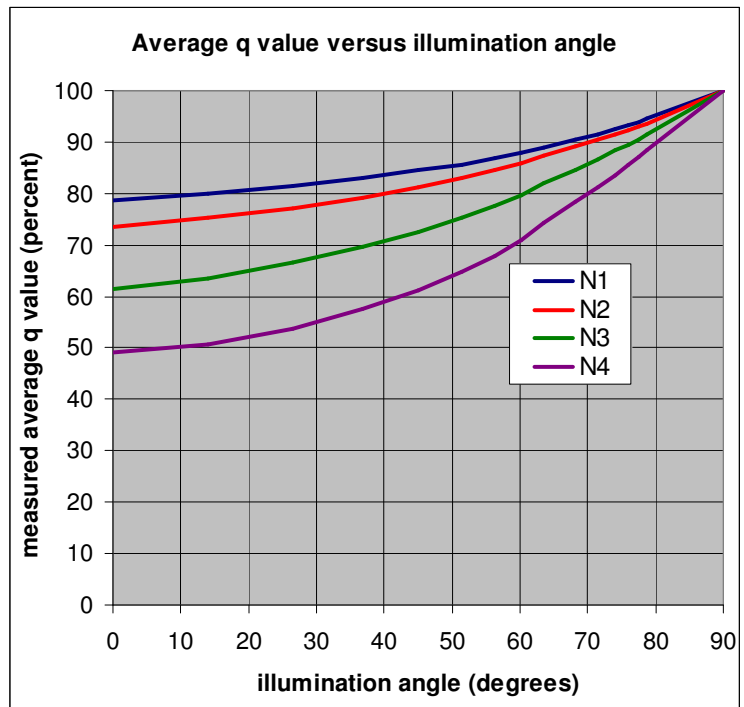


Figure E.10:
Typical average q values obtained with a truncated illumination system and shown for the reflection tables N1, N2, N3 and N4.

Figure E.10 illustrates that the average q value is smaller than the Qd value, whenever the illumination system is truncated.

It is the average q value that is measured, but the error would be unacceptable, if the average q value is presented directly as the Qd value. Therefore, the measured value is probably upscaled by means of a factor, before it is presented as a Qd value.

This means that the calibration cannot aim at giving the right proportion between luminance and illuminance (because that is the average q value), but must aim at an adjusted proportion in order to adjust the average q value to be a central representation of the Qd.

This prevents independent calibration of calibration standards. The only way of testing the calibration level is to use the instrument to measure the Qd values of a set of road marking panels with known Qd values. It is a good guess that the known Qd values of road marking panels would be obtained with old Qd30's remaining in use.

Therefore, the combination instruments do not in themselves provide trueness of Qd measurement, they only transfer the trueness provided by Qd30's that are no longer being produced.

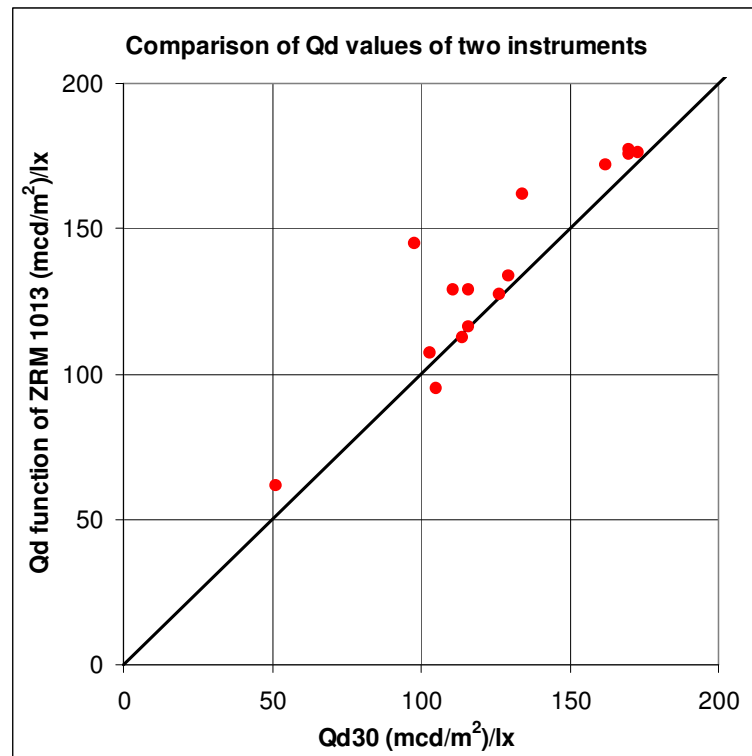
Even with a central calibration level, the truncated illumination is an additional source of uncertainty; see the variation between the N tables in figure E.10. The less than optimum arrangements of the fields of illumination and measurement is another additional source of uncertainty.

It is not surprising that the Qd function of the ZRM 1013 was not accurate. See the comparison with a Qd30 made by the Expert Panel on a road trial site, which is shown in figure E.11. The standard deviation is $33 \text{ mcd}\cdot\text{m}^{-2}\cdot\text{lx}^{-1}$ when expressed in units and 34 % when expressed in percent.

Up to twice the standard deviation can be expected to occur in practice. This is too much for a characteristic that has a total variation of perhaps $100 \text{ mcd}\cdot\text{m}^{-2}\cdot\text{lx}^{-1}$ and a spacing of classes of 30 to $40 \text{ mcd}\cdot\text{m}^{-2}\cdot\text{lx}^{-1}$ (the minimum levels for Qd classes for white road markings are 100, 130, 160 and $200 \text{ mcd}\cdot\text{m}^{-2}\cdot\text{lx}^{-1}$).

NOTE: The results for some plastics panels giving large deviations have been excluded from figure E.11 as they were deemed to be not representative for road markings.

Figure E.11:
Comparison of Qd measurements
between a Qd30 and an ZRM 1013.



In spite of this, combination instruments became popular, and DELTA was for competition reasons forced to equip a version of the LTL 2000 with the additional illumination system for Qd measurement. This happened some years after the ZRM 1013 emerged. This is also the reason that the demand for Qd30's stopped, and the production stopped

The ZRM has since been modified. The production of the LTL 2000's has ceased, but a version of the LTL-X has been equipped with a different illumination system for the Qd measurement.

The accuracy of these instruments depends among else on the above-mentioned matters, but it is not attempted to account for the individual instruments.

E.6 Requirements to handheld reflectometers

The annex A of EN 1436 and the ASTM E 2302 provide stringent and similar requirements for handheld Qd reflectometers.

It is not directly a requirement in neither ASTM E 2302 nor EN 1436 that a handheld reflectometer is based on the collimating principle, but in practice this should be requested because of advantages in terms of accuracy of measurement.

Additionally, it is not a requirement that a portable reflectometer has the arrangement A of the fields of illumination and measurement (the illuminated field encloses the measured field with reserves), but in practice this should also be requested because of the improved repeatability. Refer to E.3.

It is a requirement in EN 1436 that a portable reflectometer has a minimum tolerance to lifts, refer item e in the list of requirements provided below. However, it is an advantage if the tolerance is larger than the

minimum, as this is necessary when measuring profiled road marking with profiles higher the minimum tolerance (2 mm).

Both EN 1436 and ASTM E 2302 provide a number of direct requirements. Those of the EN 1436 are the most complete and are listed below:

- h. the luminance uniformity of the illumination system shall be minimum 0,8 (ratio of the smallest to the largest luminance)
- i. angles and aperture angles are in accordance with the 30 m geometry and the measured area is minimum 50 cm²
- j. the spectral match has a quality that ensures a maximum error of $\pm 5\%$ for yellow road markings
- k. the range of Qd values that can be measured is from 1 up to the maximum of 318 mcd·m⁻²·lx⁻¹
- l. daylight, in particular direct sun, does not influence the readings
- m. the Qd values measured at lifts of -1 mm, 1 mm, and 2 mm deviate maximum $\pm 10\%$ from the Qd value measured at 0 mm
- n. calibration is by means of a traceable standard sample for which independent calibration is possible.

Test methods for these requirements are provided or at least mentioned in EN 1436.

Literature

EN 1436 “Road marking materials - Road marking performance for road users” .

ASTM E 2302 “Standard Test Method for Measurement of the Luminance Coefficient Under Diffuse Illumination of Pavement Marking Materials Using a Portable Reflectometer”.

CIE 15.2 “Colorimetry”.

Annex F: Visibility of road markings

F.1 Introduction and discussion

This annex is a summary of some of the contents of the COST action 331 report “Requirements for horizontal road marking”. The report deals mainly with longitudinal lines in the form of edge lines, centre lines and lane dividing lines. Transverse lines and symbols etc. are only mentioned.

An experiment regarding the visibility of road markings in headlamp illumination is introduced in F.2. The results can be explained by the simple understanding that visibility conditions are in the domain of Ricco at the low levels of headlamp illumination. In this domain, the stimulus is the illumination on the eyes of the observer from the object to be seen. Accordingly, the following factors are equally important:

- the R_L value of the road marking minus the R_L value of the surrounding road surface
- the effective width of the road marking
- the luminous intensity of the headlamps.

R_L is the coefficient of retroreflected luminance, refer to annex B. The effective width of a road marking is the actual width of a continuous line, and a reduced width of a broken line. The reduction is so that a continuous line with the reduced width takes up the same area as the actual broken line.

The R_L value of the road marking is mostly much higher than the R_L value of the road surface. This shows that it is not the contrast of the road marking to the road surface that is important, but the excess luminance of the road marking.

EXAMPLE: A road marking with an R_L of $110 \text{ mcd}\cdot\text{m}^{-2}\cdot\text{lx}^{-1}$ on a road surface with an R_L of $10 \text{ mcd}\cdot\text{m}^{-2}\cdot\text{lx}^{-1}$ has a high contrast, while a road marking with an R_L of $130 \text{ mcd}\cdot\text{m}^{-2}\cdot\text{lx}^{-1}$ on a road surface with an R_L of $30 \text{ mcd}\cdot\text{m}^{-2}\cdot\text{lx}^{-1}$ has a lower contrast. However, the visibility is the same.

It may be a bit surprising that the effective width is as important as the R_L value. It does mean that a road marking with a low R_L value can work well, if it is wide.

It may also be a bit surprising that the luminous intensity of the headlamps is as important as the other factors. It does mean that a driver with powerful headlamp can see road markings, even if their R_L may be low.

It is another consequence that distance is very important for the stimulus. The reason is that the illumination on the observer's eyes is influenced twice by the square distance law of illumination, first the light has to reach the road marking, and next it has to reach back to the observer after being partly reflected into that direction. This makes the stimulus depend on distance in the inverse proportion of the distance to the power of four.

The effect is that it takes a high raise of the product of the above-mentioned factors to raise the visibility distance significantly. For instance to double the visibility distance takes an increase of the product by a factor of 16 (!). For this reason, when driving with the low beam, the visibility distance is mostly at the cut-off by the headlamps or somewhat within the cut-off.

On the other hand, if the product is reduced to half, for instance by a depreciation of the R_L value of the road marking, the effect is a reduction of the visibility distance of only 16 %. Even a poor road marking will be visible at some distance.

The visibility model derived by Werner Adrian is applied as explained in F.3, where also the freeware program Visibility, which is based on the visibility model, is introduced. Further it is demonstrated that the predictions of the program agree with the results of the above-mentioned experiment.

This visibility model is useful, as it extends the applications of the program to include factors like the age of the driver and glare from for instance headlamps of oncoming vehicles. Additionally, the applicability of the program is extended to include daylight and road lighting, and it is argued that the predictions are sufficiently accurate for practical application. Further extensions are obtained by the inclusion of vehicle geometries corresponding a car, a lorry and a motorbike, and the inclusion of realistic headlamp light distributions

The need for visibility of longitudinal road markings is considered in F.4 as based on experiments carried out on the driving simulator at the VTI in Sweden. The need is expressed by means of preview time.

Preview time is the time it takes to drive the distance at which the road marking is visible. If too short, it is a difficult and exhausting task for the driver to keep the vehicle within the driving lane. If comfortably long, the driver can find a convenient course through curves and has time for other tasks like looking in the rear view mirror. The Visibility program also provides the preview time at an input driving speed.

It is concluded that the absolute minimum for safe driving is a preview time of 1,8 seconds, while longer preview times are less exhausting and leaves time for other tasks like looking in the rear view mirror. Some consideration is given as to when a sufficient preview time is obtained.

F.2 An experiment regarding the visibility of road markings in headlamp illumination

Figure F.1 shows four longitudinal road markings that were used to determine visibility distances to road markings in headlamp illumination. The geometries of the road markings are indicated in table F.1.

Table F1: Four longitudinal road markings.

Line	Width	Line length	Gap length	Effective width
#1	10 cm	3 m	9 m	2,5 cm
#2	10 cm	3 m	3 m	5,0 cm
#3	10 cm	continuous		10 cm
#4	30 cm	continuous		30 cm

The effective widths indicated in table F1 for the two broken lines #1 and #2 are derived as if the same amount of material had been placed as continuous lines. For the two continuous lines #3 and #4, the effective widths equal the actual widths.

The four lines existed actually in two versions, one with an R_L of approximately $100 \text{ mcd}\cdot\text{m}^{-2}\cdot\text{lx}^{-1}$, varying a bit from line to line, and another with an R_L of approximately $400 \text{ mcd}\cdot\text{m}^{-2}\cdot\text{lx}^{-1}$. The road surface had an R_L value of $8 \text{ mcd}\cdot\text{m}^{-2}\cdot\text{lx}^{-1}$.

The visibility distances were determined for three luminous intensity values of the headlamps, which were approximately 1200 cd, 7000 cd and 25000 cd.

This provides a total of 4 times 2 times 3 equal to 24 test situations. A total of nine test persons determined their individual visibility distances for each of the 24 test situations. During driving at night, a test person pressed a button as soon as he saw a road marking. The visibility distances for the nine persons are averaged, resulting in average visibility distances for each of the 24 test situations.

Figure F.1: Four longitudinal road markings.



Figure F.2 illustrates a road marking at a point in time during the approach. Because of the perspective, the road marking has the shape of a triangle. Additionally, the road marking luminance decreases with distance (upwards in the figure) because of the distance law of illumination.

It is assumed that the stimulus for visibility is the excess illumination on the observers eyes from that triangle, meaning illumination in addition to what the road surface would have provided if there had been no road marking. This is the same as assuming that visibility is in the domain of Ricco, which is typical for the low luminance conditions in night time driving.

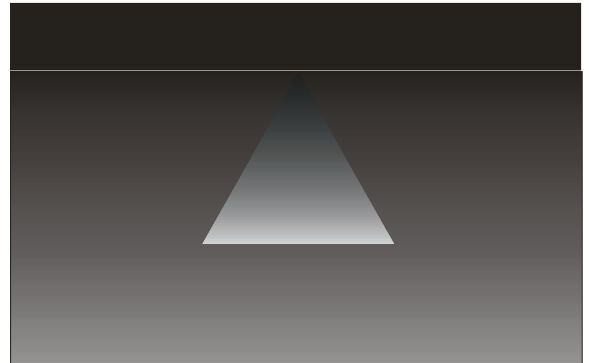


Figure F.2: A road marking seen during approach.

At a given distance, the additional illumination on the observers eyes will be in proportion to the product of three factors:

- the effective road marking width
- the R_L value of the road marking minus the R_L value of the road surface
- the luminous intensity of the headlamps.

Such a product may be called the product affecting the stimulus. Accordingly, the visibility distances determined in the experiment are plotted against these products in figure F.3.

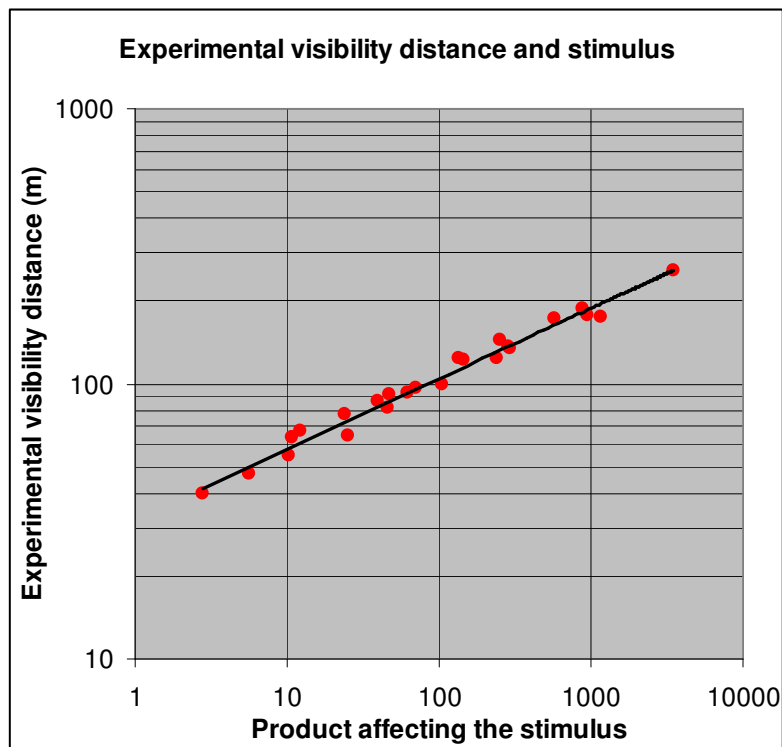


Figure F.3: Visibility distances plotted against the product affecting the stimulus.

It is seen that the correlation is good, even very good. This matter and more detailed analyses confirm the assumption about visibility being in Ricco's domain.

It is noted that the stimulus increases rapidly when approaching a road marking. If for instance the distance is reduced to half, the illuminance at the road marking increases by a factor of four because of the square distance law of illumination at the road marking. Additionally, the apparent road marking area also increases by a factor of four. This makes the illumination on the observers eyes increase by a factor of 16. Refer to the illustration in figure F.4.

Therefore, the visibility distance is expected to be in proportion to the above-mentioned product raised to a power of 0,25. This is actually the slope of the regression line shown in figure F.3.



Figure F.4: A line shown at a long distance (left) and a shorter distance (right) illustrating that both luminance and apparent size increase, when approaching a line.

F.3 The Visibility program

On this basis, the visibility model derived by Werner Adrian is applied after converting the actual triangular object with varying luminance to an equivalent circular object with constant luminance on a background of constant luminance. This is done in two steps:

- assume the constant luminance of the equivalent object is the luminance of the road marking in the forefront and that constant luminance of the background is the luminance of the road surface at the same distance
- select the circular object with a size that gives is the same luminous intensity as the actual object.

Details are provided in the COST action 331 report.

The visibility model is implemented in a freeware program Visibility. The combined input/output window is shown in figure F.5.

The visibility distances calculated with this program for the conditions of the experiment are compared to those obtained in the experiment in figure F.6. It is seen that the agreement is good.

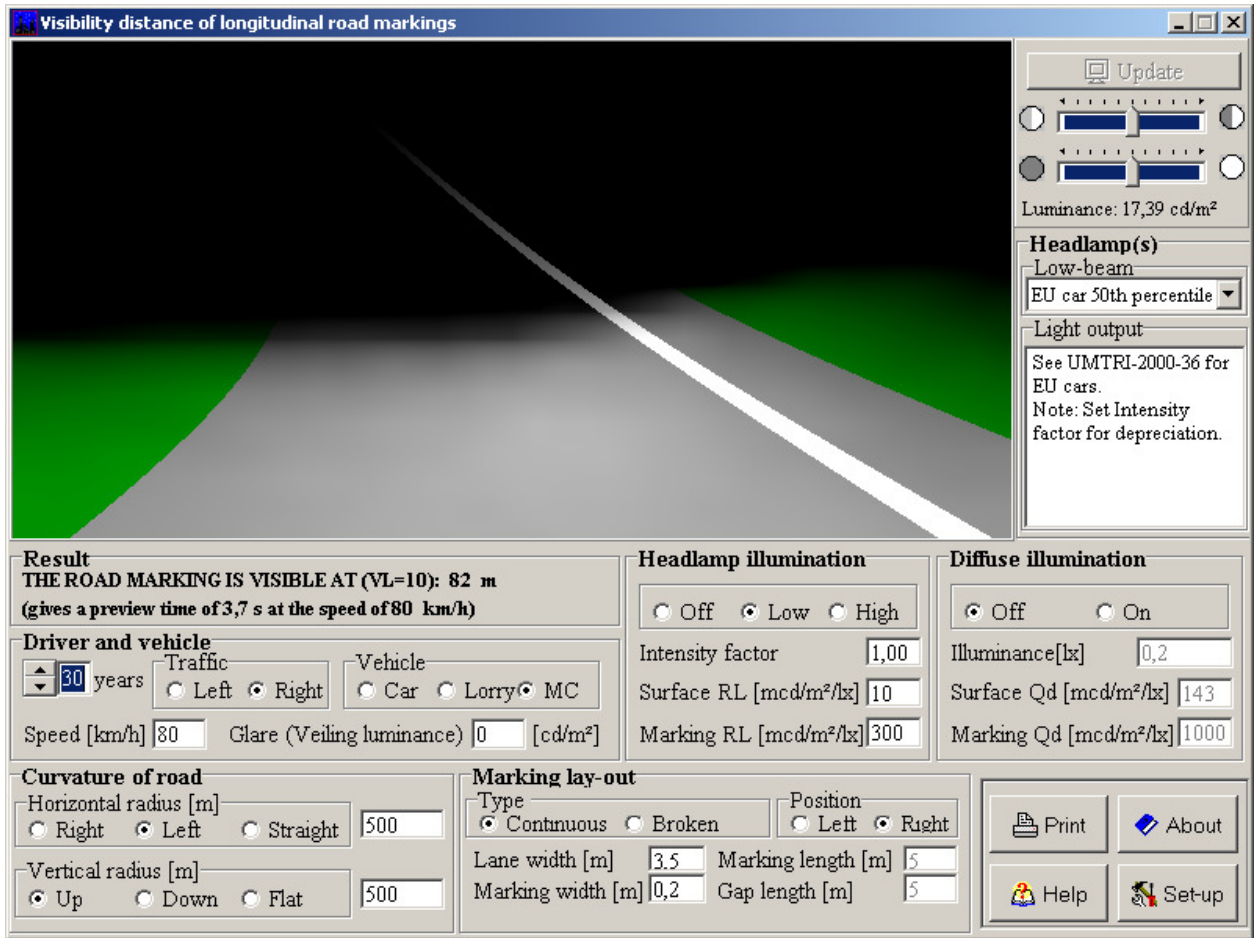


Figure F.5: The visibility program.

Figure F.6:
Comparison of calculated and
experimental visibility distances.

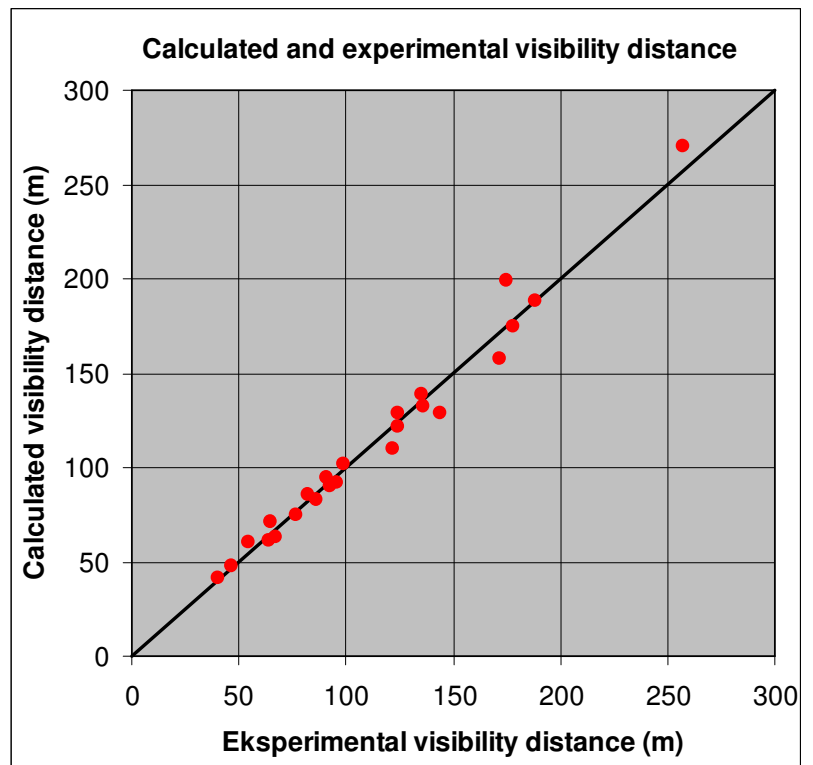


Figure F.7 shows some results of calculations with the Visibility program. It is seen that the visibility distance of an edge line increases with increasing R_L value of the line and also with increasing width. The R_L value of the road marking was set to $25 \text{ mcd}\cdot\text{m}^{-2}\cdot\text{lx}^{-1}$.

It is now tested if the Visibility program supports that the line width is as important as the R_L value of the line. This is done by plotting the calculated visibility distance against the product of two factors:

- the R_L value of the line minus the R_L value of the road surface
- the line width.

This plot is given in figure F.8. It is seen that the various points form a single curve, which confirms that the Visibility program gives the same importance to the line width as to the R_L value of the line.

Figure F.7:
Example of results obtained with the Visibility program.

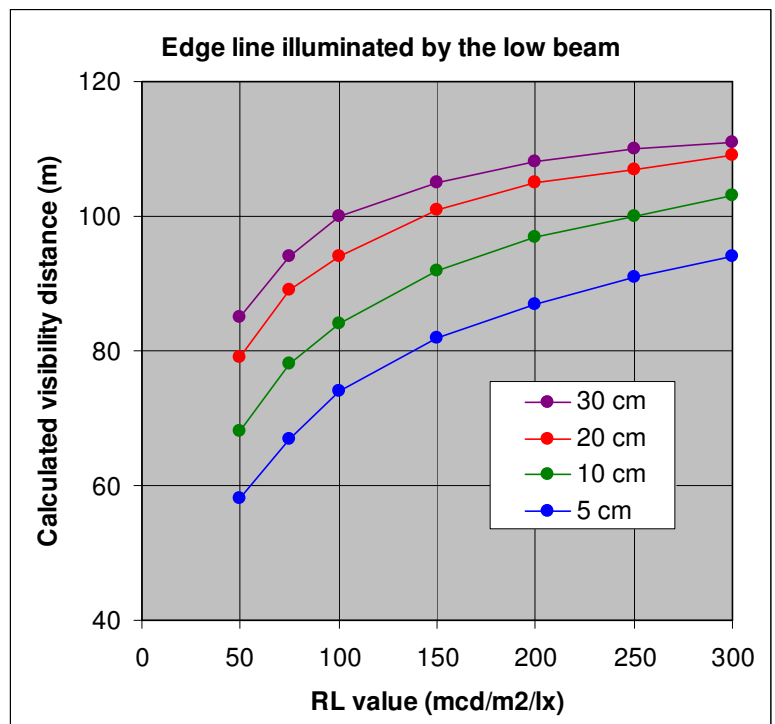
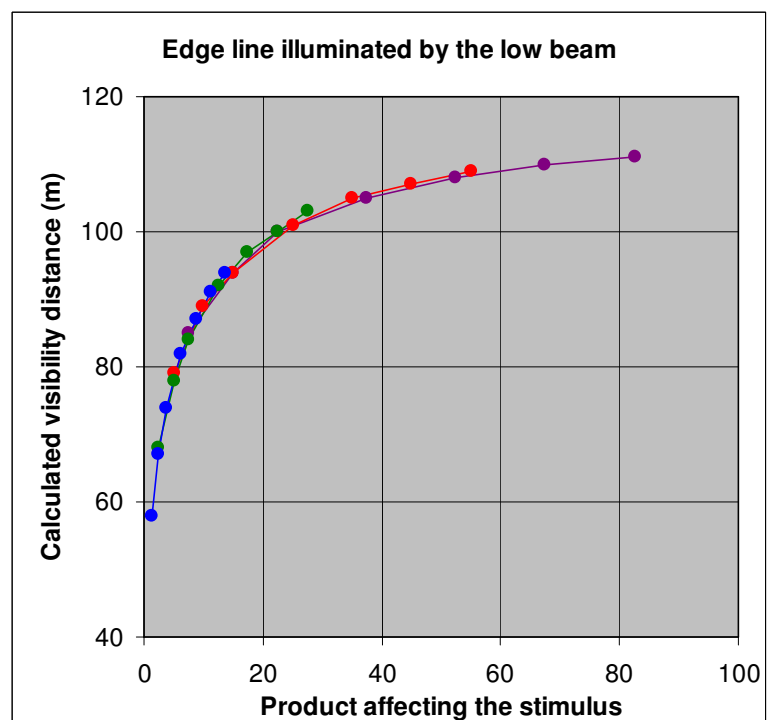


Figure F.8: Calculated visibility distance as a function of the product affecting the stimulus.



The program includes not only the night driving situation, but also day lighting and road lighting. The performance of the Visibility program was not tested for these lighting conditions and, therefore, the matter is discussed below.

In daytime, the luminance level is so high that visibility conditions are in the domain of Weber. This means that the actual luminance level is not important, only the contrast of the road marking to the road surface. This is almost like an on/off criterion. If the contrast is above a low threshold level, the road markings are visible at long distances. If not, the road markings are hardly visible at any distance.

It may be that the Visibility program does not provide the accurate threshold value, but it does reflect the nature. In view of the large variations of contrast that may appear in varying daylight conditions, this should be satisfactory in practical applications.

Road lighting in combination with headlamp illumination is in between pure headlamp illumination and day lighting. Therefore, the luminance level as well as the contrast may be expected to have an influence. The Visibility program confirms this expectation and is probably adequate for practical applications.

Other factors of Werner Adrian's model like the age of the driver and glare are included as well.

Age is included by means of two factors, one for loss of light in the eyes of elderly persons and one for increased sensitivity to glare. The two factors vary with age in a typical manner, but they do not apply for individual persons.

The vehicle can be either a passenger car, a lorry or a motorcycle. The input R_L value is for the 30 m geometry, but the program converts the value to the geometry of the selected vehicle by means of the model of reflection presented in annex B.

Realistic headlamp intensity distributions are installed as copied from UMTRI reports.

F.4 The need for visibility of longitudinal road markings

It is generally considered that a driver needs a preview time to longitudinal road markings in order to steer the vehicle properly through curves and keep it well within the driving lane.

Preview time is the time it takes a driver to drive the distance at which he can see the road marking. In a way, it is the time he has got to detect for instance a bend of the road and start steering accordingly. If for instance the speed is 90 km/h, which is 25 m per second, and the visibility distance is 50 m, then the preview time is 2 seconds.

Accordingly, there are two ways to increase the preview time, to reduce speed and to raise the visibility distance.

An experiment to determine the need for preview time was conducted at the driving simulator at the VTI, Statens väg- och transportforskningsinstitut in Sweden. A number of test persons drove through simulated road scenario with a variety of curves and straight sections, different limitations of the visibility distance and either free choice of speed or fixed speed set by cruise control.

The conclusion is that a preview time of 1,8 seconds is the absolute minimum for safe driving. It is possible to keep the vehicle on the road with less preview time, down to 1 second, but the task is exhausting and the driving is uncertain with overshooting in curves. With more

preview time, driving becomes more relaxing and it is possible to drive conveniently through curves.

Figure F.9 shows the driving simulator, while figure F.10 shows some road scenes with different visibility distances.

Calculations for night driving show that even fairly poor road markings (low R_L value and/or small effective width) mostly offer a sufficient preview time, when conditions are good. The road markings have, on the other hand, to be fairly good (higher R_L value and/or larger effective width), when conditions are adverse such as for older drivers, dirty headlamps and glare from opposing vehicles on narrow roads. Refer to the COST Action 331 report. It is also possible to test the conditions by means of the Visibility program, which includes the preview time at an input driving speed.

The most adverse case is the one of wetness, where the R_L values of most road markings fall to very low values. Only road markings with profile or other means to maintain retroreflection in wet conditions will provide some R_L value during wetness.

In daytime, preview time is ample when there is sufficient contrast between the road marking and the road surface. Poor visibility can occur in some lighting situations, in particular when the road surface is more shiny than the road markings,

At the luminance levels obtained by road lighting of traffic roads, several factors influence the visibility of road markings; the actual luminance level, the contrast and the effective road marking width. Illumination by the headlamps improves the visibility somewhat by raising both the luminance level and the contrast. The visibility distances will normally be at least adequate.



Figure F.9: The driving simulator at the VTI.



Figure F.10: Some road scenes with different visibility distances to road markings as indicated.

Literature

COST action 331 report “Requirements for horizontal road marking”.

Annex X: Lighting concepts and units used for road equipment

X.1 Summary

Light, production of light and principles of light measurement are introduced in X.2. Light is electromagnetic radiation in a narrow range of wavelengths corresponding roughly to solar radiation. Radiation with these wavelengths acts on biological processes without being unduly harmful to life.

The concept of luminous flux is introduced. Incandescent lamps and other light sources are briefly mentioned. Additionally, principles of light measurement are mentioned. The luminous flux is provided in the technical documentation of light sources.

The concepts of luminous intensity and illuminance are introduced in X.3. It is pointed out that luminous intensity relates to a direction from a lamp and is most easily understood as the ability to provide illumination of objects or surfaces located in that direction. The illuminance is derived by means of the distance law of illumination. Additionally, when the illuminance is to be derived for a plane that is not perpendicular to the particular direction, the cosine law of illumination has to be taken into account as well.

The concept of luminous intensity is used in technical specifications for luminaires and signal lights. Illuminance, on the other hand, measures the level to which a surface is illuminated and is the target for the design of some indoor and outdoor lighting installations.

The concepts of reflection and luminance are introduced in X.4. Luminance is the stimulus for the eye. Only objects possessing a luminance by some process (light emission, reflection or scattering) can be seen. A particular characteristic for reflection, the luminance coefficient, represents the ability of the illuminated surface to produce luminance.

Reflection is the subject of specifications for sign faces, road markings and other surfaces. The road surface luminance is the target for the design of road lighting installations of traffic roads.

In X.5 it is explained that nature really works in a simple way:

- The illuminance at a location on a plane is π times the average luminance of all the objects in front of the plane as seen from that location.
- A reflecting surface gets its luminance as an image of the surfaces in front. The luminance is normally reduced because of absorption in the surface and there may be more emphasis to some directions than to other directions due to shininess or other features of reflection.

Therefore, the concepts of luminous flux, luminous intensity, illuminance and reflection are not needed in order to understand how a surface gets its luminance. However, the concepts are practical in terms of applications by giving roles to specification writers, producers, testing laboratories and installation designers.

X.6 provides an introduction to the colour of light and of surfaces.

The concepts, units and definitions are summarized in table X.1.

It is easy to find literature on the internet. CIE 15:2004 “Colorimetry” is the bible on the rather difficult aspects of colour.

Table X.1: Concepts, units and definitions.

Concept	Unit	Definition
Luminous flux, Φ	Lumen (lm)	The total amount of light emitted by a light source.
Luminous intensity, I	candela (cd)	The density of light in a direction, or the ability to produce illuminance on surfaces in a direction in conjunction with the laws of illumination.
Illuminance, E	lux (lx)	The density of light falling on a field of a surface
Luminance, L	candela/m ² (cd/m ²)	The density of luminous intensity from a field of a surface. Luminance is the stimulus for the eye.
Luminance coefficient, q	cd·m ⁻² ·lx ⁻¹	The ratio between luminance and illuminance of a field of a surface in specified conditions of illuminance and observation.
x, y		CIE Chromaticity co-ordinates.

X.2 Light, production of light and principles of light measurement

Electromagnetic radiation is characterized by its wavelength. In principle, there is no limit to the wavelength, but in practice it may be considered to be from less than 10^{-10} m up to more than 100 m. Radiation within that range is subdivided into gamma rays, X rays, ultraviolet radiation, visible radiation, infrared radiation, radio waves and heat radiation. See figure X.1

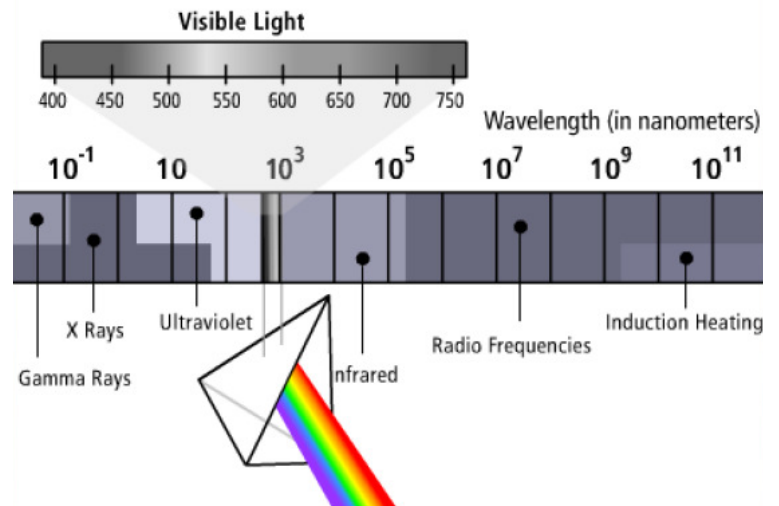
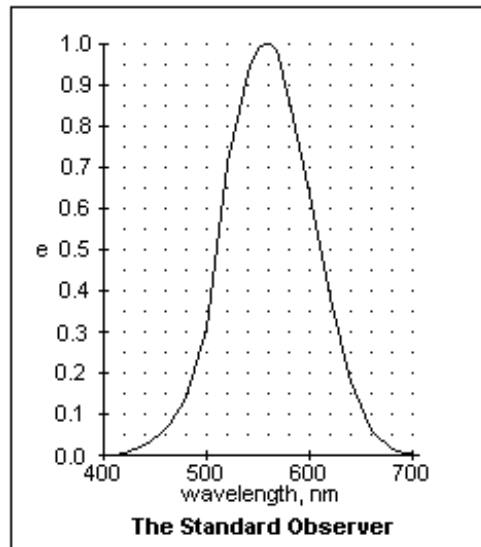


Figure x.1:
Electromagnetic radiation and light.

Visible radiation is found at wavelengths in a narrow band about 500 nm (1 nanometer equals 10^{-9} m). In principle, light is the radiant power summed up with relative weights of the so-called $V(\lambda)$ curve and multiplied by a factor of 683 lumen/Watt. The $V(\lambda)$ curve represents the spectral sensitivity of the eye, while the factor is there for historical reasons to provide a link to early definitions. The $V(\lambda)$ curve is illustrated in figure X.2.

Figure X.2:
The $V(\lambda)$ curve representing the spectral sensitivity of the eye (the standard observer).



Light summed up this way is called luminous flux Φ and has the unit of lumen (lm). The unit is rather small due to the above-mentioned factor of 683 lm/Watt. Because of this, a light source should be able to generate a large number of lumens compared to the number of Watts it consumes. The ratio is called the luminous efficacy.

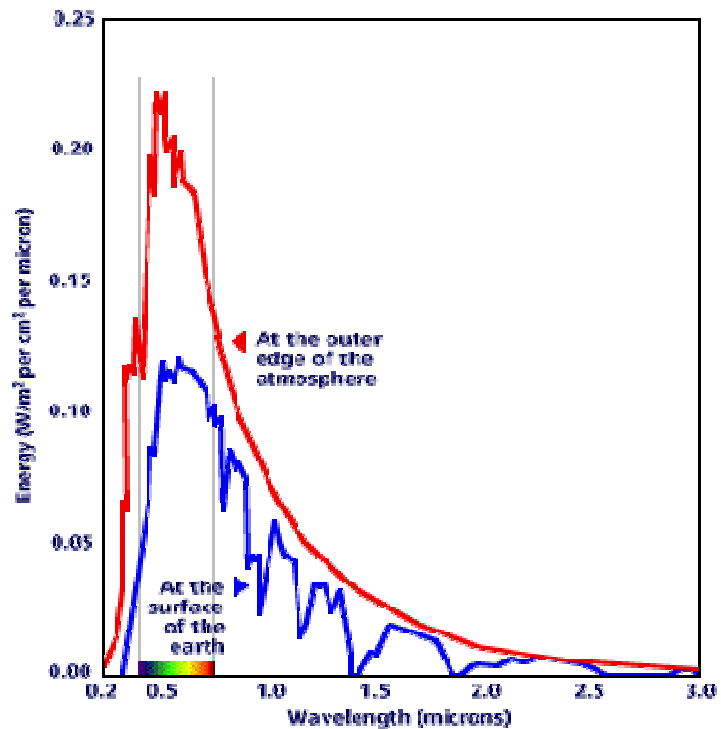
As also illustrated in figures X.1 and X.2, light can be split up into the different wavelengths, and each of these is associated with a colour of the rainbow. Colour is considered in X.6.

The energy of electromagnetic radiation comes in small packets called photons. The energy of a photon is in inverse proportion to the wavelength; it is large for gamma rays of short wavelengths and decreases gradually with increasing wavelength.

Electromagnetic radiation with short wavelengths up to and including ultraviolet radiation has sufficient energy to cause damage to biological molecules and is thus harmful to life. The energy of radiation with longer wavelengths from infrared radiation and upwards is not sufficient to interact with biology, except when concentrated to provide a heating effect as in a microwave oven.

Visible radiation is just in between, it can drive the chlorophyll process of plants and it can stimulate the sensors of the eye without being undue harmful. It is a wonder that the solar radiation spectrum at sea level has its maximum in the visible range with only some ultraviolet radiation and some additional infrared radiation. See figure X.3.

Figure X.3:
The solar radiation spectrum
(a micrometer equals 10^{-6} m).



The sun emits its radiation because it is hot at the surface, approximately 5250 °C. Any hot object emits radiation with a spectrum that depends on its temperature.

This is the principle of an incandescent lamp, which has a tungsten filament that is heated by the conduction of an electrical current. Unfortunately, the tungsten filament can be heated to only approximately 2300 °C or its life will be short. At this temperature, most of the radiation is infrared with only a low proportion in the visible range. Therefore, the luminous efficacy is low, normally in the range of 6 to 14 lm/Watt depending on the type of lamp.

Incandescent halogen lamps has a halogen gas surrounding the filament that allows a higher temperature of the filament and thereby a somewhat higher luminous efficacy, normally in the range of 10 to 20 lm/Watt depending on the type of lamp.

Actually, because electromagnetic radiation is the carrier of the electromagnetic force, there are numerous other processes for generating light than high temperature. Whenever an electron is disturbed, a quantum of electromagnetic radiation is emitted. The practical problem is to generate electromagnetic radiation that falls within the visible range and to allow it to leave. However, the principle is used in great variety of discharge lamps and other light sources like light emitting diodes (LED). In some of these lamps, radiation of short wavelengths is converted to radiation of longer wavelengths by fluorescence. Luminous efficacies are higher than for incandescent lamps, mostly in the range of 50 to 100 lumen/Watt.

Light is measured by means of photometers. These have a photo sensitive element, mostly a photodiode, whose spectral sensitivity has been corrected to match the $V(\lambda)$ curve to an acceptable degree. The correction is mostly by colour filters. Photometers also have suitable means to make them accept light from parts of the space around them with defined directional sensitivity.

The luminous flux of a light source is measured in an integrating sphere that accepts light uniformly from all directions of space. Other photometers are mentioned in the following.

The luminous flux is provided in the technical documentation of light sources.

Luminous flux is used not only in connection with light sources; it makes sense also to speak about the luminous flux falling on a surface or a field of a surface.

X.3 Luminous intensity and illuminance

Naked light sources are sometimes used for illumination, but normally they are mounted in a lamp with optics or shades to direct or reduce the light into specific directions.

NOTE: The word lamp is used in the following as a generic term for luminaires, lanterns, signal lights and other lighting devices.

The lamp, therefore, modifies the directional distribution of the light emission. In each particular direction, the intensity of light is described by a luminous intensity, I in the unit of candela (cd).

Luminous intensity has a definition of its own which, however, is complex. It is more easy to think in terms of figure X.4, which shows a luminous surface with a luminous intensity I in a direction towards a surface facing the luminous surface at a distance D . The luminous surface can for instance be the aperture of a headlamp.

The concept of illuminance applies for a field of a surface. It is the ratio between the luminous flux falling on the field and the area of the field. As the unit of luminous flux is lumen (lm), one might think that the unit of illuminance is lumen per square meter (lm/m^2). This is true, but with the modification that an individual unit of lux (lx) has been introduced.

The luminous surface causes an illuminance E on the illuminated surface given by: $E = I/D^2$. Accordingly, luminous intensity can be understood as the ability to produce illuminance. The equation illustrates the distance law of illumination - that the illuminance is in inverse proportion to the square of the distance.

EXAMPLE 1: A headlamp with a luminous intensity of 10.000 cd illuminates a surface at a distance of 50 m. The illuminance at the surface is $10.000/50^2 = 4$ lx.

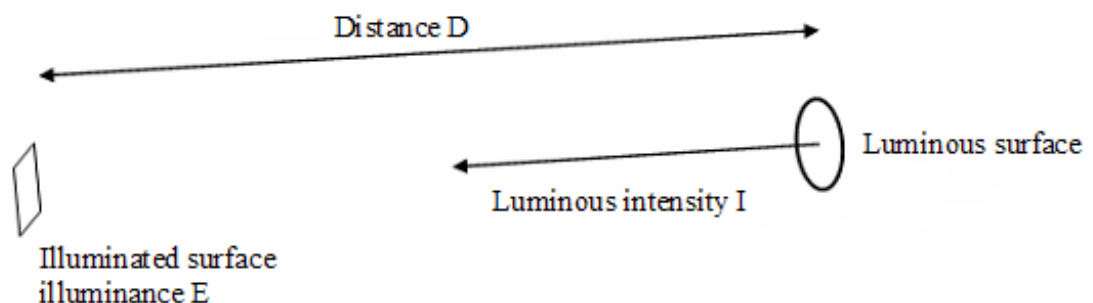


Figure X.4: A luminous surface with a luminous intensity I in a direction towards an illuminated surface at a distance D causes an illuminance of I/D^2 .

There is an additional law of illumination, which is to be applied when the illumination is measured on a plane that is not perpendicular to the direction of illumination. The direction of

illumination is described by an angle of incidence v , which is shown in figure X.5. The resulting illuminance is reduced by the factor $\cos v$ in accordance with the cosine law of illumination.



Figure X.5: The angle of incidence.

Consequently, the complete expression for illuminance is $E = I \cos v / D^2$. Contributions from more than one luminous surface can be summed up to a total illuminance.

Illuminance can be measured by means of a luxmeter, which is a photometer that accepts light from the hemisphere in front of the luxmeter with a directional sensitivity in accordance with the cosine law of illumination. A luxmeter can either be turned towards the light, or it can be placed with its back on the surface on which the illuminance is to be measured.

A luxmeter can either be anything from a cheap handheld instrument up to an expensive laboratory photometer.

The distance law of illumination is used for calculations of illuminance but can also be used to determine the luminous intensity of a lamp by means of the inverse equation, $I = E \times D^2$. The illuminance E is measured by means of a luxmeter at a known distance D and I is determined. This is the basis for laboratory measurement of luminous intensities of lamps.

EXAMPLE 2: A headlamp produces an illuminance at 20 m distance of 25 lx. The luminous intensity is $25 \times 20^2 = 10,000$ cd.

The luminous intensity from a lamp depends generally on the direction relative to the lamp.

As an example, a low beam headlamp has large luminous intensities in directions below the cut-off, and much lower luminous intensities in directions above. Refer to figure X.6, which shows the distribution of average luminous intensity from a number of headlamps in use, after cleaning (the distribution for dirty headlamps is broader).

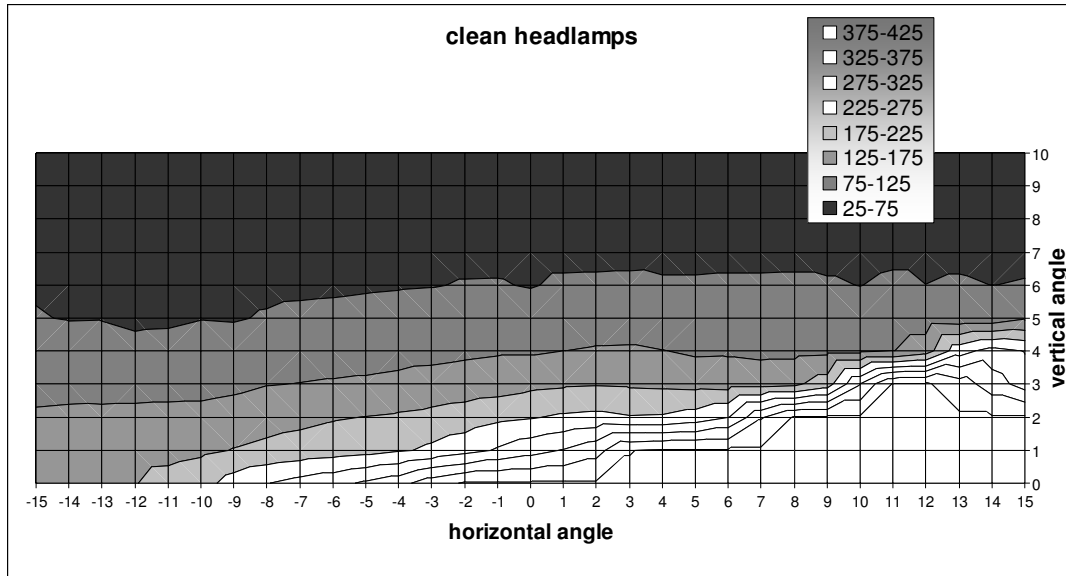
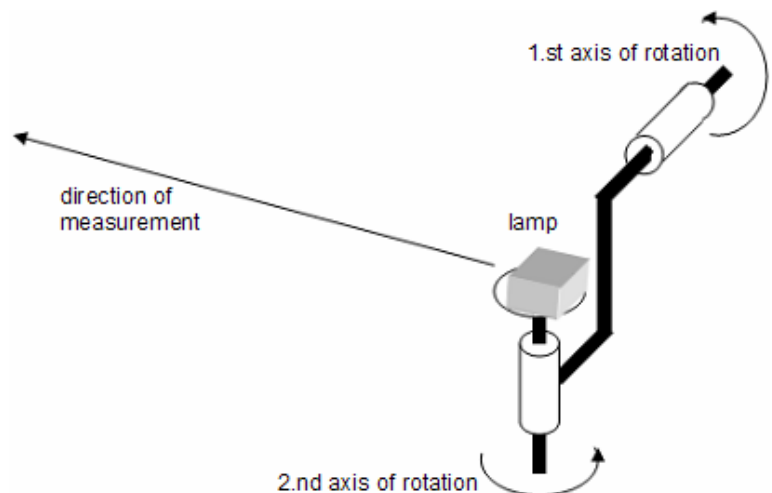


Figure X.6: Average intensity distribution of some clean headlamps in use (cd).

In this example, the purpose is to provide a reasonably high illumination at some distance in front of the vehicle without causing strong glare to oncoming traffic. Most luminaires and signal lamps have optics designed to provide variations in the luminous intensity for similar purposes.

Therefore, it is in general necessary to measure the luminous intensity in several directions relative to the luminaire or signal lamp. The particular set of direction is often defined in technical specifications, which in some cases also set requirements for the luminous intensities in the individual directions.

The most common method of establishing different directions is to keep a fixed horizontal measuring direction, but to turn the lamp in a goniometer with two axes of rotation. See figure X.7.



**Figure X.7:
A lamp placed in a goniometer.**

In another method, the luminaire is turned about a fixed vertical axis, while the measuring direction is varied with respect to the horizontal by tilting a large mirror (this is not illustrated). This method takes up more space, but is preferable for lamps with light sources that cannot be tilted, or light sources that changes luminous output when tilted.

A complete table of luminous intensity values is called a luminous intensity distribution or a light distribution. It is sometimes illustrated by means of a diagram as shown in figure X.6, and sometimes in other ways.

The concept of luminous intensity is used in technical specifications for various luminaires and signal lights. Illuminance is the target for the design of some indoor and outdoor lighting installations.

Luminous intensity is used not only in connection with lamps; it makes sense also to speak about the luminous intensity emitted by reflection from a surface or a field of a surface.

X.4. Reflection and luminance

A surface that is illuminated by a lamp obtains a luminance L by reflection as seen by an observer, see figure x.8.

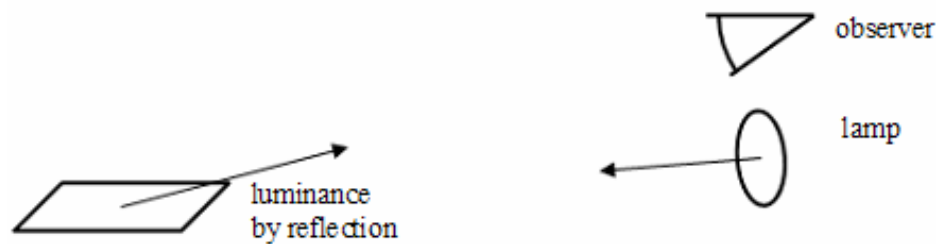


Figure X.8: A surface obtains a luminance by reflection as seen by an observer.

The luminance L of a field of a surface is $L = I/A$, where I is the luminous intensity of the field and A is the apparent area of the field. The luminance, the luminous intensity and the apparent area refer to a particular observation direction. The unit for luminance is candela per square metre (cd/m^2).

By apparent area of a field is meant the projection of the actual area of the field onto the direction of observation. Refer to figure X.9.

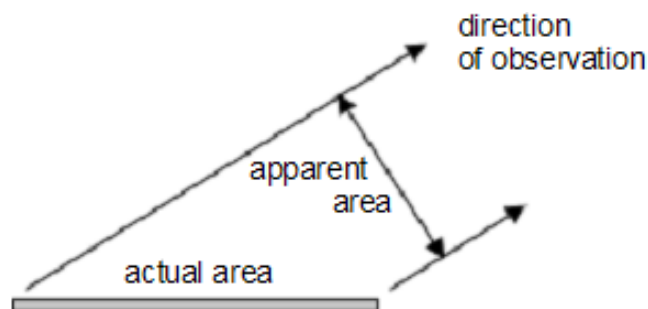


Figure X.9: Actual and apparent area.

Luminance is the stimulus for the eye. Objects that obtain a luminance by some process (light emission, reflection or scattering) can be seen, light as such cannot.

Luminance is measured by means of a photometer called a luminance meter, which has optics to allow light only from a field confined by a small cone. The size of the cone is measured by its angular diameter, which may typically be $6'$, $20'$, 1° or 3° . The field confined by the cone is called the measuring field.

A luminance meter is a handheld instrument looking somewhat like a video camera, in which the measuring field is indicated in a search image. A luminance meter can be rather cheap, or it can be fairly expensive with measuring fields down to 6 minutes of arc.

The road surface luminance is the target for the design of road lighting installations of traffic roads.

The luminance L obtained by reflection is in proportion to the illuminance E . The ratio between the two is called the luminance coefficient q ; i.e.: $q = L/E$. The unit is $\text{cd}\cdot\text{m}^{-2}\cdot\text{lx}^{-1}$. The luminance coefficient is a measure of the ability of a surface to create luminance.

In a theoretical case, when the surface has perfect diffuse reflection, the value of q is independent of the geometry of illumination and observation. If so, the luminance coefficient is given by $q = \rho/\pi$ where ρ is the reflectance of the surface. The reflectance is a measure of the degree to which incoming light is reflected and is maximum 1. Therefore, for diffuse reflection, the maximum value of q is $1/\pi$ equal to approximately 0,318.

Diffuse reflection is approximated by surfaces of matt finish and is sometimes assumed as a simplification in some lighting conditions. However, in most practical cases that are relevant for road equipment, the luminance coefficient varies with the geometry of illumination and observation.

Reflection is the subject of specifications for sign faces, road markings and other surfaces. The specifications are based on particular characteristics and they define the geometry of illumination and observation. Additionally, specifications include the spectral composition of the incoming light; refer to X.6.

EXAMPLE 1: The luminance coefficient in diffuse illumination Q_d of a surface is an average of the individual q values for the illumination directions of diffuse illumination. Diffuse illumination is obtained when the surroundings above the surface has a constant luminance and is best supplied from a photometric sphere. Q_d is used with an observation direction that forms an angle of $2,29^\circ$ to the surface.

A reflecting surface can at most show the same luminance as the luminance of the surroundings L which, on the other hand, creates an illuminance of $\pi \times L$. Therefore, the maximum value of Q_d is $L/(\pi \times L) = 1/\pi$.

Q_d is used for road markings, but can as well be used for road surfaces.

EXAMPLE 2: The coefficient of retroreflected luminance R_L of a surface has the same definition as the luminance coefficient q , except that the illuminance is measured on a plane perpendicular to the direction of illumination – instead of on the plane of the surface. This makes an R_L value smaller than a q value, but the same unit is used.

The R_L is used for road markings, but can as well be used for road surfaces. The R_L is normally used for a geometry that simulates that the driver of a passenger car looks on the surface 30 m ahead.

EXAMPLE 3: The coefficient of retroreflection R_A of a surface has the same definition as the luminance coefficient q , except that the area of the surface is the full area – not the apparent area in the observation direction. This makes an R_A value smaller than a q value. The unit is not $\text{cd}\cdot\text{m}^{-2}\cdot\text{lx}^{-1}$ as for a luminance coefficient, but $\text{cd}\cdot\text{lx}^{-1}\cdot\text{m}^{-2}$ in order to stress the difference in the use of the area.

The R_A is used for retroreflective sign face materials and sign faces.

X.5 A bit more about luminance

In X.3 it was shown that a luminous surface with a luminous intensity I creates an illuminance of $E = I/D^2$ at a distance D .

Actually, the luminous intensity I of the luminous surface is given by $I = L \times A$, where L is the luminance and A is the area of the luminous surface. The illuminance is then given by $E = L \times A / D^2 = \omega \times L$, where ω is the solid angle of the luminous surface as seen at the distance D and as given by $\omega = A / D^2$. Solid angles are really without dimension, but are formally given the unit of steradian (sr).

The expression $E = \omega \times L$ shows that the illuminance on the illuminated surface is really caused by the presence of a luminous surface in the surroundings. The concept of luminous intensity is not needed to explain the illuminance, but it is practical in terms of technical applications. In other cases, it is more practical to think in terms of luminance.

An example is illumination by the sun, where it is not really practical to determine the luminous intensity as the product of luminance and area, and then apply the distance law of illumination. It is enough to multiply the luminance with the solid angle. The luminance of the sun is approximately $1.000.000.000 \text{ cd/m}^2$, and its angular diameter is 32 minutes of arc corresponding to a solid angle of $0,000086 \text{ sr}$, so that the illuminance is approximately 86.000 lx . In practice, the illuminance by the sun depends on the height position of the sun and on atmospheric conditions.

The above-mentioned illumination by the sun is on a plane perpendicular to the direction of the sunlight. The illumination on the horizontal plane is reduced by the cosine to the zenith angle of the sun.

Another example is illumination by the sky on the horizontal plane. Assume that the sky has a uniform luminance L of 5.000 cd/m^2 and be aware that the solid angle of the hemisphere is 2π and that the average cosine of all directions in the hemisphere is $1/2$. The illuminance is then $E = \pi \times L = 15.700 \text{ lx}$.

This example makes it clear that the illuminance at a location on a plane is simply π times the average luminance of all the objects in front of the plane as seen from that location. There is nothing fundamental in the presence of the factor π , it is only due to the units of illuminance and luminance. See figure X.10.

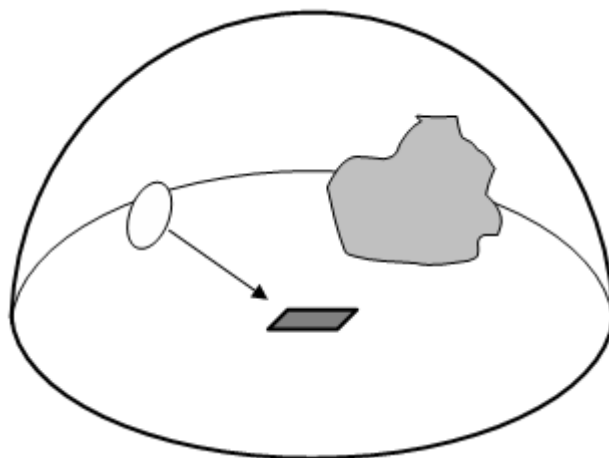


Figure X.10: The illuminance on a plane is π times the average luminance of all the objects in front of the plane.

In X.4 it was stated that an illuminated surface obtains a luminance by reflection given by $L(\text{illuminated surface}) = q \times E$, where q is the luminance coefficient. Inserting E gives $L(\text{illuminated surface}) = q \times \omega \times L(\text{luminous surface})$. This expression raises the suspicion, that the illuminated surface simply shows an image of the luminous surfaces in front of it.

This is true. A reflecting surface gets its luminance as an image of the surfaces in front. The luminance may be reduced because of absorption in the surface and there may be more emphasis to some directions than to other directions due to shininess or other features of reflection. The image is mostly diffused or blurred depending on the properties of the reflecting surface.

As an example, a road surface with a reflectance of 0,25 under a uniform sky has a luminance 0,25 times the sky luminance.

Therefore, the concepts of illuminance and luminance coefficient are not really needed in order to explain how an illuminated surface gets a luminance, but the concepts are practical for technical applications.

X.6 Colour of light and surfaces

The CIE 1931 colour space is the most widely used colour system for technical specifications of colours.

The tri-stimuli values X , Y and Z are found as weighted summations of the spectral radiant power. The weights are in accordance with the curves $\bar{x}(\lambda)$, $\bar{y}(\lambda)$ and $\bar{z}(\lambda)$ indicated in figure X.11. The curve $\bar{y}(\lambda)$ is actually the same curve as the $V(\lambda)$ and appears in this connection with a different designation only.

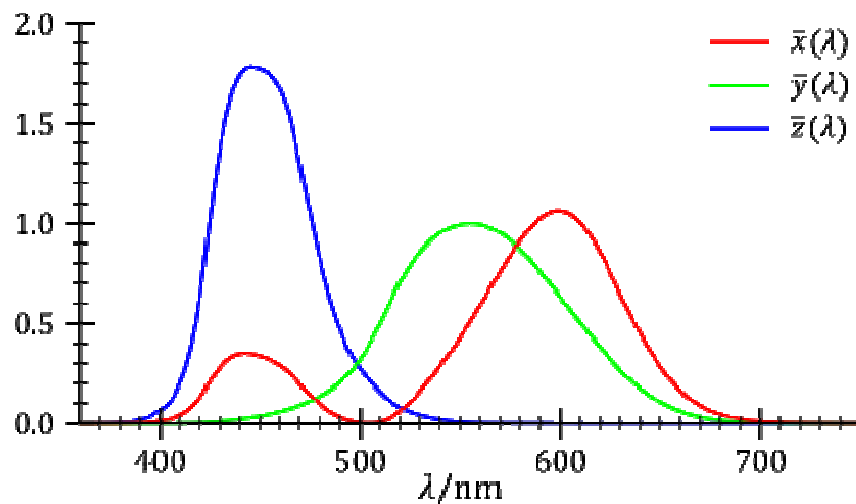


Figure X.11: The curves $\bar{x}(\lambda)$, $\bar{y}(\lambda)$ and $\bar{z}(\lambda)$ used to derive the tri-stimuli values X , Y and Z .

The two chromaticity co-ordinates x and y are found by $x = X/(X+Y+Z)$ and $y = Y/(X+Y+Z)$. Those two co-ordinates determine a location in the CIE chromaticity diagram shown in figure X.12. The numbers indicated around the curving part of the triangular colour region refer to the wavelengths of light of a single wavelength, i.e. to the colours of the rainbow. The curving part is called the spectrum locus. All other colours are mixtures of these colours.

Permissible colours of signal lights are generally indicated by colour regions or colour boxes in the chromaticity diagram.

Colours of light of light sources are indicated in similar ways or with reference to a curve for temperature radiators by means of a correlated colour temperature (this curve is not indicated in figure X.12).

Permissible colours of reflecting surfaces are also indicated by colour boxes in the chromaticity diagram. The surfaces represent for instance sign faces or road markings. However, the chromaticity of a reflecting surface depends on the illuminant used to illuminate the surface and on the geometry of illumination and observation. These matters are therefore specified and lie behind the requirements. The value of Y has a meaning as a measure of the reflection.

The illuminants are generally standard illuminant A, which represents a headlamp with an incandescent lamp, or standard illuminant D65, which represents daylight. The most used geometry of illumination and observation is the 45°/0° geometry. The value of Y is mostly in the scale of a luminance factor, which is π times the scale of a luminance coefficient.

As an example, the chromaticity boxes of retroreflective sheeting materials are shown in figure X.13. These apply for standard illuminant D65 and the 45°/0° geometry. The boxes include only non-fluorescent materials, as fluorescent materials have separate boxes.

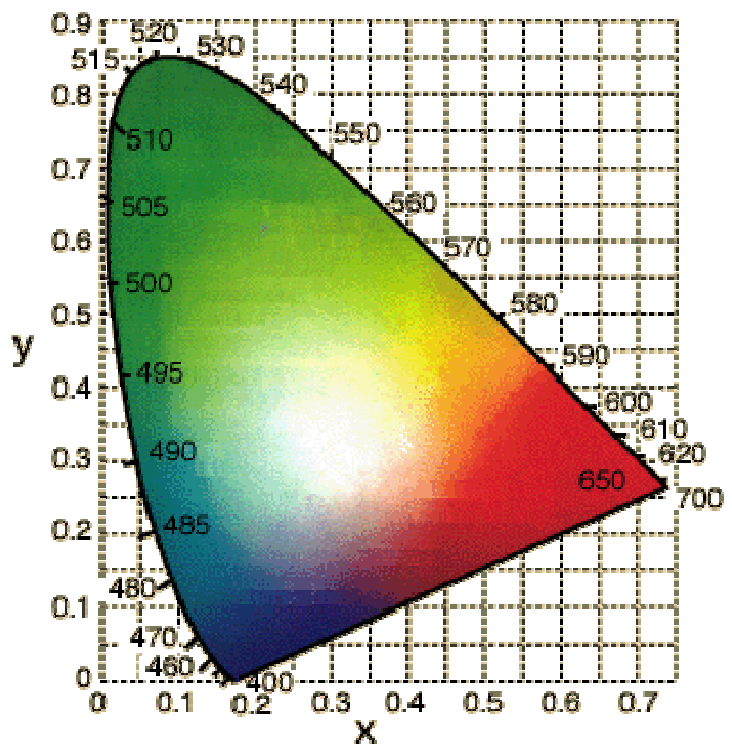
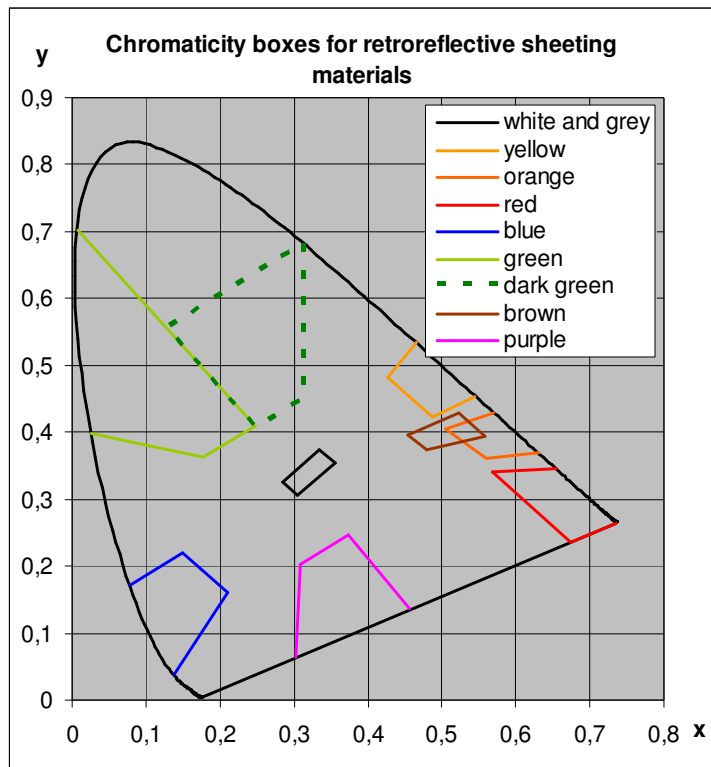


Figure X.12:
The CIE chromaticity diagram.

Figure X.13:
Example of colour boxes.



NOTE: The sizes of the colour boxes do not necessarily indicate the permissible variations of colour within the boxes, as the distances in figures X.12 and X.13 do not indicate degrees of visual distances.

Literature

CIE 15.2 "Colorimetry".